AD-A056 953 CONTROL DATA CORP MINNEAPOLIS MINN F/G 17/9
DIGITAL MODULAR CHANGE DETECTOR.(U)
MAY 78 R DENNY, M BAYNES, W MCLURE F30602-73-C-0141
UNCLASSIFIED RADC-TR-78-104 NL

1 OF 3
AD A056953

LEVEL II

RADC-TR-78-104
Final Technical Report
May 1978

DIGITAL MODULAR CHANGE DETECTOR

R. Denny
M. Baynes
W. McLure
et. al.

Control Data Corporation

Approved for public release; distribution unlimited.

ROME AIR DEVELOPMENT CENTER
Air Force Systems Command
Griffiss Air Force Base, New York 13441

This report contains a large percentage of machine-produced copy which is not of the highest printing quality but because of economical consideration, it was determined in the best interest of the government that they be used in this publication.

This report has been reviewed by the RADC Information Office (OI) and is releasable to the National Technical Information Service (NTIS). At NTIS it will be releasable to the general public, including foreign nations.

RADC-TR-78-104 has been reviewed and is approved for publication.

APPROVED: Ronald B. Haynes

RONALD B. HAYNES
Project Engineer

APPROVED: H Davis

HOWARD DAVIS
Technical Director
Intelligence & Reconnaissance Division

FOR THE COMMANDER: John P. Huss

JOHN P. HUSS
Acting Chief, Plans Office

If your address has changed or if you wish to be removed from the RADC mailing list, or if the addressee is no longer employed by your organization, please notify RADC (IRRE) Griffiss AFB NY 13441. This will assist us in maintaining a current mailing list.

Do not return this copy. Retain or destroy.

UNCLASSIFIED
SECURITY CLASSIFICATION OF THIS PAGE (When Data Entered)

REPORT DOCUMENTATION PAGE

READ INSTRUCTIONS BEFORE COMPLETING FORM

1. REPORT NUMBER: RADC-TR-78-104	2. GOVT ACCESSION NO.
3. RECIPIENT'S CATALOG NUMBER	
4. TITLE (and Subtitle): DIGITAL MODULAR CHANGE DETECTOR	5. TYPE OF REPORT & PERIOD COVERED: Final Technical Report. 9 Mar 73 - Jan 78
6. PERFORMING ORG. REPORT NUMBER: N/A	
7. AUTHOR(s): R. Denny, M. Baynes, W. McLure et. al. V. Froehlich R. Rigles	8. CONTRACT OR GRANT NUMBER(s): F30602-73-C-0141
9. PERFORMING ORGANIZATION NAME AND ADDRESS: Control Data Corporation, 2800 East Old Shakopee Road, Minneapolis MN 55420	10. PROGRAM ELEMENT, PROJECT, TASK AREA & WORK UNIT NUMBERS: 63746F; 11530122
11. CONTROLLING OFFICE NAME AND ADDRESS: Rome Air Development Center (IREE), Griffiss AFB NY 13441	12. REPORT DATE: May 1978
	13. NUMBER OF PAGES: 12 198 P.
14. MONITORING AGENCY NAME & ADDRESS (if different from Controlling Office): Same	15. SECURITY CLASS. (of this report): UNCLASSIFIED
	15a. DECLASSIFICATION/DOWNGRADING SCHEDULE: N/A

16. DISTRIBUTION STATEMENT (of this Report)

Approved for public release; distribution unlimited.

17. DISTRIBUTION STATEMENT (of the abstract entered in Block 20, if different from Report)

Same

18. SUPPLEMENTARY NOTES

RADC Project Engineer: Ronald B. Haynes (IRRE)

19. KEY WORDS (Continue on reverse side if necessary and identify by block number)

Radar Exploitation
Radar Change Detection
Digital scan converters
Displays

20. ABSTRACT (Continue on reverse side if necessary and identify by block number)

This report describes the development of a Digital Modular Change Detector (DMCD). One method of Interpretation of Synthetic Aperture Side-Looking Airborne Radar (SLAR) images is based on the comparative analysis of two images of the same area exposed at different times to detect any differences or changes in detail that have occurred during the interim period. Recent improvements in SLAR technology have advanced the operational state-of-the-art in collection system where radar imaged data can be obtained over wide swath widths at rates of many thousand of square nautical miles per hour. To ex-

DD FORM 1 JAN 73 1473 EDITION OF 1 NOV 65 IS OBSOLETE

UNCLASSIFIED
SECURITY CLASSIFICATION OF THIS PAGE (When Data Entered)

096300

ploitate intelligence in a timely manner from this data requires on-line automated processing, screening, and display of changes pertinent to an interpreter. This program designed, fabricated, tested and demonstrated a digital modular change detection system for SLAR imagery. The modular approach uses a programmable module, provides the capability for system growth potential and adaptability to meet new Air Force SLAR imagery processing requirements.

PREFACE

This report has been prepared by the Digital Image Systems Division of Control Data Corporation under Air Force Contract F30602-C-73-0141. This project has involved the building, demonstration and installation of the Four Channel Modular Change Detection equipment and applicable software.

The Control Data program manager was M. Sandahl. Specific technical responsibility was as follows: R. Denny, M. Baynes, and W. McLure - hardware design and configuration; V. Froehlich, R. Rigles, B. Becker, K. Enstrom, G. Grisbeck, W. Webber, and M. Murphy - software implementation; S. Clark - diagnostic software system; R. Bogott - Display OPS analysis, B. Glish - Digital Imagery analysis.

The contractor would like to acknowledge the technical guidance provided by the Air Force Program Monitors, Mr. J. Maier and Mr. J. Horne.

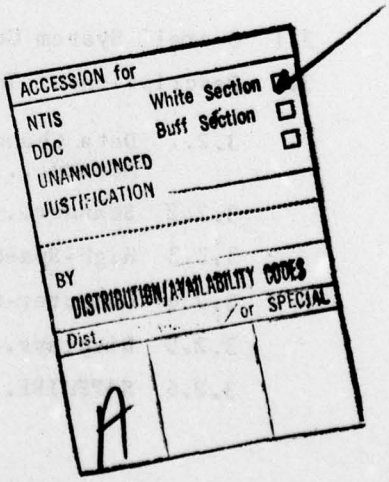

TABLE OF CONTENTS

TABLE OF CONTENTS (Cont.)

LIST OF FIGURES

LIST OF FIGURES (Cont.)

LIST OF FIGURES (Cont.)

LIST OF FIGURES (Cont.)

LIST OF TABLES

EVALUATION

The work completed under Contract #F30602-73-C-0141 is significant because it has developed an automated system for separating change events between two side-looking-airborne-radar (SAR) images. With the development of high resolution large area reconnaissance radar surveillance system capable of producing wide swaths widths of data at rates of many thousands of square nautical miles per hour requires special exploitation techniques be developed. The digital modular change detector was developed, tested and successfully demonstrated under this effort. This now allows automatic on-line change detection necessary for extracting intelligence data in a timely manner from near real time data linked reconnaissance radar images.

The work accomplished under this effort falls directly under TPO-R2C, Ground Target Detection and Identification, whose objective is to improve the Air Force's real-time all-weather surveillance exploitation capabilities.

The system developed under this effort is being applied to developing the advanced UPD-4 Side Looking Radar exploitation system scheduled for conceptual demonstration in USAFE in 1980.

Ronald B Haynes

RONALD B. HAYNES
Project Engineer

1.0 INTRODUCTION

1.1 HISTORY

Control Data Corporation has been involved in various image processing programs since 1968. The primary emphasis of Digital Image Systems Division has been the study of Synthetic Aperture Side-Looking Airborne Radar (SLAR) data. Computer simulations, using large general-purpose computers, have proven the feasibility of automatic digital change detection between pairs of SLAR film images. These studies have developed realizable digital procedures for the matching of the scenes between two film images. The digital techniques developed for registration of the film pairs proved to be more exact than any current (1970 vintage) analogue capabilities. The analogue techniques, such as the Cedertron, corrected only linear distortions in the geometry of the image scenes. The Control Data studies clearly indicated that the scene brightness and contrast were equally important in the matching of the SLAR image scenes and the geometry corrections were more complicated than simple linear correction. The CDC algorithms developed included all these corrections in the digital processes. Once the SLAR images were matched (registered and photonormalized), simple differences between the scenes became apparent. This differencing process represents SLAR digital change detection.

These simulation studies led to the development of a hardwired processor to perform the matching and change detection algorithms. The matching process was fabricated as a registration process for the geometric corrections and a photonormalization process for the radiometric corrections. This equipment, known as the ARRES 1280 System, was delivered to Rome Air Development Center in August of 1972 and demonstrated, on-line, in October of that same year at Rome, New York.

Since the development of the ARRES 1280 equipment, various refinements and additions to the simulation software indicated the need for a change detection system with the flexibility to adapt to algorithm refinements

and the possibility of additional processing requirements of the system. In addition to the functional flexibility required of a new change detection system, a system must have improved reliability and maintainability. To meet the above-mentioned requirements, a breadboard special-purpose processor, the Flexible Processor (Figure 1-1) was built and demonstrated to RADC personnel in January 1973. This processor was a programmable unit capable of communicating to other similar units at a 256 million-bit rate and to a small general-purpose computer at various rates down from 32 million bits to whatever could be accepted by the general-purpose computer.

An Advanced Development* Model of a change detection system was then to be constructed utilizing this processor as the common module (See Figure 1-2). This program began in March 1973.

* An item used for experimentation or tests to (a) demonstrate the technical feasibility of a design, (b) determine its ability to meet existing performance requirements, (c) secure engineering data for use in further development and, where appropriate, (d) establish the technical requirements for contrast definition. Depending on the complexity of the equipment and the technological factors involved, it may be necessary to produce several successive models, to achieve additional objectives. The final advanced model approaches the required form factor and employs standard parts (or nonstandard parts approved by the agency concerned). Serious consideration is given to military requirements such as reliability, maintainability, human factors and environmental conditions.

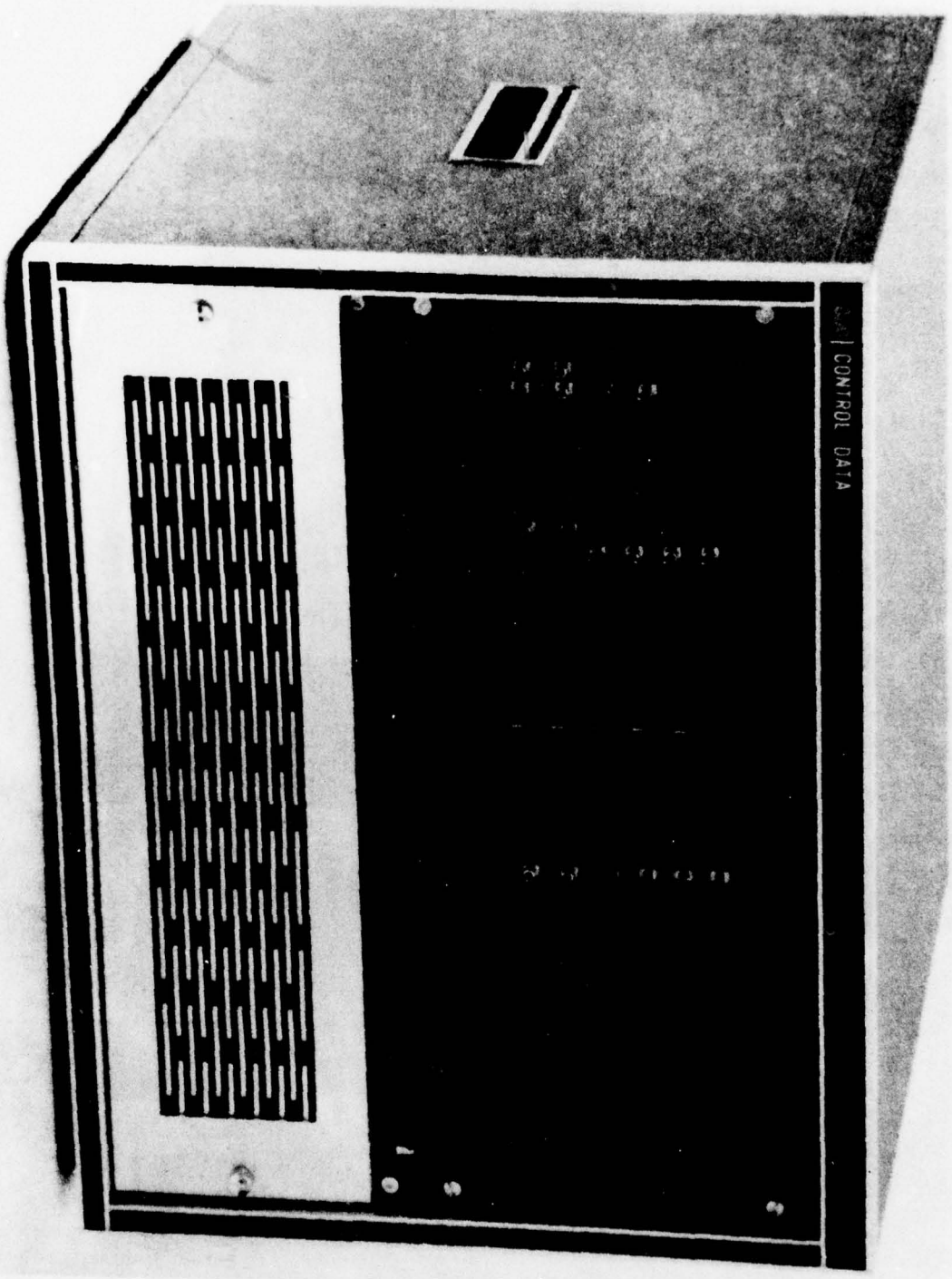

Figure 1-1. The Flexible Processor

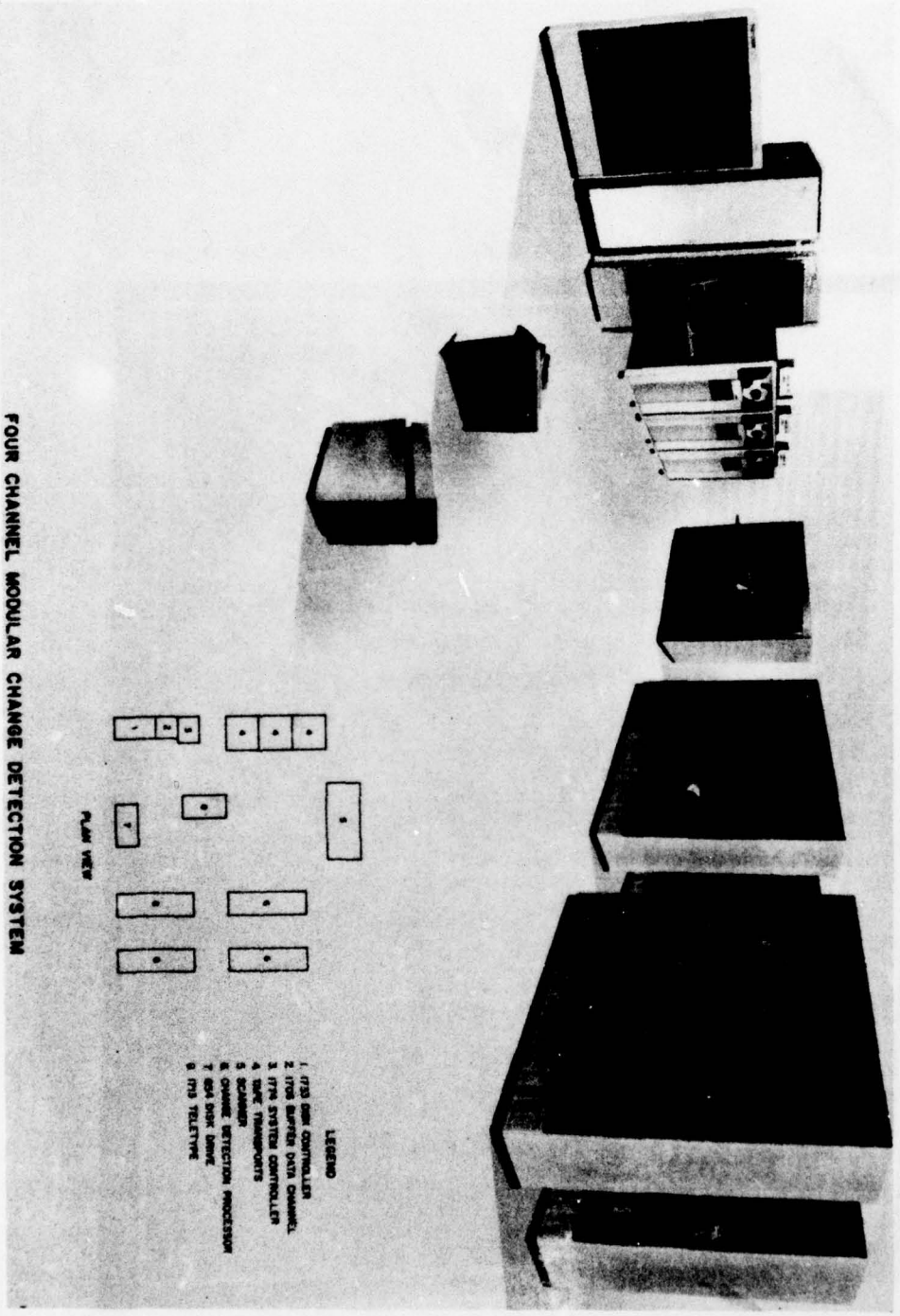

Figure 1-2. Advanced Development Model of a Change Detection System

1.2 PROGRAM OBJECTIVES

The major objective of the Digital Modular Change Detection (DMCD) program was to design, fabricate, test, and demonstrate a modular change detection system for SLAR imagery. This modular design approach using a programmable module was to provide the capability for greater system growth potential and the adaptability to meet new Air Force SLAR imagery processing requirements.

A second objective of the program was to apply a common module and component engineering construction approach to the then existing change detection functions. This engineering model would significantly reduce future production, test, and maintenance costs of SLAR imagery processing systems. This approach reduced the total amount of different printed circuit board types within the system, lowering the cost of spare parts, allowing production methods of construction (flow soldering, semiautomatic wire-wrapped back panels, etc.) and the utilization of fault isolation diagnostics at the modular level.

A third objective of the program was to provide the Air Force with second generation change detection equipment having increased functional capabilities in SLAR imagery processing, and to which new capabilities could be added in the future through its modular and programmable approach. The increased functional capabilities included a process to reduce the false alarm rate due to the scintillation effect in SLAR and a process for the initialization or start-up of a system. A summary of the initial program requirements is presented in Table 1-1. This summary highlights the original program statement of work, dated 18 July 1972.

1.3 PROGRAM HISTORY

The original program statement of work was modified with eight amendments, the first of which occurred before the contract for the program was consummated. The program amendments are summarized in

TABLE 1-1.

SUMMARY OF ORIGINAL PROGRAM REQUIREMENTS

1. Determine Operational Constraints Imposed by the Physical Characteristics of UPD-4, Senior Crown, and Senior Lance Data
2. Define Display Interface Requirements to be Satisfied by the Program Equipments
3. Implement processes to Screen SLAR Change Detected Data and Discard False Alarms Resulting from Dissimilar Reflections of Scene Features
4. Determine Design Requirements to Scale Data to Aerial and Ground Mapping Systems
5. Determine the Most Cost-effective General-purpose Support Computer
6. Fabricate a Four Channel Change Detector as Follows:
   - Use FP modules
   - Use ARRES 1280 Scanner
   - Output changes in context of SLAR imagery background or to a general-purpose computer
   - Operator parameter selection and operator-assisted initiation
   - Computer programs to perform the change detection
   - Process film input pair at up to 14 IPS
   - Register to one resolution cell
   - Normalize image density differences
   - Suppress shadows
   - Output resolution commensurate with UPD-4 SLAR data
7. The System MTBF shall be 100 hours excluding display, with M_{ct} = 30 minutes and $M_{max\ ct}$ = 60 minutes
   - MIL-STD-883 Class C Parts Shall be Used
   - Reliability Qualification Tests in Accordance to Test Plan VIII, MIL-STD-781B Test Level A
   - Predict Maintainability Using Procedure II of MIL-HNDK-472
8. Provide Routine Maintenance Software Package
9. Conduct Design Review
10. Develop Preliminary Acceptance Tests
11. Develop Final Acceptance Tests
12. Provide Operator Training for the System

TABLE 1-2.

SUMMARY OF AMENDMENTS TO PROGRAM REQUIREMENTS

Amendment	Date	Effect
1	8 Dec. 1972	• Limit System output resolution to that of input device (the ARRES 1280 Scanner)
		• Specified a MTBF of 40 hours for the system
		• Require ceramic microcircuits
		• Require contractor to provide any spare parts which fail in excess of the MTBF specified for the first twelve months
2	12 March 1974	• Slant Range Conversion to be operator selectable
		• To require processing of SLAR data with up to 2^{o} of rotational deviation in relative image flight tracks
		• To require operation with direct SAPPHIRE data and digital data on magnetic tape
		• Mosaic UPD-4 data to remove channel gaps
		• Provide a means for initial alignment of SLAR data from digital sources
		• Provides means for storage of scene data in digital form for 500 sq. KM
3	10 June 1974	• Analyze the impact of digital SLAR radar correlation on the change detection processes by processing FLAMR and HIRSADAP data
4	10 March 1975	• Require the hardware and software for direct interface to SAPPHIRE for input data to the DMCD
		• Require implementation of interface tests and test procedures
5	24 Sept. 1975	• Require the hardware and software to record DMCD output at full resolution and full swath width on the SAPPHIRE laser beam recorder
6	25 June 1976	• Measure UPD-4 non-parallel and irregular channel gaps
		• Select final acceptance test data from 10 pairs of GFE SLAR data

TABLE 1-2.

SUMMARY OF AMENDMENTS TO PROGRAM REQUIREMENTS

Amendment	Date	Effect
		• Develop test data by mosaicking and pre-processing selected data and record on magnetic tapes
		• System repeatability shall be demonstrated by developing test data from the same source data and processing to achieve essentially the same results
		• Supply mounting hardware for new laser in ARRES 1280 scanner
7	10 Nov. 1976	• Supply three months of maintenance upon completion of acceptance testing
8	4 May 1977	• Support the Air Force in the physical integration of the Digital Modular Change Detector to the SAPPHIRE ground processor

Table 1-2. The effect of these amendments was to redirect the program effort from the development of a film-based system with UPD-4 resolution to an all digital input system expecting sensor data characteristic of the UPD-4 film data in geometric properties but with extended radiometric resolution. In addition, the output of the change detection system was to be printed on the SAPPHIRE Laser Beam Recorder. While the original plans were for the Digital Modular Change Detector (DMCD) and the SAPPHIRE equipments to arrive on site at approximately the same time, the DMCD arrived on site a year ahead of the SAPPHIRE. As a result there was a considerable stretch-out of the phases of acceptance testing and integration to the SAPPHIRE.

1.4 PROGRAM RESULTS

A DMCD system was constructed and delivered to the U.S. Air Force at Wright Patterson AFB in Dayton, Ohio. The preliminary acceptance tests were run in November of 1975 and authorization to ship the DMCD was received. In preparation for the final acceptance tests it was discovered that the bulk of the Air Force SLAR data was grossly out of specification with regards to the test data provided in the program and with regards to the data requirements of UPD-4 SLAR. Consequently Amendment 6 to the contract specified an alternate test data preparation procedure. Problems were also incurred in procuring replacement parts for the ARRES 1280 scanner. Final acceptance tests were completed in September of 1976. However, the interface to the SAPPHIRE equipments was not available and was covered under a separate acceptance test procedure (Amendment 8). Between final acceptance of the DMCD and December of 1977, the program effort concentrated on system modifications to support SAPPHIRE and the installation of a display capability (under separate contract). The completion of the DMCD integration with SAPPHIRE equipments occurred in December of 1977.

The equipment built for the DMCD has already demonstrated its extensive flexibility during the construction phase of the software. The project equipments were originally configured to process film data.

Additional tasks to support digital input data, new interactive display systems and new hard copy output channels as required by the Air Force are examples of the growth potential and system flexibility. Other studies in progress are proposing much greater modification to the system algorithms, requiring hardware reconfiguration. These modifications are very cost-effective.

The system reliability has been outstanding except for two chronic problems. The power supplies for the modules and the memory chips both have relatively high failure rates even though the system as a whole easily meets the requirements. The failure rate on the FP module is too low to obtain reliable statistics as of yet. Typically there has been one failure per 5×10^4 hours for the FPs. The FP power supplies on the other hand are experiencing six failures in the same time frame. The memory failure rate is approximately one per 4×10^9 bit hours This is a failure on the system once every 200 system hours for over 2×10^7 bits of data.

The DMCD system has met or exceeded all of the contract requirements for performance of SLAR data matching, change detection and false alarm suppression. The final acceptance test procedures were executed successfully to demonstrate this capability. Since the integration of SAPPHIRE to the DMCD certain variances in the SAPPHIRE data with respect to UPD-4 film data have come to light and are outside the original software design requirements for the DMCD. These variances from UPD-4 data are, however, amenable to processing with the further modification of the DMCD. Thus the DMCD is performing its original function of Advanced Development hardware admirably well.

2.0 GENERAL CHANGE DETECTION PRINCIPLES

2.1 OVERVIEW

The actual process of change detection must separate change events between two side-looking-airborne-radar (SLAR) images. This requires that the changes in one image be significantly different from the background in the other image. The image from a previous reconnaissance pass is known as the reference image, and the image from the current pass is known as the mission image.

Changes between the mission and reference images are determined by an element-by-element subtraction of the registered images. From this difference image individual change events are extracted by thresholding and feature oriented processing. The feature oriented processing greatly reduces the false change events reported by the system. The feature processor suppresses scintillation noise, and shadow-induced changes. In addition, the retained events are classified by size and on which image they appear. The feature processor will report its results in two distinct forms: 1) tag the image indicating the individual pixels comprising the changes or 2) issue a coordinate value for the event. This latter option lends itself to pass-to-pass correlation of change events and presentation of change events on the display by symbol graphics.

The system is fully operable off-line using magnetic tape input sources in place of data from the radar processor. The system, therefore, may be utilized for training and analysis exercises simulating on-line conditions without the radar processor being used.

Lastly, the system is designed for high availability. The system's off-line capability permits checkout of the full processor using the change detection software. In addition, diagnostic routines may be run to detect and isolate failures.

With two images available to the processor array, the change detector performs the change detection (Steps are listed in Figure 2-1). The first step is to coarsely align the images. This step uses aircraft navigation data or assumes registration within a fixed tolerance. The coarse alignment provides the initial registration estimate for a correlation-coefficient-based geometric registration process. This metric is used to compute the resampling of the mission image within the synthetic scan buffer thereby warping the mission to conform to the reference image.

This geometric registration is followed by photometric correction of the images, and the direct picture cell (pixel) by picture cell differencing and thresholding of the images. The resultant three-level image (no difference, strong return mission, strong return reference) is supplied to the Feature Analysis routines where the shadow and noise-induced changes are suppressed.

The output data of the system includes the following: 1) the processed mission image now in the reference image coordinates, 2) the valid change event coordinates and 3) the mission or reference radar image with the change events superimposed.

The balance of Section 2 describes in greater detail the processes used in the Digital Modular Change Detection system to perform radar change detection.

2.2 AUTOMATIC ACQUISITION

2.2.1 General Description

After the two SLAR images have been converted to digital format, an automatic procedure to insure the proper initial registration of the change detection process is begun. The testing and simulation studies for this algorithm were done on UPD-4 SLAR imagery. The initial misalignment between reference and mission was to be ± 1 nautical mile but was later changed to ± 5 nautical miles, necessitating data reduction by blurring.

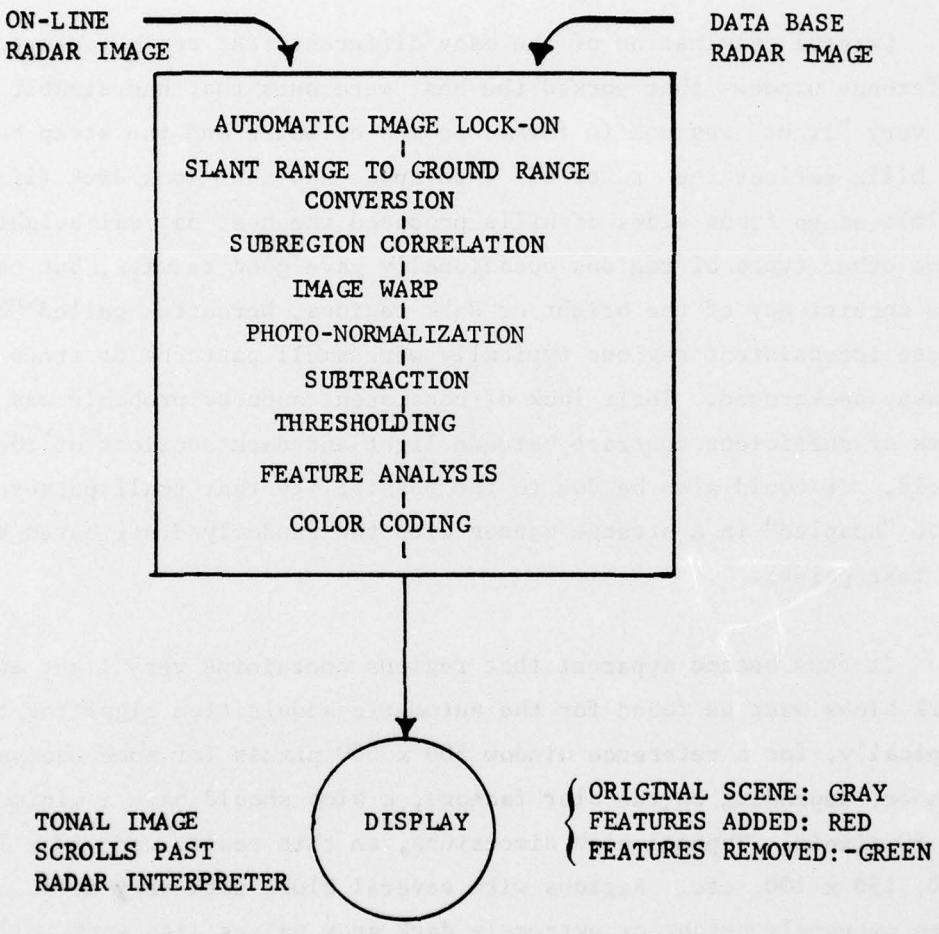

Figure 2-1. Functions Performed by Modular Change Detection System

A general class of topographical features that meets conditions sufficient for the successful operation of the search algorithm and an algorithm for finding regions containing these features, is the first step of automatic acquisition.

Careful examination of the many different test regions showed that the reference windows that worked the best were ones that had sizable very "dark" or very "light" regions in them. Bodies of water and the steep back sides of hills reflect the radar off into space and thus look dark (light on the film); steep front sides of hills produced the best natural bright returns. Some other types of regions occasionally gave good results, but not with the consistency of the bright or dark regions, hereafter called "blobs." These inconsistent regions typically were small patterns of trees on a flat grassy background. Their lack of consistent success probably was due to lack of sufficient contrast between light and dark sections of the test field. It could also be due to the possibility that small patterns may have "coupled" in a strange manner with the randomly distributed sequence of test points.

It thus became apparent that regions containing very light and/or dark blobs must be found for the automatic acquisition algorithm to work. Typically, for a reference window 500 x 500 pixels (or some equivalent number, depending on the blur factor), a blob should have a minimum dimension of 50 pixels. Typical blob dimensions, on this scale, were 50 x 100, 75 x 240, 150 x 100, etc. Regions with several blobs work very well. Blobs with extremely bright or extremely dark gray values also work well because, as one moves away from registration, the contributions to the error function become larger for each test point.

The problem of finding blobs for this type of SLAR imagery, it turns out, is best solved in a two-step process: 1) define quantitatively what is meant by a "very dark" or "very bright" region; 2) search for significant areas with these quantitative gray values. These steps will be

discussed separately.

2.2.2 Quantification of Subjective Gray Scale Interpretation

A typical gray level distribution curve for SLAR imagery looks like the one shown in Figure 2-2; a nonsymmetric, roughly bell-shaped curve with mean of 140 or so, and standard deviation of 24 to 32. Cummulative distribution curves, or percentile curves, look roughly like the one in Figure 2-3. Very bright and very dark regions are found in the extreme ends of the distribution function, Figure 2-4. Variation in the mean and higher moments of the distribution curves from one piece of imagery to the next, means fixing a density value associated with very dark (d_1, Figure 2-4) or very light (d_2, Figure 2-4), is not possible. Some inherent property of the distribution function must be used.

The simplest scheme that appeared to be adequately insensitive to variations in radar returns was to set some fixed percentile as the cutoff values for light and dark; thus, if d_1, the highest "dark" value is set at 4%, then all points tested and found to be in the lower 4% of the observed range of densities count as a "dark" point. The final values were decided upon after studying the distributions of individual regions and examining actual imagery of the relevant region. After studying several regions, a table of cutoffs was created and the final single cutoffs to be used on all regions were determined. Actual values used will be presented later.

The actual blob-finding algorithm uses four discrete subjective levels of brightness: extremely dark (XD), very dark (VD), very light (VL), and extremely light (XL) (See Figure 2-5). This four-level scheme was used because it allowed more variation in the original testing. Typical data is presented to establish gray level cutoff. Table 2-1 has the values of d_1, d_2, d_3 and d_4 as shown in Figure 2-5 for six different regions, and the final values used for the fixed percentile scheme.

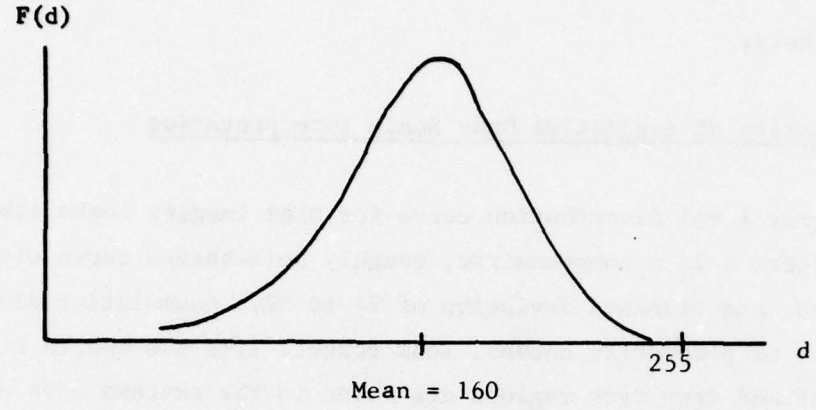

Figure 2-2. Typical SLAR Distribution*

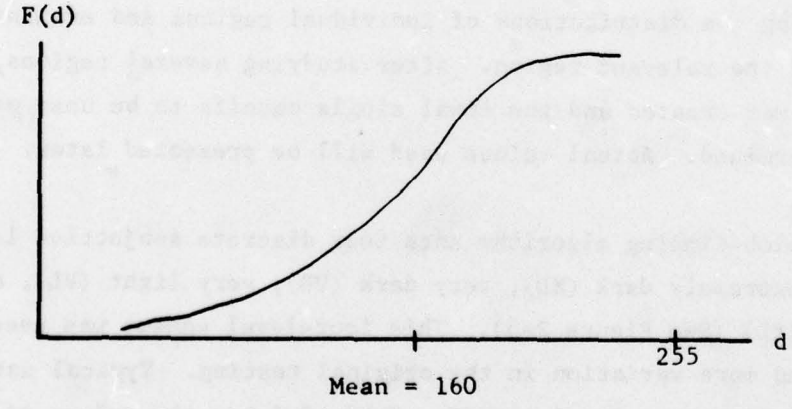

Figure 2-3. Typical Cumulative Distribution *

* d = density

F(d) = number of pixels with density, d

D3964

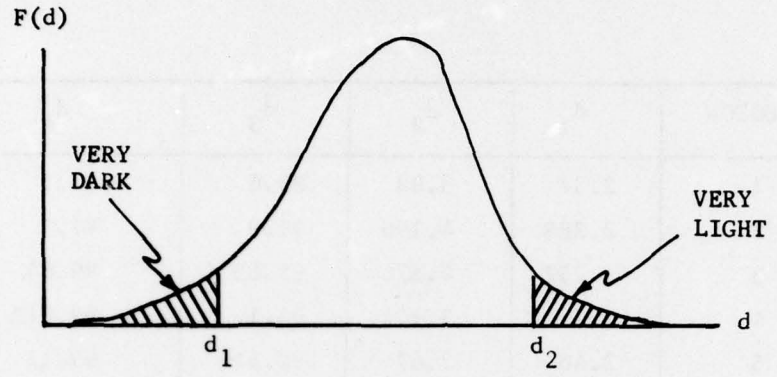

Figure 2-4. Subjective Gray Level Interpretation

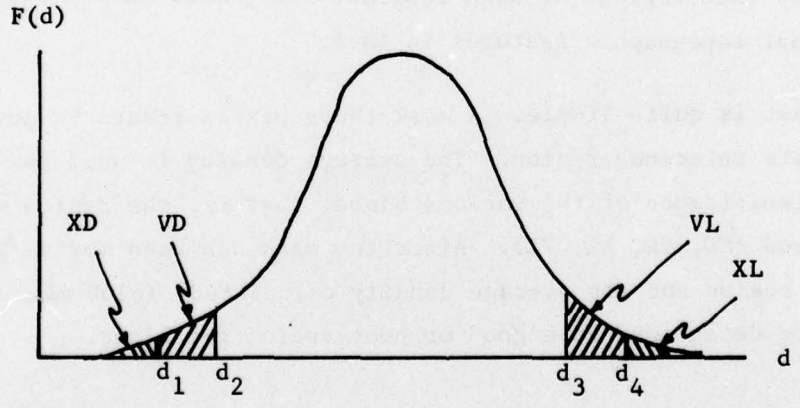

Figure 2-5. Four-Level Division of Distribution

D3965

TABLE 2-1. FIXED PERCENTILE GRAY LEVEL INTERPRETATION

REGION	d_1	d_2	d_3	d_4
1	2.37	3.99	89.6	97.5
2	2.288	4.196	91.9	97.3
3	1.752	4.576	97.65	99.64
4	1.7	3.944	94.1	99.912
5	2.46	7.67	92.5	99.11
6	1.151	6.20	95.4	99.43
FINAL	2.3	4.5	95.	99.

2.2.3 Blob and Contrast Tests

Having set the gray level cutoffs, there are two remaining tasks, the blob test and the contrast test. The contrast test does not require these gray levels, and is actually easily performed at the time the cummulative distribution function is determined. The standard deviation in the density of all the points tested is calculated; this is a rough measure of contrast. The assumption is that regions of high contrast will, more likely than not, have some relevant topographic features in them.

The blob test is quite simple. A mask three pixels square is moved over any candidate reference region. The average density is used to determine the significance of the various blobs; that is, the region within which it was found (XD, VD, XL, VL). After the mask has been moved over the entire region and its average density calculated (blob measure), the region can be determined as a good or poor region for blobs.

Having calculated the blob measure for all candidate reference windows, nine of the top blob regions are retained. The working reference window is chosen from these blob regions by picking the one with the highest standard deviation; the search procedure then begins.

2.2.4 Search Algorithm

The basic search algorithm is one described by Barnea and Silverman.[1] The two images, the reference window and the mission search area are defined as shown in Figure 2-6. The object is to search the entire mission search area and find the test region (i*, j*)- i.e. the region whose lower left-hand corner is (i*, j*) which, according to the chosen measure, is most similar to the reference window. Corresponding points in the test region S and the reference window R are called a "windowing pair." Thus P_1 and P_2 in Figure 2-6 are a windowing pixel pair.

After some initial testing, it was decided to use the constant threshold algorithm. In this scheme, for any chosen test region S, windowing pixel pairs are selected in a random fashion over the test region S. At each step, the error function $\epsilon(i,j,\vec{P})$ is calculated:

$$\epsilon(i,j,\vec{P}) = \left| S_{i,j}(\vec{P}) - R(\vec{P}) \right|$$

where $\vec{P} = (P_x, P_y)$ is the vector displacement from the test region origin (i,j) (or reference window) to the point in question. These tests are continued until the cumulative error function $E = \sum_k \epsilon(i,j,\vec{P}_k)$ exceeds some fixed value, T, called the threshold. For any given test region $S_{i,j}$, the number of tests taken before the cumulative error, E, exceeds T is saved in the array I(i,j). Moving the test region, S, around the search area in some orderly fashion, and testing $S_{i,j}$ at the chosen points (typically a rectangular grid) will produce a maximum* of I(i,j). The

*This is reasonable. For regions S and R of high similarity, each test will produce only a small contribution to the cumulative error function, thus many tests (i.e. larger value of I(i,j)) will be necessary before T is exceeded.

1. D. I. Barnea and H. F. Silvermann, "A Class of Algorithms for Fast Digital Image Registration," IEE Transactions on Computers, Vol C-21, No. 2, pp 179-186, Feb. 1972.

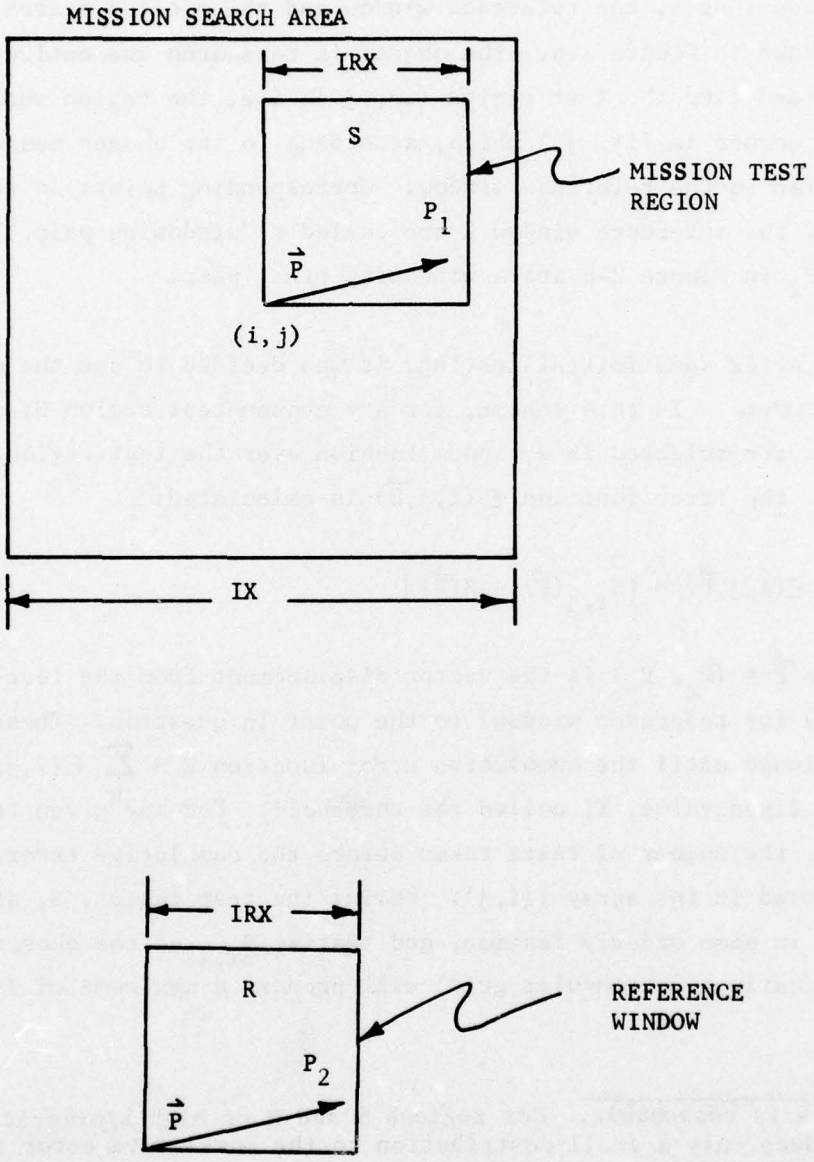

Figure 2-6. Test Regions

maximum of I(i,j) defines the point (i*,j*) and is considered the point of maximum similarity; or of best registration.

Figure 2-7 illustrates the process of cumulative error accumulation for two sets of regions - one close to registration, the other so far from registration as to be essentially noncorrelated. While the threshold was kept constant for all subregion tests over a given search area, the threshold did vary from one type of data to the next. The threshold was a linear function of the variance of the data; this was necessary to prevent extremely large numbers of tests (and hence long times) before crossing the threshold.

The first step of the search algorithm is described in Figure 2-8. Since there was so much data to be searched, it was decided to use a two-step process; first test the mission subregions separated from one another by some step size (N=4 pixels was finally used). Then, after searching through the entire mission search area, pick the 10 (or so) regions with the highest correlation values and do an exhaustive search around each of these; the test site among these with the highest value of correlation is considered the match point.

Since blurred pixels are being used, a quadratic interpolation is then performed. It should also be mentioned that a photonormalization between reference and mission image is done in the comparison process.

2.3 SLAR IMAGE REGISTRATION

Automatic techniques for registration utilize a systematic traversal of the reference image using a predetermined point-sampling pattern, and a search process to locate matching, conjugate points on the mission image. The match points found are used to construct the warp equations which transform the mission image such that it is in registration with the reference image. This procedure is initiated by selecting a few initial points by separate procedures and providing their coordinates to the main process.

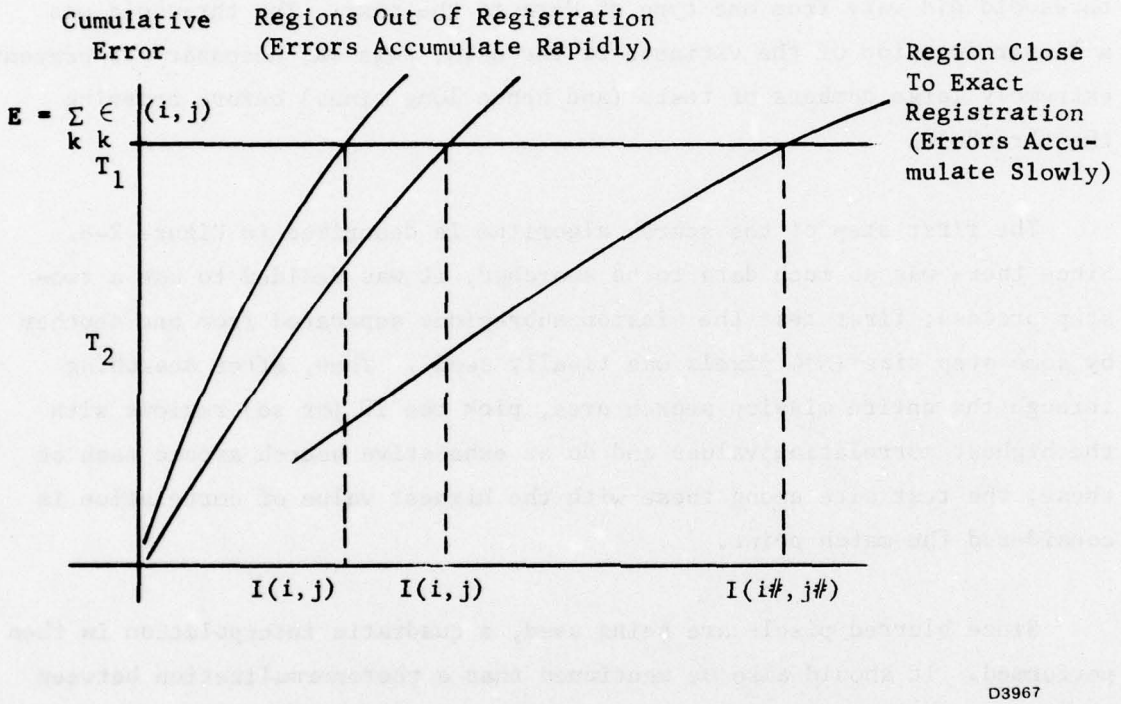

Figure 2-7. Expected Nature of the Cumulative Error Function

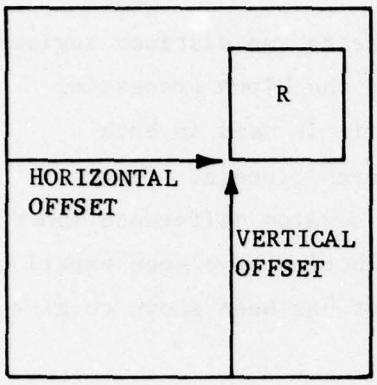

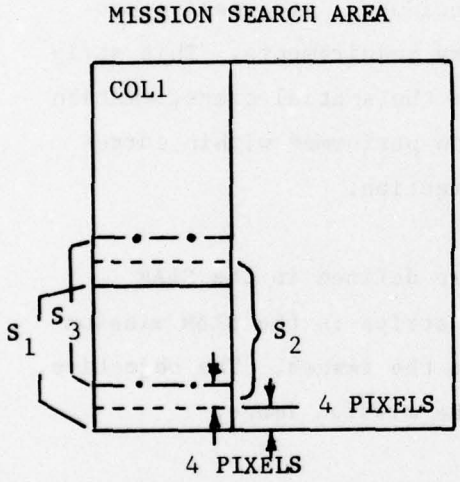

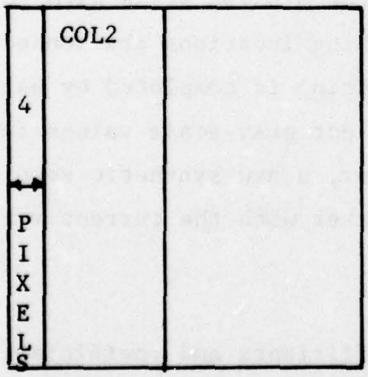

1) Pick reference window region and condense the data.

2) Condense and store data from COL1.

3) Test region S_i against R. Record I(i,j). Step up 4 pixels to S_2.
Test region S_2 against R. Record I(i,j + 4). Step up 4 more pixels to S_3.
Test region S_3 against R. Record I(i,j + 4)

.
.
etc.
.
.

Until COL1 is completed.

4) Step 4 pixels to the right. Condense and store new data (that part of COL2 not in COL1).
Test COL2 as did COL1 (see 3 above).

.
.
etc.
.
.

Repeat 4) until finished with whole mission search area.

Figure 2-8. The Coarse Search Algorithm D3968

Different methods of image traversal give rise to two distinct registration approaches; the strip processing approach and the block processing approach. However, a correlation coefficient metric is used in both approaches as the matching metric in the point-search process. Other matching metrics such as the difference function, squared difference function, inner product function, and cosine of the angle function have been experimented with at CDC, but the correlation coefficient has been shown to give the most satisfactory results.

To register SLAR strip imagery, the continuous strip processing approach is applicable. The technique allows continuous, progressive processing of image data with minimum time and memory requirements. This strip approach utilizes recursive computation to update the spatial transformation for each scan line on the basis of the correlation performed within correlation paths or strips running in the process direction.

Two to twelve strips, each N pixels wide, are defined in the SLAR reference image (Figure 2-9). The corresponding strips in the SLAR mission image are distorted by some existing warp between the images. The objective, then, is to find the location of the strips in the mission image.

Matching conjugate locations in the reference and mission strips are identified by evaluating tentative positions in the mission strip with the correlation coefficient (Figure 2-10). The matching locations are connected by straight lines between strips i and i+1. Bridging is completed by using a nearest-neighbor interpolation criterion to select gray-scale values for pixels along these bridging lines. In this manner, a new synthetic scan line is generated from the mission image to register with the current reference image scan line.

Statistical moments for the correlation coefficients and coefficients for the spatial warp transformations are computed "on the run." That is, as the strips progress acr s the image, new data recursively updates the computations while old data exponentially decays.

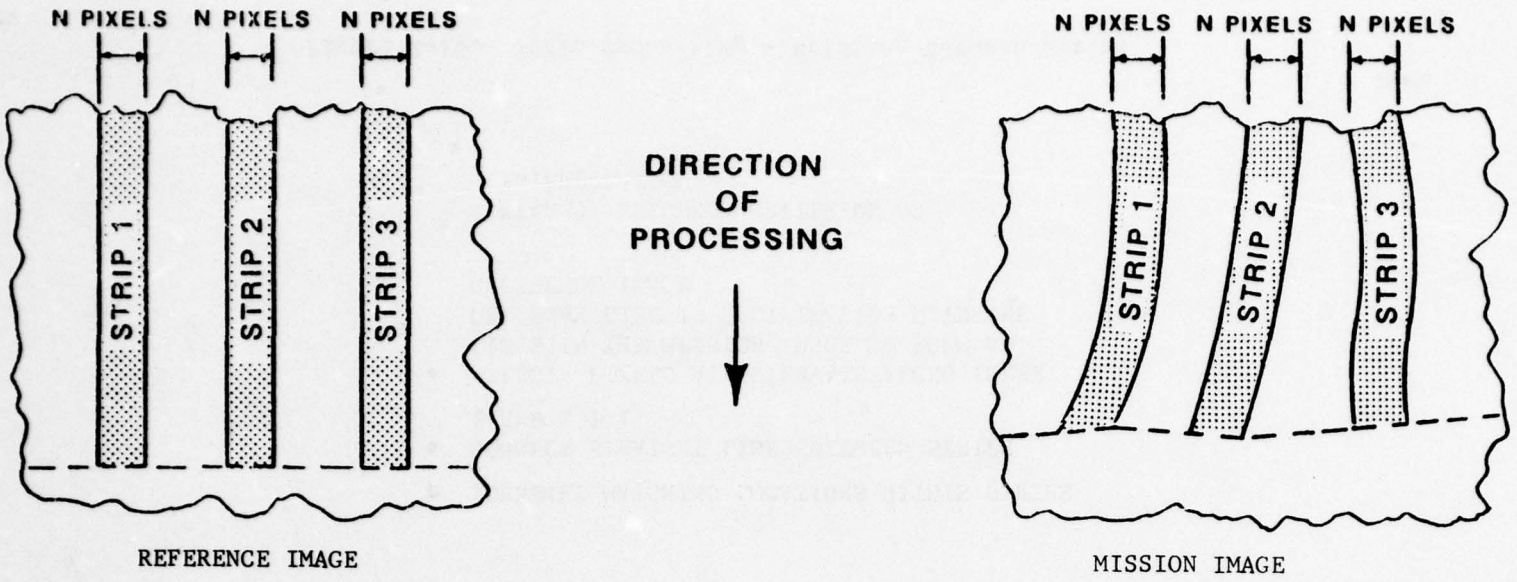

- A NUMBER OF "STRIPS" IN THE REFERENCE IMAGE ARE DEFINED
- THE CORRESPONDING DISTORTED STRIPS IN THE MISSION IMAGE ARE LOCATED
- THE CRITERION FOR MATCHING CONJUGATE POSITIONS IN THE MISSION AND REFERENCE STRIPS IS THE CORRELATION COEFFICIENT

Figure 2-9. Strip Processing - The Concept

D3969

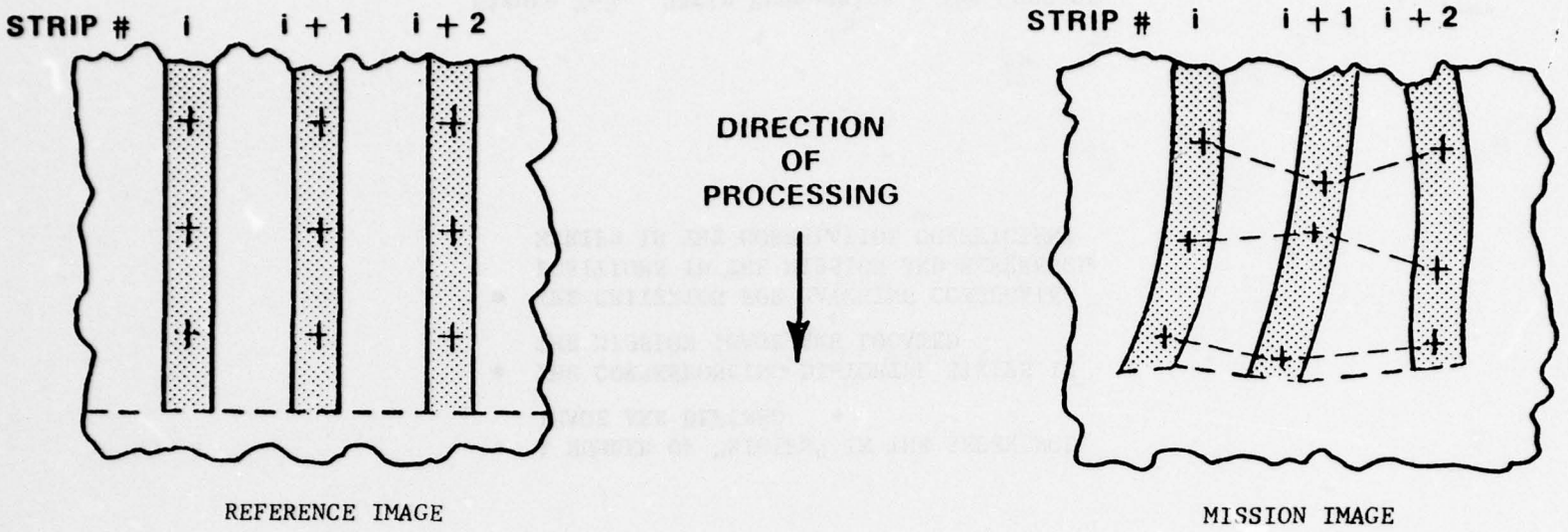

- IDENTIFY MATCHING LOCATIONS WITHIN STRIPS
- CONNECT STRAIGHT LINES BETWEEN STRIPS i AND i + 1
- SELECT* PIXELS AT INTERVALS ALONG THESE LINES IN THE MISSION IMAGE TO FORM A NEW SCAN LINE IN REGISTRATION WITH THE REFERENCE IMAGE

* NEAREST NEIGHBOR CRITERION OR INTERPOLATION

D3970

Figure 2-10. Strip Processing - Bridging Between Strips

Synthetic scan line generation is accomplished through the concept of a numerical scanner (Figure 2-11). The current reference or independent scan line (K pixels) is stored until the synthetic mission image scan line has been computed. The latter is obtained from a random access memory (M by K pixels) where data for M mission image scan lines is stored. This mission image "window" is maintained so that the synthetic scan lines are at the leading edge. The numerical scanner memory is updated with each scan image, while the oldest line is dropped. The image is also centered in the range direction by "sliding" the mission input window within the mission line buffer memory.

2.4 PHOTONORMALIZATION

Once the synthetic mission scan line has been generated, its gray-scale values are adjusted statistically to match the reference image as closely as possible in average value and contrast. This process, which is known as photonormalization, applies a linear regression line to fit the joint distribution of reference and mission gray-scale values within each correlation strip (Figure 2-12). The adjusted gray-scale values for the synthetic scan lines are obtained by statistical manipulation of the regression line. Photonormalization is critical in change detection because it ensures the generation of a low-noise subtraction image with a minimum of false change events.

The calculation is:

$$A_N = A \cdot C + D$$

where A_N = Normalized Mission Pixel

A = Mission Pixel

C = Contrast Correction Factor

D = Density Correction Factor

The correction factors, C and D, are modified continuously so that each mission pixel is adjusted to match the corresponding reference pixel. The

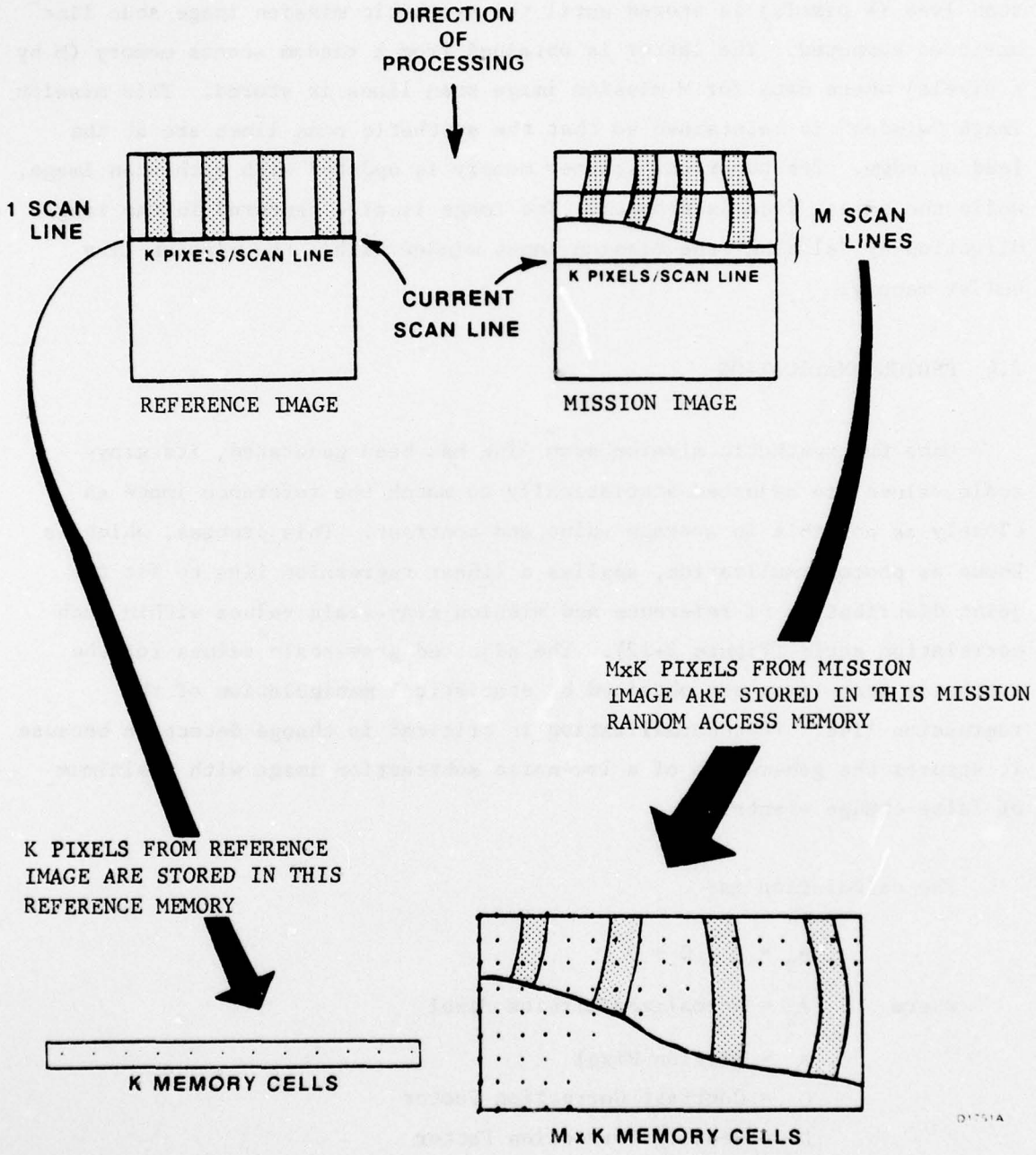

Figure 2-11. Numerical Scanner Concept

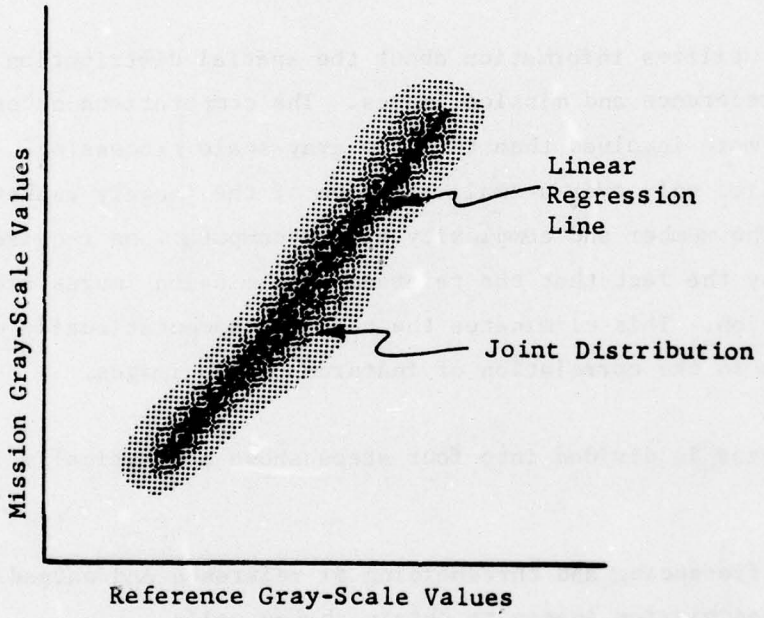

Figure 2-12. Linear Regression Line for Photonormalization

calculations for these correction factors are done using the statistics determined during the registration process.

2.5 FEATURE ORIENTED PROCESSING

Feature oriented processing significantly enhances the change detection process by:

1) Identification and suppression of false alarms
2) Verification of change features in noisy environments

The process utilizes information about the spatial distribution of features on the reference and mission images. The computations necessary are considerably more involved than those in gray-scale processing. However, they need be applied only over a small fraction of the imagery rather than at each point. The number and complexity of the computations required is further reduced by the fact that the reference and mission images are in precise registration. This eliminates the need for computationally costly search procedures in the correlation of features on two images.

The FOP process is divided into four steps shown schematically in Figure 2-13.

1) Image differencing and thresholding of reference and warped/normalized mission images to obtain change cells
2) Change cell linkage to link cells into change event features
3) Image classification tests to judge whether a feature is a legitimate change, false alarm, or shadow-induced change
4) Modify event cues to suppress false alarms from output image.

Associated with the FOP process is a circular buffer (FOP MEMORY). The FOP Memory holds the selected background image and change cues. This memory serves as a delay between the input and the display output. During this delay, the change features are classified. Each word in the FOP Memory contains two 6-bit pixels and a 4-bit tag field. The tag field indicates

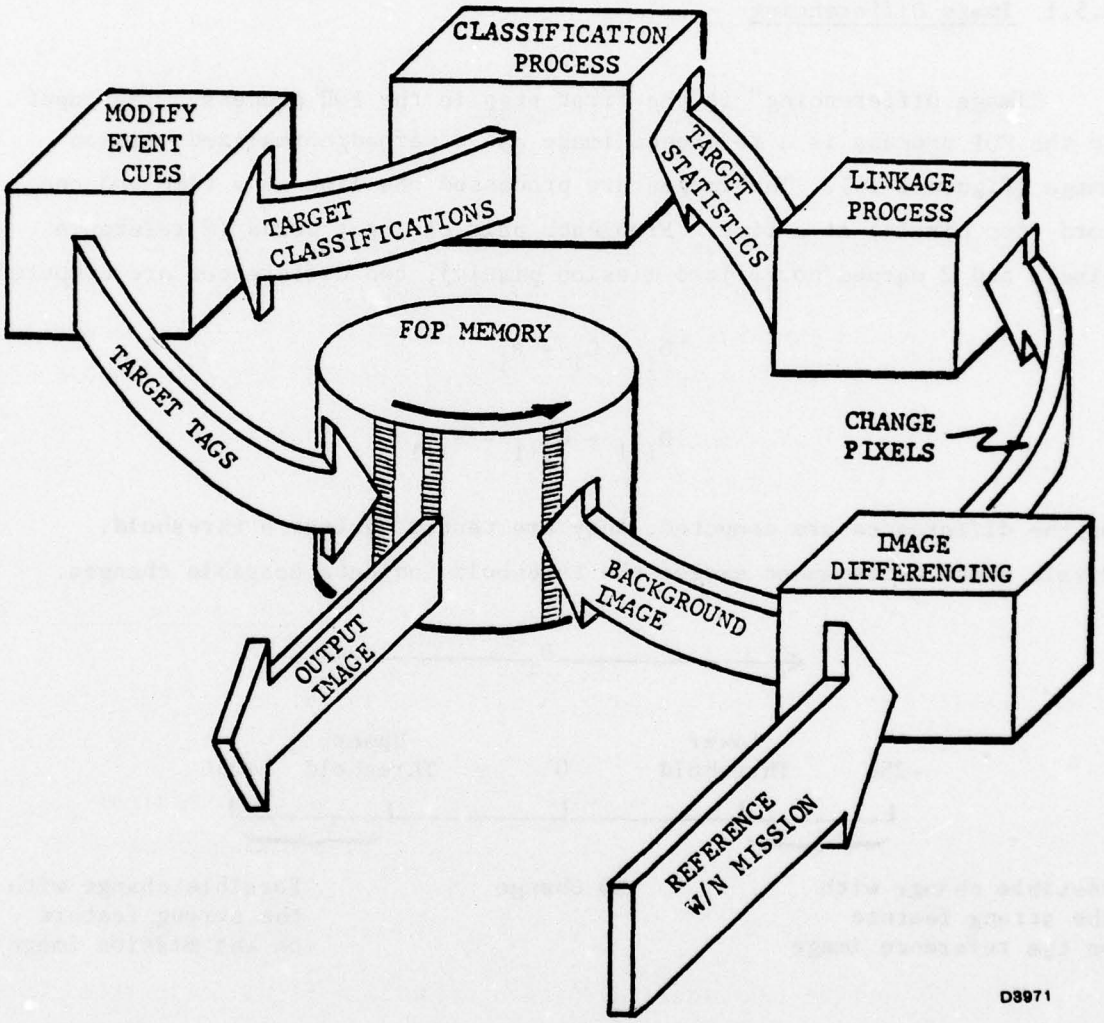

Figure 2-13. Feature Oriented Processing Data Flow

the class of each change feature (see Table 2-2). Either the reference, warp/normalized mission, or difference image may be selected as the background image. The FOP Memory contains 32K words which allows 12.8 lines of delay for a line containing 5120 elements.

2.5.1 Image Differencing

"Image Differencing" is the first step in the FOP process. The input to the FOP process is a reference image and a warped/normalized mission image (Figure 2-14). The images are processed one line at a time and one word (two pixels) at a time. From each pair of input words (2 reference pixels and 2 warped/normalized mission pixels), two differences are computed:

$$D_i = C_i - R_i$$

$$D_{i+1} = C_{i+1} - R_{i+1}$$

As the differences are computed, they are tested against a threshold. Pixels whose differences exceed the threshold indicate possible changes.

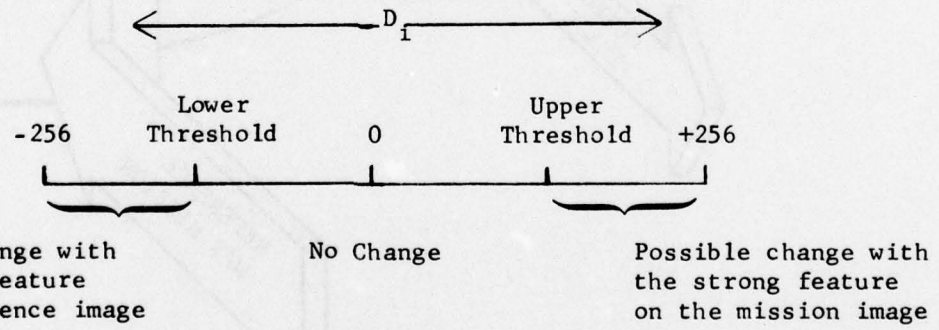

If the thresholding indicates a possible change, the reference word, mission word, and y coordinate (position in the current scan line) are sent to the "Linkage" process. The tag field in the FOP memory is set to indicate a possible change.

TABLE 2-2. CLASSES OF CHANGE EVENTS

Value of T_n	Class of Change
0	No change
1	Not used
2	Possible change added
3	Possible change subtracted
4	Legitimate change added
5	Legitimate change subtracted
6	Weak change added
7	Weak change subtracted
8	Scintillation-induced false alarm added
9	Scintillation-induced false alarm subtracted
10	Shadow-induced false alarm added
11	Shadow-induced false alarm subtracted
12-15	Not used

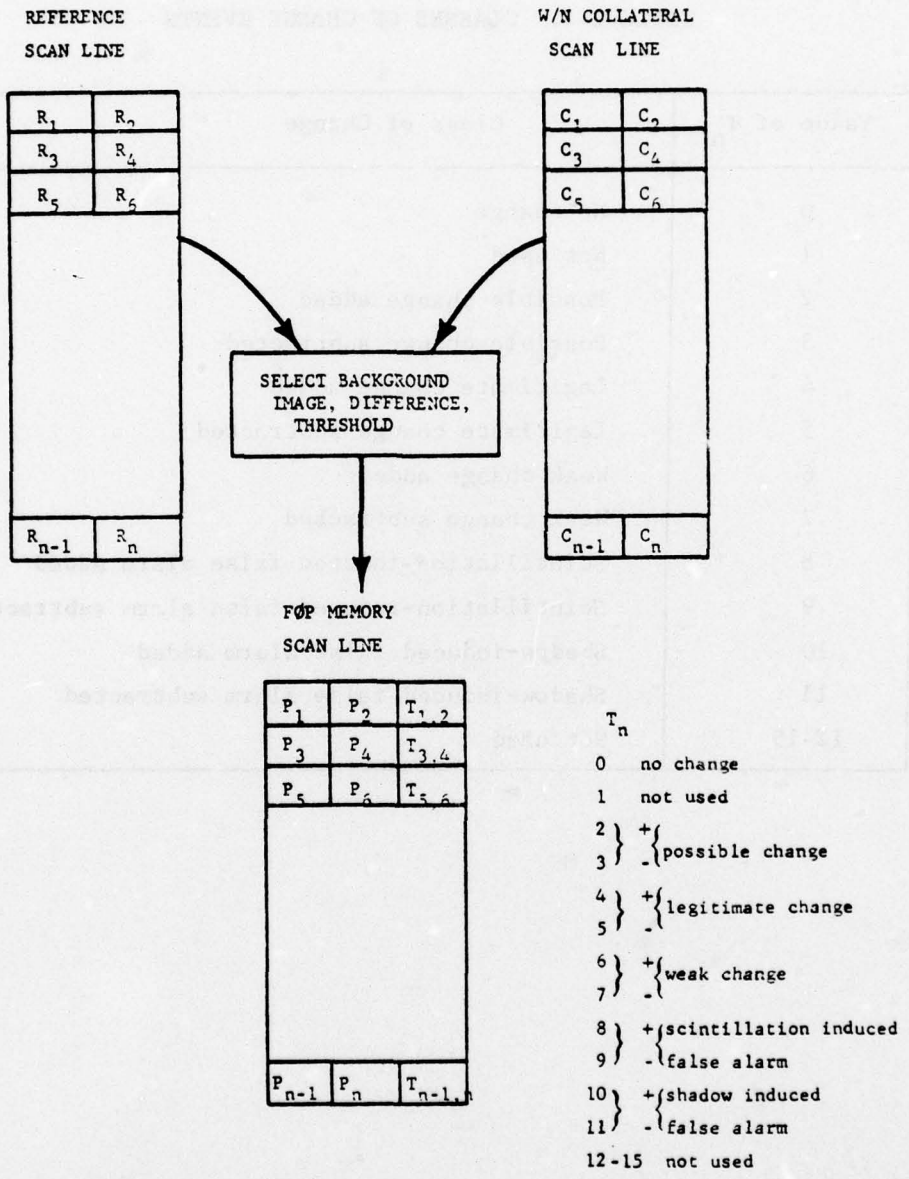

Figure 2-14. Image Differencing

Linkage Process

The "Linkage" process groups change cells into change event features (See Figure 2-15). The process requires three steps:

1) Link change cells on the current scan line into change events
2) Link change events on the current scan line to change event features on the previous scan line
3) Accumulate statistics of change features and send statistics to "Classification Process"

During the "Linkage" process, the change event features are kept in linked lists ordered by polarity of change and image coordinate. The linked lists greatly reduce the search time. Change event features are removed from the lists and sent to the "classification" process when:

1) No change events from the current scan line were linked to it, or
2) The number of scan lines in the change feature equal 12.8 (the amount of delay in the FOP memory)

Classification Process

Completed change features must go through a classification procedure to determine whether the feature is:

1) Legitimate change
2) Weak target
3) Shadow-induced change
4) False alarm

The classification logic is linear, nonprobabilistic and assumes non-overlapping classes. Seven tests are performed:

1) Correlation coefficient
2) Weak target
3) Shadow
4) Background feature

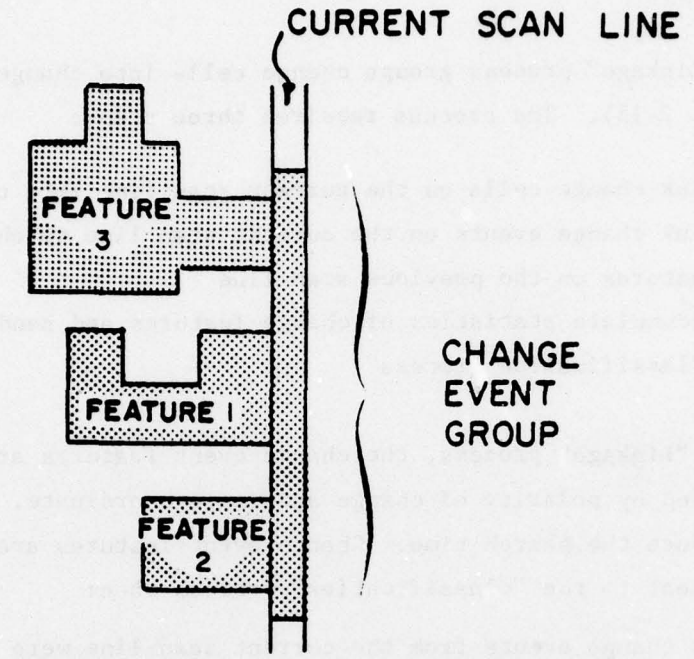

(a) LINKAGE OF THE FIRST TYPE

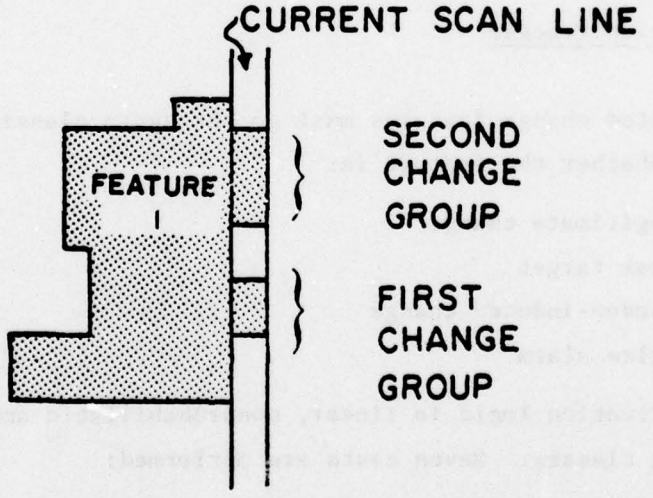

(b) LINKAGE OF THE SECOND TYPE

D2226A

D3973

Figure 2-15. Feature Oriented Processing Change Event Linkage

5) Regression line

6) Maximum correlation

7) Standard deviation perpendicular to regression line

Modify Tag Process

The Modify Tag process receives a feature descriptors package for each change feature. Included in this package are feature classification and image coordinates. The Modify process calculates the address of the feature in the FOP MEMORY. The pixel tags in the FOP Memory are then modified to indicate the correct classification, Table 2-2. The data flow for the change detection process is shown in Figure 2-16.

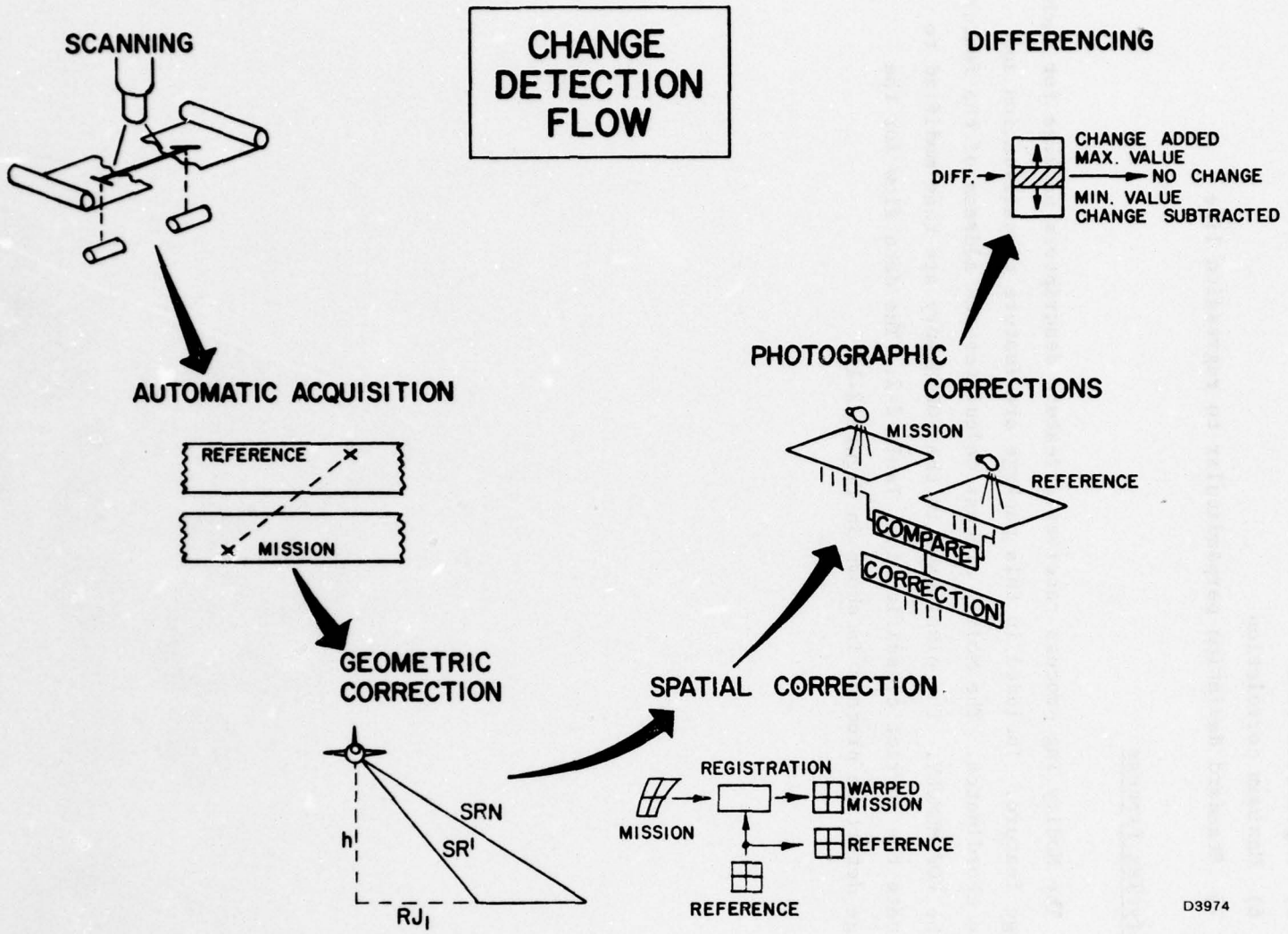

Figure 2-16. Change Detection Flow

3.0 SYSTEM DESCRIPTION

3.1 OVERALL SYSTEM CONFIGURATION AND CONTROL

The previously-described functions were implemented by utilizing a modular microprogrammable processor, the Flexible Processor. The processor is constructed with a common backpanel for every processor; then from 27 board types, a processor is configured by insertion of the proper board modules for the specific function it is to perform. The Digital Modular Change Detection System (DMCD) has 40 Flexible Processors connected in serial and parallel pipelines to perform the change detection job. A block diagram of the Modular Change Detection System is shown in Figure 3-1. The system consists of two image input sections, reference and mission; four processing sections, each computing on one fourth of the data stream; an output section; and a supervisory computer section.

The DMCD was designed to provide maximum functional and construction modularity and flexibility. The operational capabilities of the DMCD are summarized in Table 3-1.

The DMCD performs on-line processing at all RF-4 collection rates. The system is tolerant of flight path variations including ground track heading variations of up to $\pm$2.0 degrees. In addition, large variations in common coverage with the stored reference image are allowed. This flexibility greatly reduces the data collection restrictions which might be imposed to perform this process. This ability is achieved through well proven registration algorithms.

The system is configured to perform on-line with SLAR imagery collected in real time with the characteristics shown in Table 3-2.

The overall block diagram of the system (Figure 3-1) shows the peripheral and external interfaces to the processor array. All primary interfaces are made through the Data Channel Controllers and their

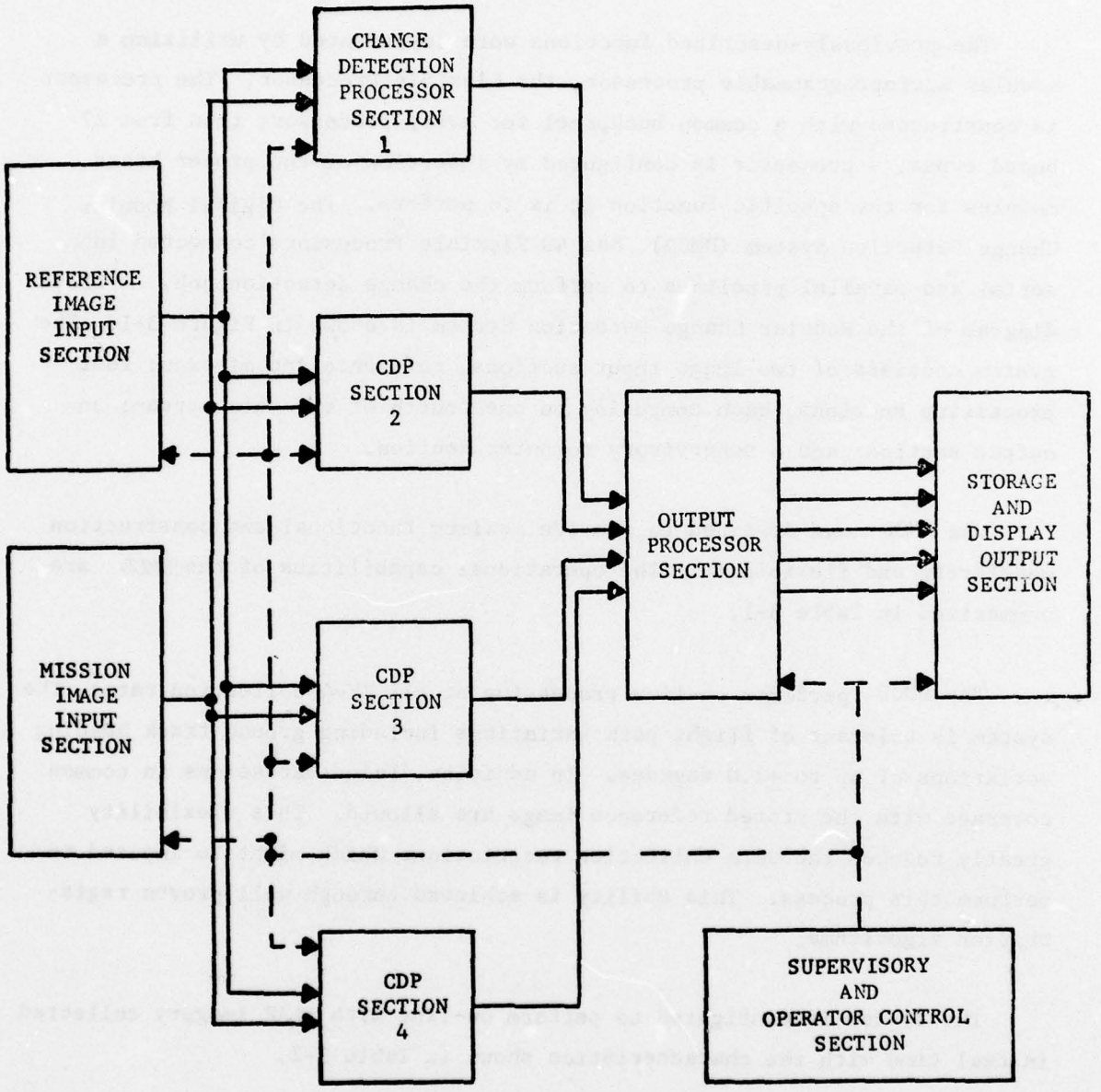

Figure 3-1. Modular Change Detection System Block Diagram

TABLE 3-1. DMCD OPERATIONAL CAPABILITIES SUMMARY

On-Line Performance

- RF-4 Collection Rates
- Tolerant to Heading and Ground Track Variations

Change Event Feature Processing

- Noise Suppression
- Shadow-Induced Change Suppression
- Event Classification: Strong, Weak, Added, Deleted

Restitution

- Overlay Events on Reference or Mission Imagery

System Availability

- Extended Diagnostics
- Full Off-Line Operational Ability

TABLE 3-2. SLAR IMAGERY CHARACTERISTICS

FORMAT:	8 Bits Per Picture Element (Pixel)
	5120-Pixel Image Width
COLLECTION RATE:	150 Lines Per Second Maximum
FLIGHT PATH:	±2.0 Degrees Heading Deviation
Repeatability	25 Percent Minimum Initial Common Coverage if Navigation Data Available (75 Percent if Not Available)
	25 Percent Minimum Common Coverage (Post Acquisition)
Pass Length	No Limitation

associated buffer memories within the array. Data is then accessed from the buffer by the processor array.

A Data Channel Controller consists of an interface from the control processor, over which commands are issued, and one peripheral controller for each data interface in the system.

The functions of automatic initial registration, change detection, and off-line processing functions of display and data formatting are each implemented by a set of programs or modules. A module is a collection of routines for the SC 1700 and the Flexible Processor, stored in the MSOS system. The programs are written in assembly language. Some of the general system characteristics are shown in Table 3-3.

The DMCD required an operating system that would control the change detection algorithm, provide debugging aids, and provide diagnostic capability. To provide these features, the Check Out Resident or COR operating system was developed. It is a stand-alone system written in assembly language and requiring application routines to be in assembly language. The system is maintained and built using the assembler and loader available on the standard CDC Mass Storage Operating System (MSOS) for 1700 systems.

The operating system's general requirements are shown below:

- System Initialization
- Operator Interface Structure
- Interrupt Processing Structure
- Overlay Structure
- Flexible Processor Control Structure
- Flexible Processor Program Library

TABLE 3-3. MODULE OPERATIONAL CHARACTERISTICS

INSTRUCTIONS PER SECOND	320 (10^6)
PIXELS PER SECOND (FROM TWO IMAGES)	
Peak	1 (10^6) Each Image
Average (5120 Samples/Line)	.8 (10^6) Each Image
FILM SPEED	14.4 Inches/Minute 150 Lines/Second
RELIABILITY	
Contract Requirement	40 Hours
Predicted (MIL-STD-785A)	41 Hours
Acceptance Test Results	119 Hours
MAINTAINABILITY	
Contract Requirement	30 Minutes
Predicted (MIL-HDBK-472)	18 Minutes
Acceptance Test Results	9 Minutes

The support features that exist in COR can be classified in the following four areas:

- Internal Structure
- File System
- Operator Interface
- Support Utilities

Internal Structure

The internal structure of COR consists of a group of resident routines and a series of overlays. The standard hardware autoload structure is used to load and start executing the absolutized resident section of COR from disk. The disk also has absolutized overlays stored on it which contain the logic for processing the various commands. An ordered command table links a given command with an overlay and a location in the overlay to start execution for the command. The resident routines, command tables, and overlays are built and stored on the disk by a special program that runs under MSOS, the standard 1700 operating system. MSOS utilities are used to manipulate the programs and absolutize them from relocatable form.

The structure of the COR resident routines permits inclusion of interrupt processing routines. This structure is used to control operator I/O and application programs in the Flexible Processors. The current operator station handling has a limited multi-station capability. When entering independent commands, the system will support more than one terminal. However, if a series of dependent commands are executed, such as editing a file, then only that one terminal may be active during the series.

File System

The COR system contains a file system which manages the disk space on the system disk. The file system was designed to support the general disk storage needs of COR which are independent of the bulk image or data base

storage requirements for the change detection process. The file system contains three types of files which provide a storage structure for flexible processor microcode binary programs, command files, and editor files.

The file system uses a random allocation strategy to store a file on disk. This strategy permits a file's length to vary during its lifetime on the disk. A file can be created or removed by a command from a user terminal. A file is referenced on the system by specifying its name. A protective feature is provided by means of a password for each file. This restricts access to the files for modification or removal operations.

Operator Interface

Commands are entered into the COR system from operator terminals. The command format is a series of one to nine parameters delineated by one or more separator characters. The parameters may be one to six characters long. The legal separators are shown below:

.	;
/	blank
(	)
*	

The first parameter of the input string is assumed to be the particular command to be executed. COR uses its command table to verify the existence of the command and specify the appropriate overlay or resident location where the code to process the command is located.

The COR system has a Command File feature which greatly reduces operator entry requirements. The purpose of a command file is to permit a user to execute a series of commands by entering a single command. The commands are stored on a disk file, and COR reads the file instead of requesting input from the terminal. Command files provide three significant capabilities to the system:

- Reduces entries to system.
- Executes a series of accurate commands faster than operator entry.
- Provides a facility for constructing higher order functions from basic commands.

Command files are created and modified using the EDITOR at the user terminal. The special format procedure file is created from the EDITOR file using the COPYTF function. This ease of manipulation is an important feature since it permits users to quickly construct files and makes them useful even for short series of commands. Three other features of procedure files, namely multilevel, a list option and an optional operator input, reduce composition time, and made their operations easier.

The multilevel ability is available to three levels deep. Thus, instead of entering a string of identical commands several times in a command file, the strings can be replaced with a single command file command call. This is similar to a programming subroutine call. Since executing a series of commands rapidly can cause a user to be saturated with output messages, a list control on the output to the character display is provided. The default mode inhibits listing of both the executed command and the command's output. Alternate options list the command output or the command call on the character display.

When a user constructs a command file, a special comment option can be used. Any command file command that has stars as the first two characters is always listed on the character device. This is useful for general prompting of the operator or displaying an operator's options, when the optional operator entry feature of command files is used. The comment lines scroll upon the screen and then the command file interrupts its execution and waits for the operator's entry via the operator input feature described below.

In many cases a user can set up a command file to be everything desired except for one or two parameters. The operator input feature consists of

stopping execution of the file and waiting for an operator input character string which is inserted into the command before it is subsequently executed. This feature is triggered during the command processing stage when each command is prescanned and checked for a #, the special interrupt character. These commands are formed as normal in the EDITOR except that # characters are placed where a string of characters from the operator is to be inserted.

Support Utilities

The COR system contains the following five support utilities which provide off-line capabilities for assisting the system user:

- Debug Commands
- File Creation
- File Purge
- Copy Functions
- Editor

Debug Commands

The COR system contains several commands which aid programmers in debugging software. A basic set is included to debug the 1700 code and an extensive set is included to debug microcode. These provide the ability to logically connect a user terminal to a specified FP and then investigate the status of the FP. This would include displaying the contents of storage locations and micromemory.

File Creation

A file can be created in the file system from a user terminal using the CREATE command. This file remains in existance until the user removes it with a PURGE command. The system requires a user to specify the 1-6 character file name and file type (Microcode Binary, Command, or Editor). An optional

password of 1-6 characters can be supplied to limit access to the file. If no password is supplied, the name of the file is used as a password.

File Purge

A file may be removed from the system by a PURGE command. The user need only supply the file's name and password.

Copy Function

The COR system provides two transformation commands. COPYTE transforms command and microcode binary files into editor files. COPYTF transforms editor files into command and microcode binary files. This transformation permits the general-purpose editor to be used to manipulate the contents of the files. Users can, therefore, easily generate and manipulate command files at the terminal. Programmers can use this feature to change microcode program during development.

Editor

The COR system contains a general-purpose editor to manipulate text. The text file is divided into equal length lines and all commands reference these line numbers. All or a series of lines may be listed. A line or lines may be deleted and a new line or lines inserted. A line or lines may be inserted anywhere in the file. The editor can be used to create new command or microcode binary files, or existing files can be transformed into editor files by the COPYTE command. The COPYTF command is used after editing is completed to transform back to the proper file format.

The COR PROCESSING STRUCTURE is divided into seven priority levels (Figure 3-2)--LEVEL 0, COR IDLE LOOP and BACKGROUND COMMANDS; LEVEL 1, COR COMMANDS and COMMAND INTERPRETER; LEVEL 2, LINE START (SLIDING MISSION); LEVEL 3, LINE START PROCESS CONTROL ROUTINE; LEVEL 4, 210 CRT and TTY INTERRUPT ROUTINES; LEVEL 5, OCA INTERRUPT ROUTINE; LEVEL 6, CDP INTERRUPT

LEVEL 6

CDP INTERRUPT ROUTINE
REFERENCE PROCESS INTERRUPT ROUTINE
MISSION PROCESS INTERRUPT ROUTINE
OCB PROCESS INTERRUPT ROUTINE
TCM PROCESS INTERRUPT ROUTINE
REFERENCE DCC INTERRUPT ROUTINE
REFERENCE HSDT INTERRUPT ROUTINE
REFERENCE SCANNER INTERRUPT ROUTINE
REFERENCE OUTPUT PROCESS INTERRUPT ROUTINE
MISSION DCC INTERRUPT ROUTINE
SAPPHIRE INTERRUPT ROUTINE
MISSION HSDT INTERRUPT ROUTINE
MISSION SCANNER INTERRUPT ROUTINE
MISSION OUTPUT PROCESS INTERRUPT ROUTINE
OUTPUT DCC INTERRUPT ROUTINE

LEVEL 5

OCA INTERRUPT ROUTINE
FOPM → CCT INTERRUPT ROUTINE
FOPM → LBR INTERRUPT ROUTINE
OLBM → CCT INTERRUPT ROUTINE
TCM → CCT INTERRUPT ROUTINE
GETLIN

LEVEL 4

210 CRT INTERRUPT ROUTINE
TTY INTERRUPT ROUTINE
GETLIN

LEVEL 3

LINE START PROCESS CONTROL ROUTINE

LEVEL 2

LINE START (SLIDING MISSION)

LEVEL 1

COR COMMAND INTERPRETER
COR COMMANDS

LEVEL 0

COR IDLE LOOP
COR BACKGROUND COMMANDS
RUN REPOS
STRT SETPOS

Figure 3-2. COR Processing Structure

ROUTINES. Levels 4, 5, and 6 are hardware-generated interrupt routines and levels 1, 2, and 3 are entered from software interrupts originating at higher levels. The LOW COR words that define the state of the system are: LEVEL, contains one bit for each level available and is set when it becomes active; SAVEP (save pointer), contains the address of the save routine for the level currently executing; NEWLVL (new level), specifies new interrupts for levels 1, 2, and 3; and MASKL (mask level), is the interrupt mask word for NEWLVL to determine whether the new level can be entered or not. To clarify this structure the following example is presented:

> When a hardware interrupt occurs (levels 4, 5, or 6) during lower level processing (levels 0, 1, 2, and 3), execution terminates, registers are stored in the save area of the level that was executing (SAVEP), and execution is transferred to the interrupt routine. If the interrupt routine requires that another level be executed after its termination, then it sets the new level bit in NEWLVL. When any level exits, an exit routine will select the highest priority level between the present level (LEVEL) and the new level (NEWLVL) to determine the next level to be processed. Before that level is entered, the registers are restored from that save area...then the cycle repeats.

The Line Start program is a routine which controls all inputs to and outputs from the DMCD; in its design, it is a testing and controlling routine providing for the various legal combinations of input and output mediums. The data flow block diagram, Figure 3-3, illustrates all input and output modes available, with the processes that control them and the memories that interface these processes. All processes are dependent upon the information or lack of information available in the memories; and since the memories link the processes together, all processes are indirectly dependent upon one another. Therefore, the rate of the flow will synchronize with the slowest process.

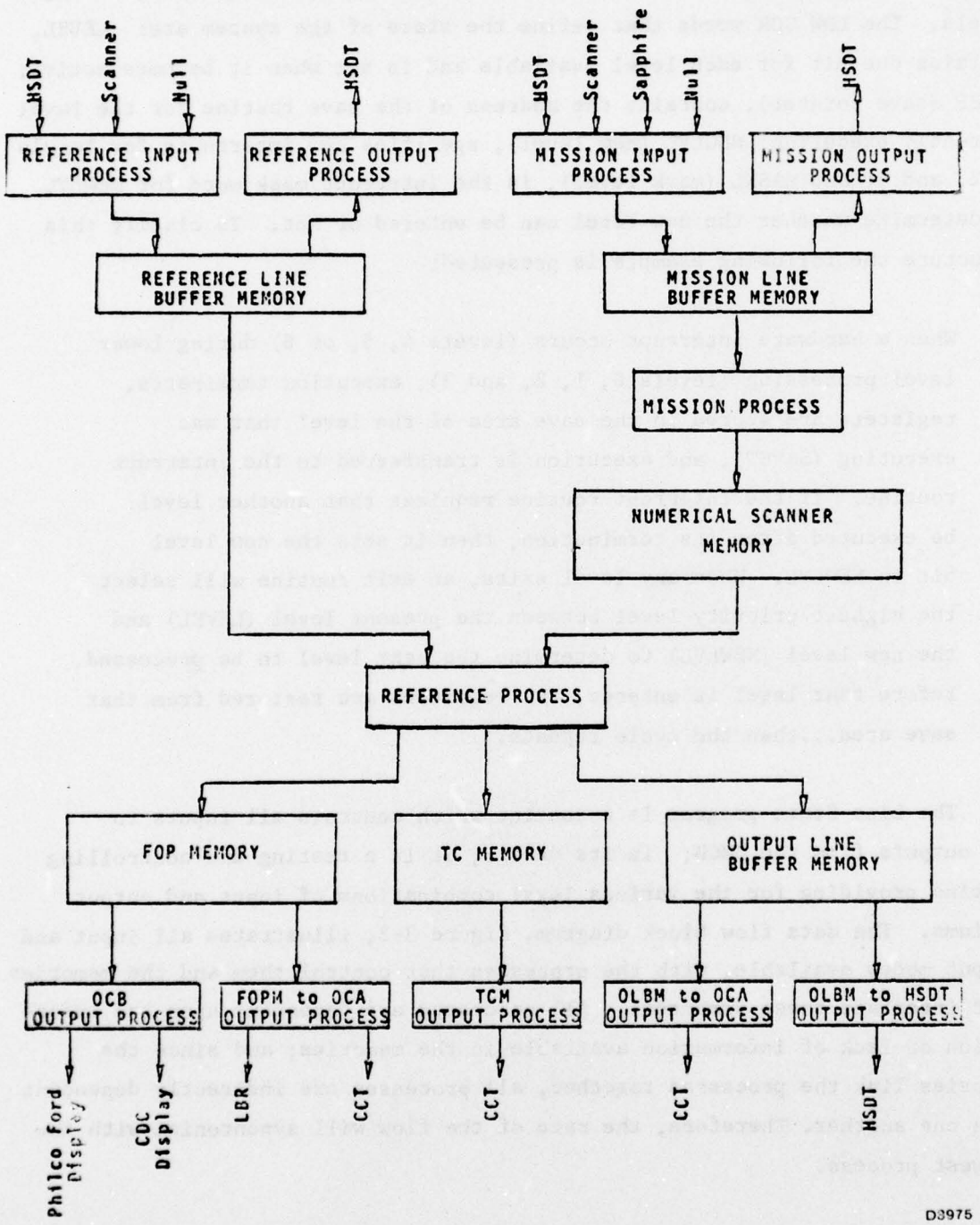

Figure 3-3. Data Flow

Figure 3-4 is the configuration of the present design for the Line Start Process Control Routine. It calls for a polling of all processes; a process is checked only when not already in progress. When a process is checked, the interfacing memories are tested for availability of information (input) and space (output); if space and information are available, the process is executed; if not, it is exited.

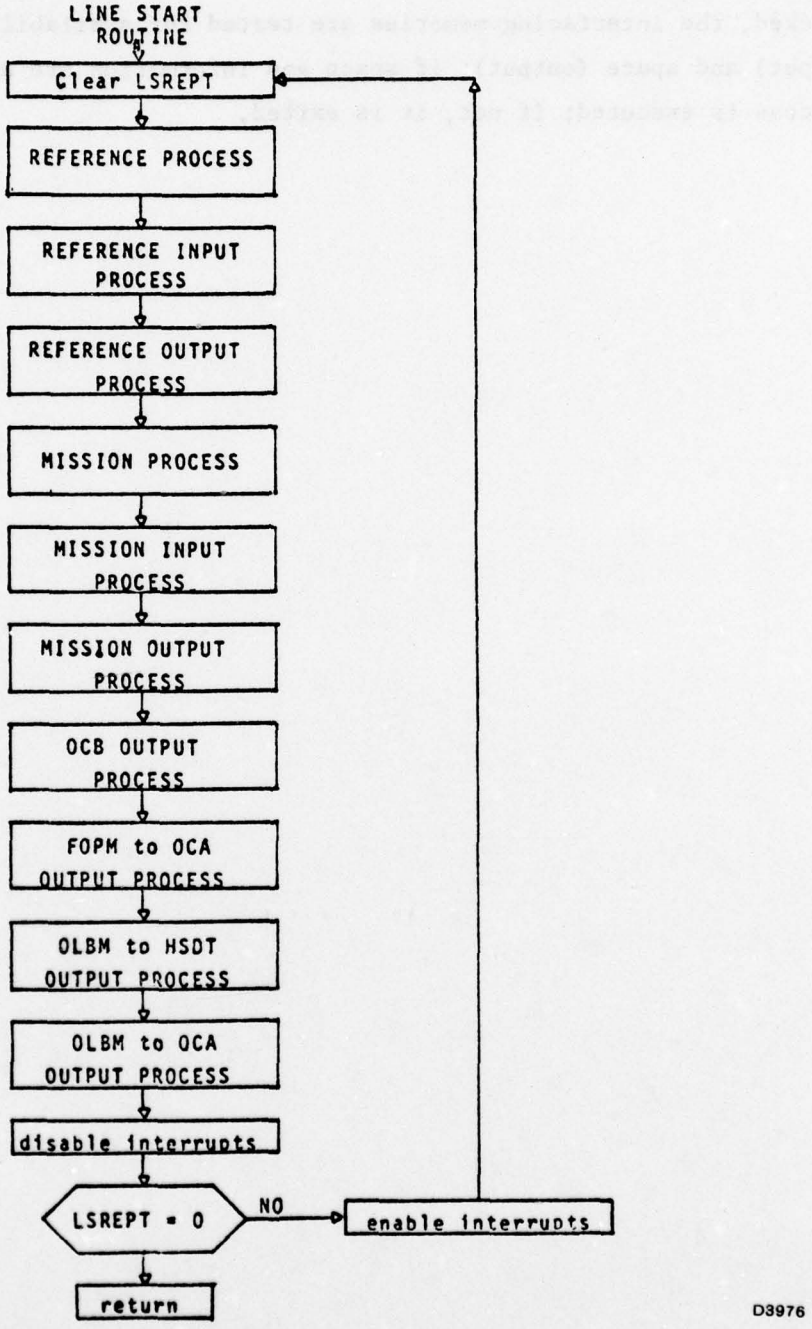

Figure 3-4. Line Start Process Control Routine

3.2 DESCRIPTION OF INPUT/OUTPUT DEVICES

3.2.1 Data Channel Controller/Line Buffer Memory

The DMCD system includes three Data Channel Controllers and their associated Line Buffer Memories.

The Data Channel Controller (DCC) is a general-purpose device designed to provide a streamlined, buffered, record-oriented, data interface between a peripheral device and a random-access "Line Buffer Memory" (LBM). It is capable of handling up to six such interfaces under the control of a single supervisory computer (See Figure 3-5).

The three DCC/LBM's in the DMCD are designated: Reference, Mission, and Output.

The Reference DCC/LBM includes the following interface controllers:

- Film Scanner (right side)
- High-Speed Digital Tape Unit
- 1700 Supervisory Computer

The Mission DCC/LBM includes:

- Film Scanner (left side)
- High-Speed Digital Tape Unit
- SAPPHIRE
- 1700 Supervisory Computer

The Output DCC/LBM includes:

- High-Speed Digital Tape Unit
- 1700 Supervisory Computer

SCANNER CONTROLLER

The scanner controller, a part of one station in the DCC, interfaces one side of the Dual Film Laser Scanner to a Line Buffer Memory. This

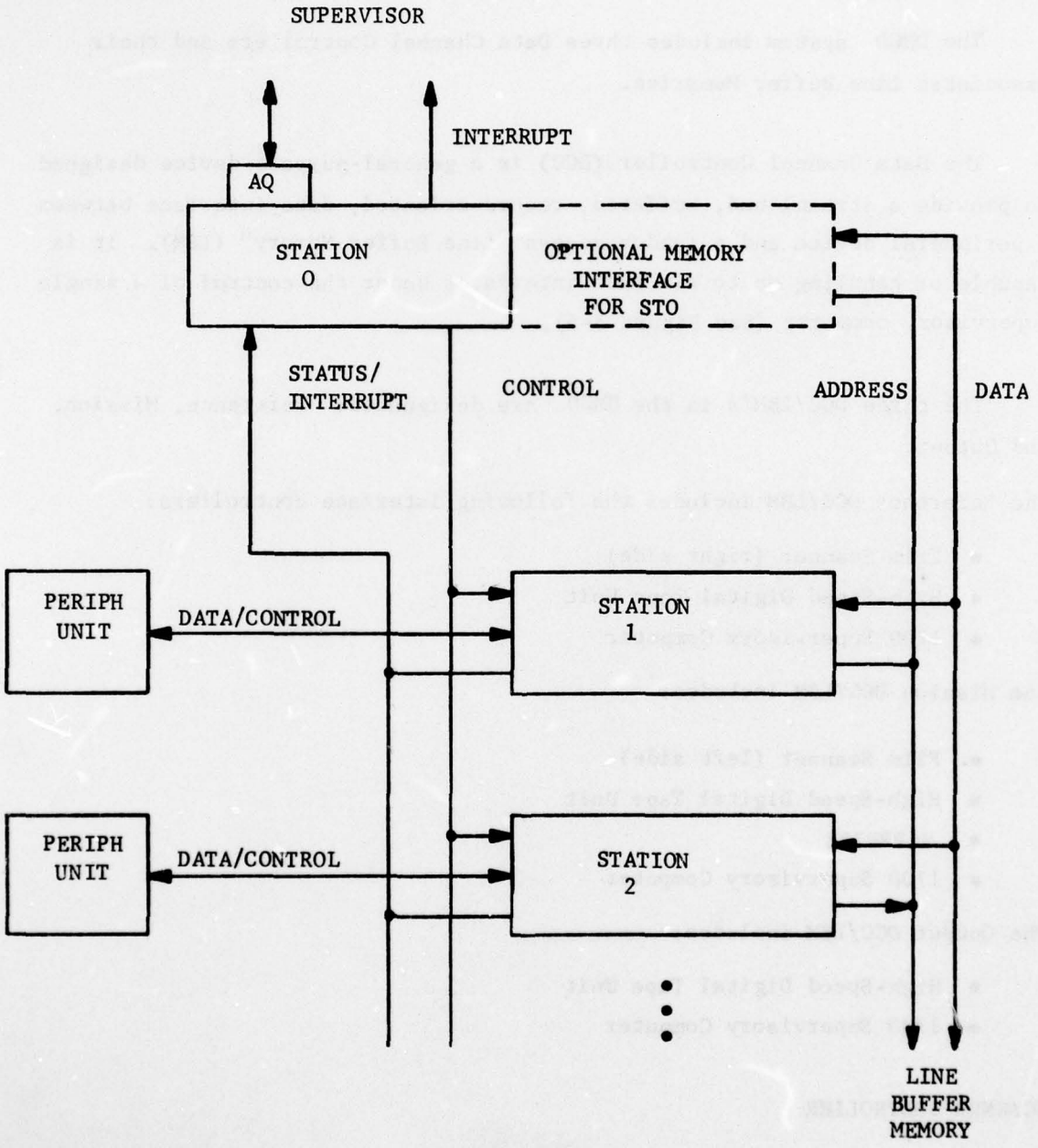

Figure 3-5. General DCC Block Diagram

D3977

controller provides a control interface for the 1700 to direct the operations of the scanner and packs the 8-bit data stream from the scanner into 16-bit words, for storage in the Line Buffer Memory.

HIGH-SPEED DIGITAL TAPE CONTROLLER

The High-Speed Digital Tape drive interfaces with the Data Channel Controller through one of its six interface stations. A tape controller may presently control one IBM 3420, Model 8, tape drive and contains a reloadable control memory of 64 16-bit words. Separate microprograms are necessary to read or to write tape. Both microprograms contain rewind and primitive status handling capabilities.

The tape unit reads and writes eight 8-bit characters every 6.125 microseconds; it will always write and read a multiple of eight characters. A non-multiple of eight characters record will be rounded up to eight and a file error status will result. The 8-bit characters are packed into 16-bit words and passed through a 16-word FIFO and then into the Line Buffer Memory.

SAPPHIRE CONTROLLER

The SAPPHIRE Digital Correlator is interfaced to the Module Change Detector via one station of the Mission Data Channel Controller. This SAPPHIRE controller is a microprogrammable device which contains 256 16-bit words of program memory. It also contains a 256 by 16-bit buffer primarily for SAPPHIRE's Auxiliary Data output. However, this buffer may also be written from microprogram or from the supervisory AQ Channel. Under firmware control, a selected portion of this buffer is transferred to the Mission Line Buffer Memory at the beginning of each record as a record header.

LINE BUFFER MEMORY

The Line Buffer Memories hold two to four full swath scan lines of up

to 8192 pixels each. This memory is used as a first in/first out line buffer between the selected peripheral devices and the Change Detection Processors (CDP's).

The reference and mission Input Line Buffer Memories are also used to partition the full swath scan lines into four segments for parallel processing by the four CDP channels. The Output Line Buffer Memory is used to assemble the four-channel segments back into a continuous full swath scan line for use by its associated DCC and selected peripheral device.

3.2.2 Scanner

The dual transport Laser Film Scanner was originally constructed by CDC and delivered to the Air Force in 1972 as a part of the ARRES 1280 correlator contract. The film transport and optics were originally designed for four-channel film scanning but the electronics were designed for only one channel. For the DMCD contract this equipment was supplied GFE back to CDC where the electronics were upgraded to four channel capability and the appropriate DCC interface was installed.

A description of the optical, mechanical and electrical construction of the scanner follows.

OPTICAL CONSTRUCTION

Top and side views of the optical scanning elements are illustrated in Figure 3-6. The laser beam is expanded approximately five times to obtain the 0.23 inch beam. The vertically oriented beam is horizontally deflected and separated by the beamsplitter. These collimated beams are directed to the rotating 8-facet mirror and scanned through the focussing lenses which form the 1.56 mil spot at each film plane. The spot position is repeatable to 1/6 spot size, or .25 mil. This is an equivalent error angle of

$$\alpha = \frac{45^{o}}{9.5 \text{ inches}} * .25 \times 10^{-3} \text{ inch} = 1.19 \times 10^{-3} = 4.25 \overset{\frown}{\text{sec}}$$

a. Top View

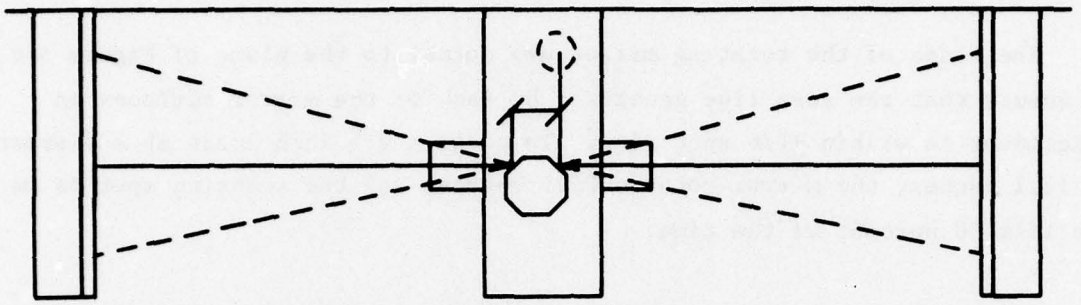

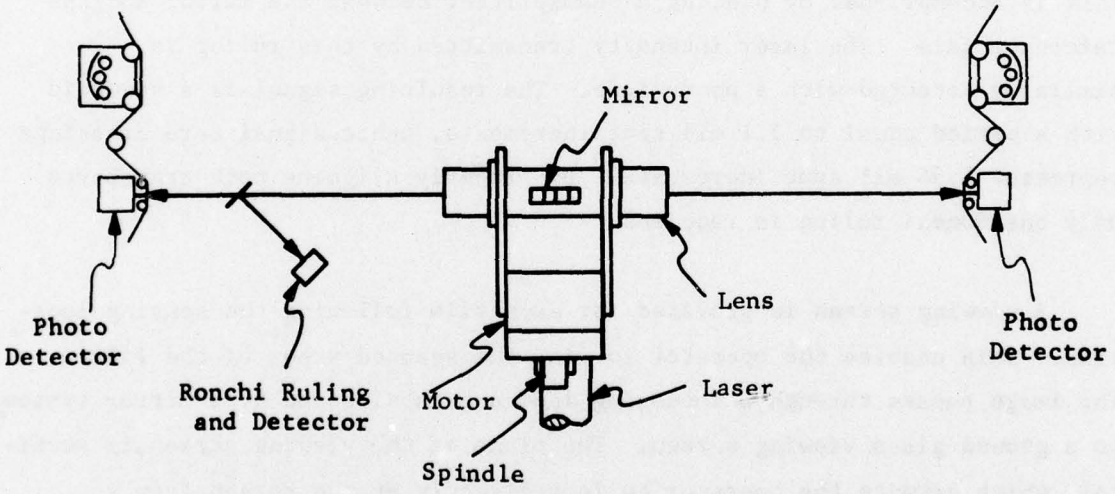

b. Front View

D1637

Figure 3-6. Spot Scanning Optical Design

Since error angles are doubled by the mirror, total mirror/spindle runout is maintained at less than 2.1 $\overset{\frown}{\text{sec}}$.

The sides of the rotating mirror are normal to the plane of Figure 3-6 to ensure that the scan line generated by each of the mirror surfaces is coincident to within $\pm 1/6$ spot size. To cover a 9.5 inch image at a distance of 12.1 inches, the mirror rotates 22.5 degrees and the scanning spot is on the film 50 percent of the time.

The intensity transmitted through the film is collected by a photodiode. The photodiode signal is amplified, log-converted and sampled for every 1.56 mil increment on film. Spot position along the film is determined by simultaneously scanning the beam across a 320-line-per-inch Ronchi ruling, which is a series of transparent and opaque line rulings. This is accomplished by placing a beamsplitter between the mirror and the reference film. The laser intensity transmitted by this ruling is similarly detected with a photodiode. The resulting signal is a sinusoid with a period equal to 3.1 mil spot increments, hence signal zero crossings represent 1.56 mil spot increments. By properly aligning both transports only one Ronchi ruling is required.

A viewing screen is provided for each film following the sensing location. This enables the operator to view the scanned areas of the film. The image passes through a focussing lens and is directed by a mirror system to a ground glass viewing screen. The plane of the viewing screen is vertical, which permits the operator to look directly at the screen from a comfortable standing position. An appropriate hood is required to minimize ambient light. The viewer presents a 6-inch-by-6-inch scene of a 2-inch-by-2-inch area on the film. The viewing screen, mirror, and lens assembly can be raised or lowered to cover the view of the entire film width. Individual viewing screens are provided for each of the two films (Figure 3-7).

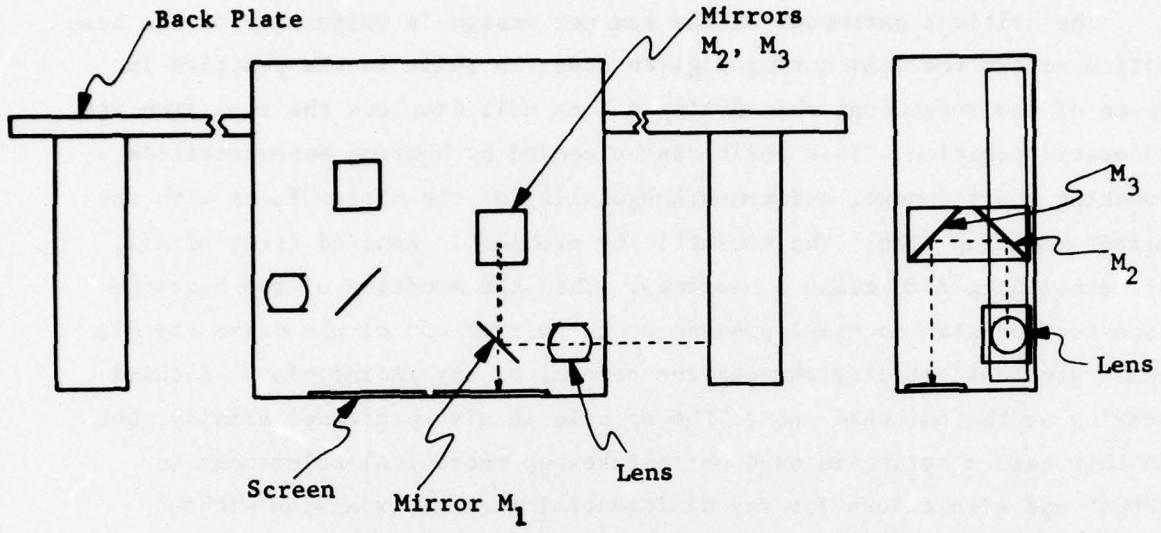

A: TOP VIEW

B: SIDE VIEW

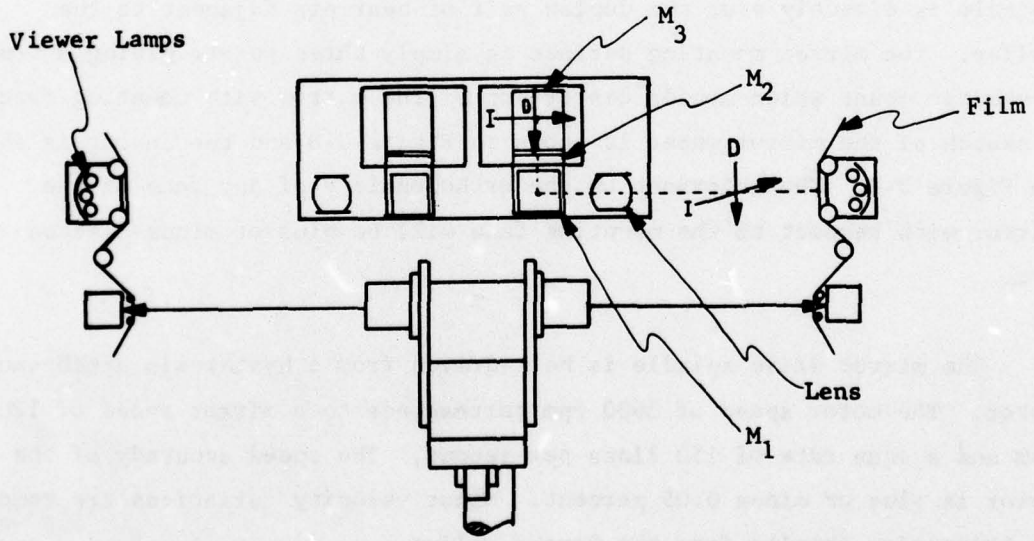

C: FRONT VIEW

D1653

Figure 3-7. Viewer Assembly Optical Design

MECHANICAL CONSTRUCTION

The critical parameter of the scanner design is uniformity of the beam motion across the film during a given scan. A shift in the position in space of the rotational axis during a scan will displace the scan from its theoretic position. This shift can be caused by bearing eccentricities, mounting shaft runout, and non-orthogonality of the mirror faces with the mirror mounting face. The eccentricity problem is handled first of all, by maintaining ABEC class 5 bearings. Then the mounting of two bearings face-to-face with an axial preload at the mirror end of the drive spindle shaft provides rigidity through the removal of any radial play. A third bearing at the outboard end of the spindle is also preloaded axially, but in this case a spring is used which takes up mechanical tolerances in length and also allows for any differential thermal expansion without resultant looseness. The drive pulley is located between the mirror and the duplex bearing pair, thus minimizing any possibility of bending of the shaft due to the drive torque on the pulley. The mounting point of the spindle is directly over the duplex pair of bearings adjacent to the pulley. The mirror mounting surface is simply three points giving a true kinematic mount which avoids distortion of the mirror with mounting forces. A sketch of the mirror mount is shown in Figure 3-8 and the layout is shown in Figure 3-9. The tolerance on the orthogonality of any face of the mirror with respect to the mounting face will be plus or minus 1 second of arc.

The mirror drive spindle is belt-driven from a hysteresis synchronous motor. The motor speed of 3600 rpm corresponds to a mirror speed of 1200 rpm and a scan rate of 150 lines per second. The speed accuracy of the motor is plus or minus 0.05 percent. Minor velocity variations are removed by triggering samples from the Ronchi ruling.

The basic film transport configuration is vertical, that is, the plane of the main mounting plate is vertical. All film reels, drive capstans and idler and follower rollers stand perpendicular to the main plate and

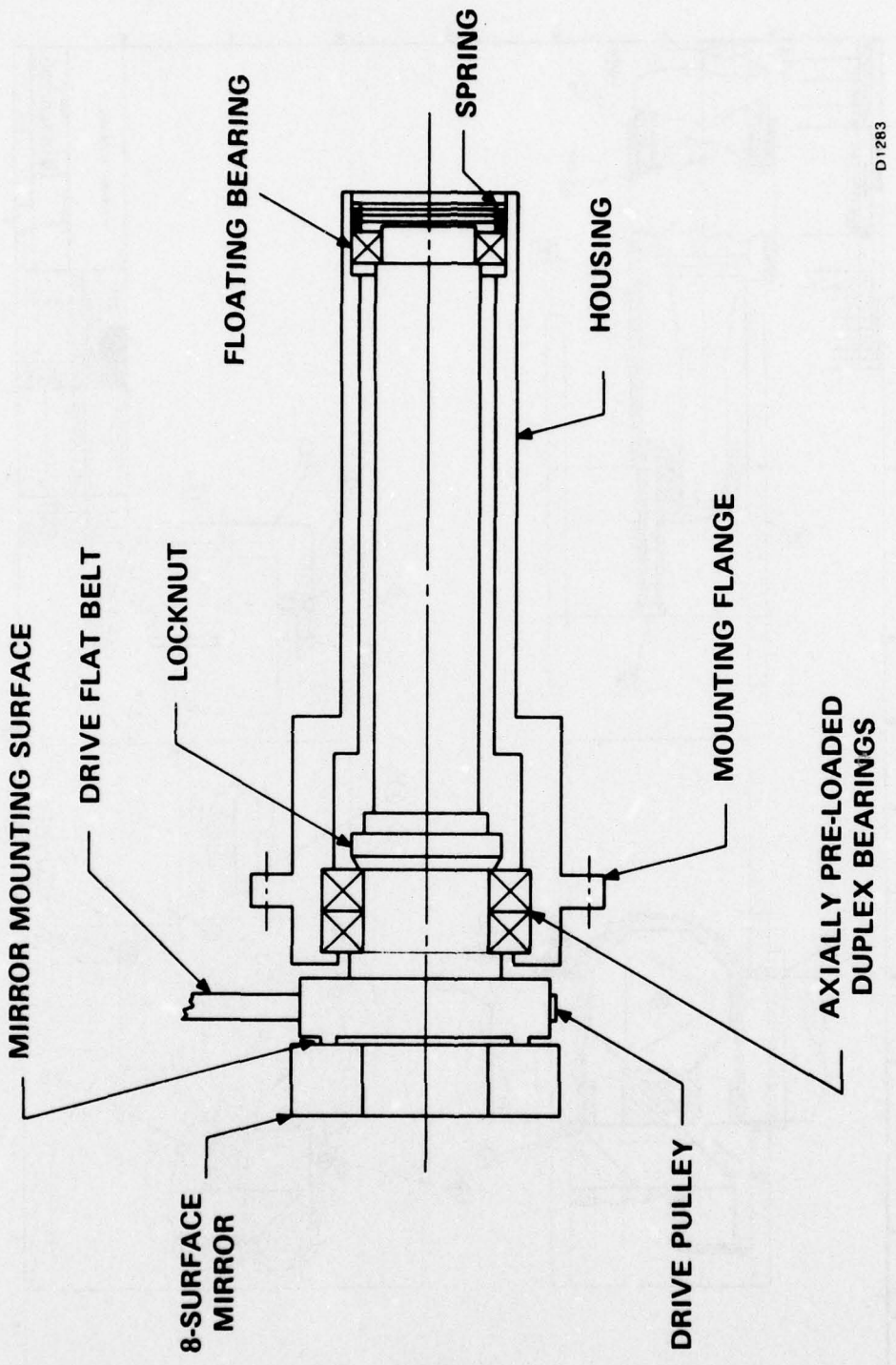

Figure 3-8. Mirror Drive Spindle

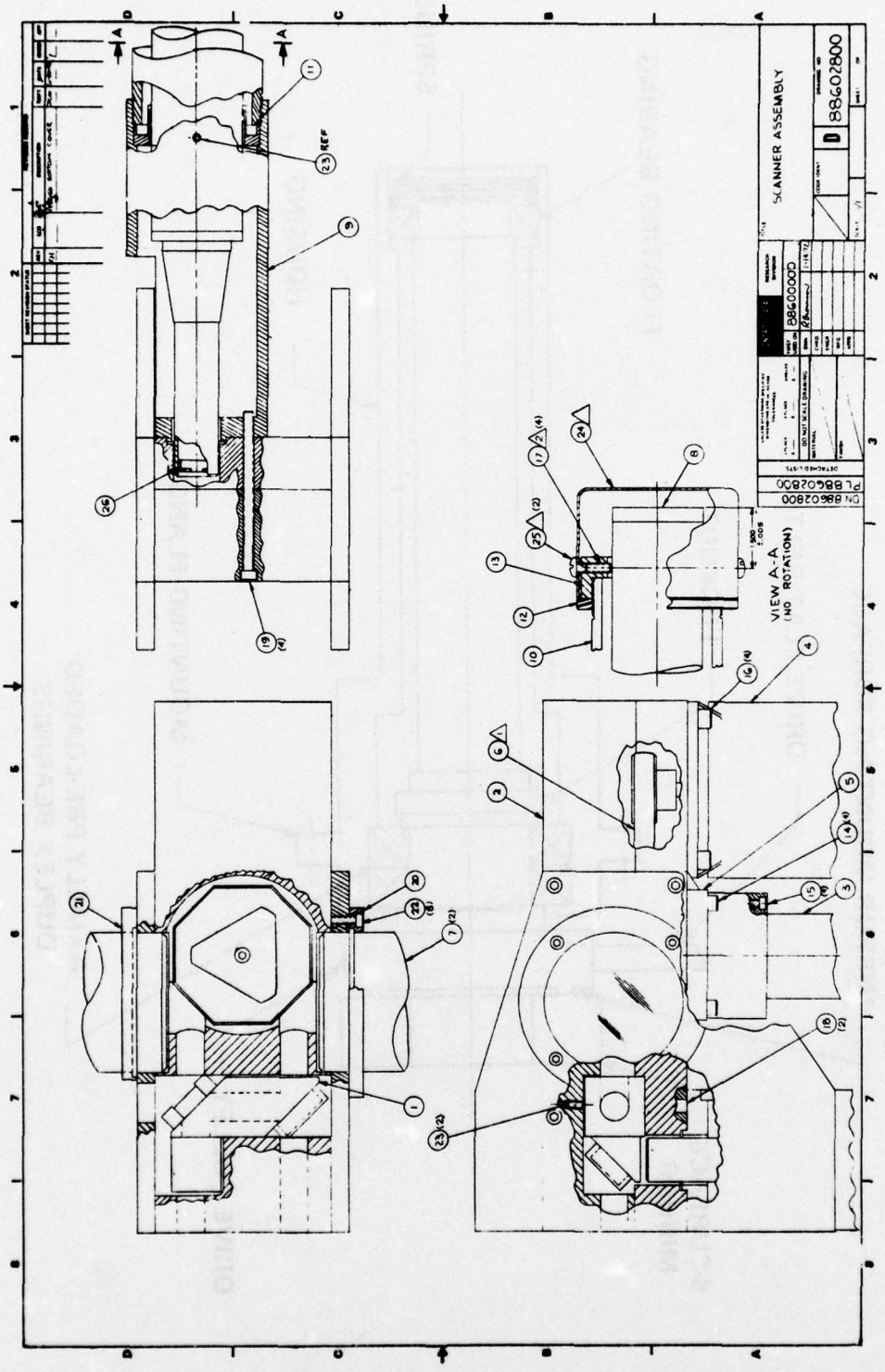

Figure 3-9. Scanner Assembly

thus their axes are horizontal. The plane of the films is vertical, with the emulsion sides facing each other and the scanning beams. Mechanical rigidity is designed into the main plate by attaching structural elements along its perimeter which increase the cross-sectional moment of inertia. The plate, in turn, is attached is a steel I-beam running horizontally across the length of the machine. This minimizes any possibility of relative flexure between the film planes at the sensing locations. The film transport plate is approximately the size of a desk. The dimensions of the scanner are approximately 72 inches high, 60 inches wide, and 26 inches deep. Appropriate covers are required for optical paths and moving machine elements. The electronic components are packaged in the lower part of the machine.

ELECTRONIC CONSTRUCTION

The scanner electronics are required to convert spot transmission power into gray scale values for each picture element, to provide the control of scanner functions, and to interface with the DMCD.

Individual samples are defined by simultaneously scanning the spot across a 320 line pair per inch Ronchi ruling. The detector response produces a cyclic wave whose zero crossings correspond to the transition edge of the line rulings. Samples are taken for each crossing of the cyclic wave in both positive and negative directions. Since the mirror has a constant angular velocity and the spot velocity is approximately a linear function of angle, all nonlinearities are eliminated by these linear sample pulses. The spot position across the film is addressed by a counter which is driven from the sample pulses. This gives a total of 6010 spot positions defined by a 1.5 mil sample interval across the 9.5 inch film.

The light energy transmitted through the film is detected by a long line photodiode. The sensitive diode area is 10 inches by 0.1 inch. The laser power incident on the film after beamsplitting and other losses is approximately 1 mw. Diode sensitivity of 0.35 A/W gives signals from 3.5 μA to 350 μA over a dynamic range of 100. This signal is superimposed

on a 20 μA dark current, which is measured between each scan line. An amplification of about 100 is required to attain the 0 to 10 volt level for A/D conversion. In order to optimize the digitizing of a given film, a capability to program the gain and bias of the input amplifiers is provided.

The functional operation of this gain/bias circuit is shown in Figure 3-10. This circuit performs the following function on each pixel

$$z = \frac{10x}{a} - b$$

where x = input pixel values

z = output pixel value

The contents of the GAIN (G) and BIAS (B) registers are loaded by the host computer, and range from 0 to 255. If

G = value in the GAIN register

$$a = \frac{-9\ G}{255} + 10$$

Therefore the effective gain for the circuit is

$$G_{eff} = \frac{10}{\frac{-9}{255} G + 10}$$

From measurements of 12 UPD-4 films the actual gain realized from the circuit was 93% of the theoretical value.

$$G_{eff} = \frac{9.3}{\frac{-9}{255} G + 10}$$

The bias factor b is a linear function of the value in the BIAS register (B). The coefficients were derived empirically from the measurement of the 12 UPD-4 films.

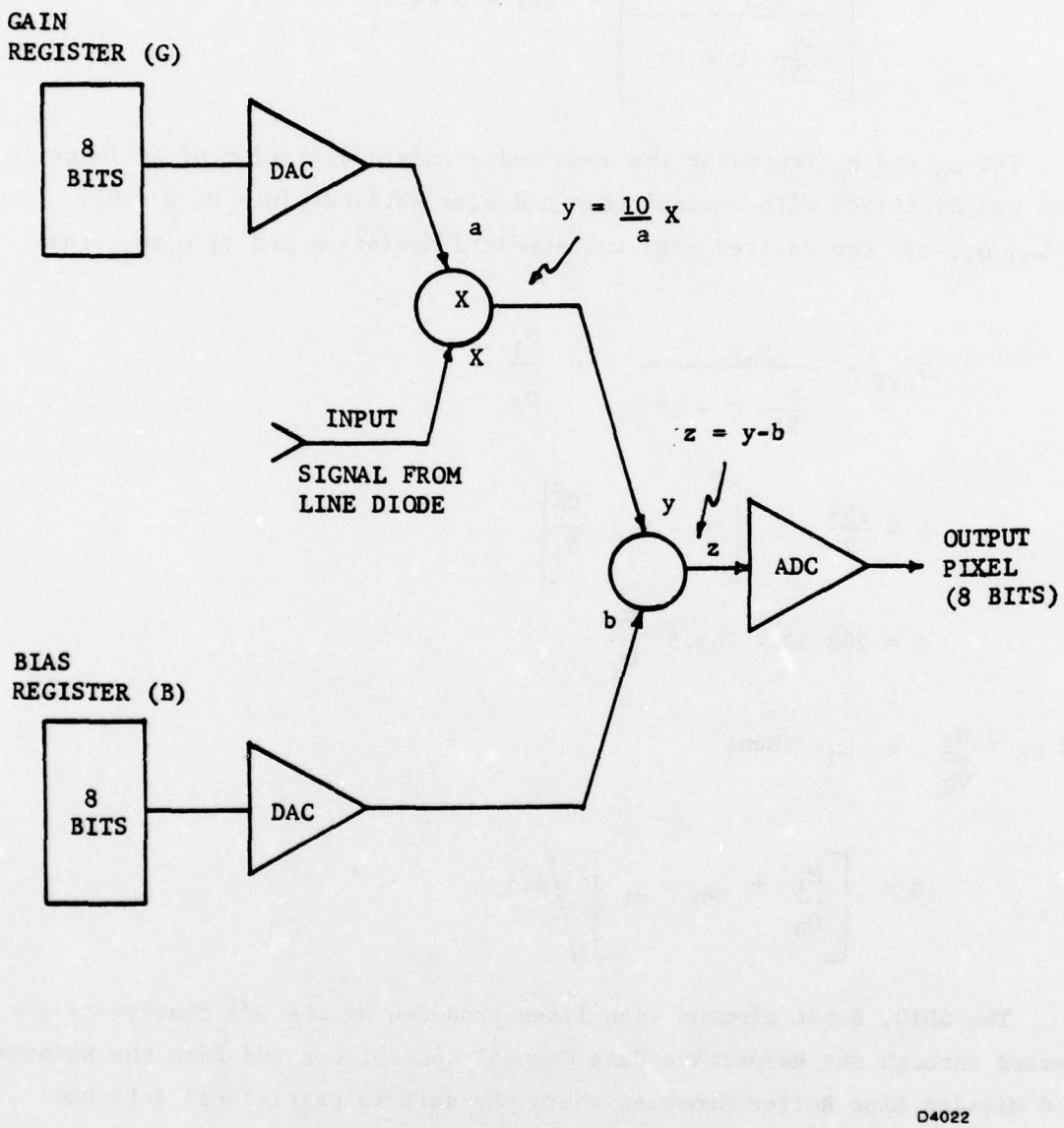

Figure 3-10. Gain/Bias Circuit

$$b = B * 4.5$$

Therefore

$$z = \left[\frac{9.3}{\frac{-9}{255} G + 10} \right] (X) - B (4.5)$$

Let μ_0 and σ_0 represent the mean and standard deviation of an image that was digitized with nominal gain and bias settings (G = 0, B = 0). If μ_1, σ_1, are the desired mean and standard deviation and if $\sigma_1 > \sigma_0$, then

$$G_{eff} = \frac{9.3}{\frac{-9}{255} G + 10} = \frac{\sigma_1}{\sigma_0}$$

$$G = \frac{255}{9} \left[10 - 9.3 \frac{\sigma_0}{\sigma_1} \right]$$

$$G = 283.33 - 263.5 \frac{\sigma_0}{\sigma_1}$$

If $\mu_0 * \frac{\sigma_1}{\sigma_0} > \mu_1$, then;

$$B = \left[\frac{\sigma_1}{\sigma_0} * \mu_0 - \mu_1 \right] \Big/ 4.5$$

The 6010, 6-bit element scan lines produced by the D/A converters are passed through the Respective Data Channel Controllers and into the Reference and Mission Line Buffer Memories where the data is partitioned into the channel segments to be used by the CDP's.

Film motion can be controlled either manually, off-line, or by the 1700 on-line. Refer to Table 3-4 for a description of the manual control

TABLE 3-4. OPERATOR CONTROL PANEL SWITCH FUNCTIONS

NAME	FUNCTION	INDICATOR
Power	Brings up 110V 1Ø power to equip	Light on when power is on
Master Clear	• Clears all transient film motion conditions • Initializes all counters and control signals • Identical to power-on-master-clear and scanner clear	None
Viewer	• Provides power to film viewer lamps. • Must be off to enable READY • Cannot be switched when READY	Light on when viewer lamps on
On-Line/ Off-Line	• In on-line mode, turns on buffer motor, and disables left supply reel. • In off-line mode, turns off buffer motor, and enables left supply reel. • Cannot be switched when READY	Dual light - one side on for on-line; one side on for off-line
Buffer Clear	Allows operator to process any film remaining in the buffer loop when on-line operation is complete	Light on when buffer clear is pushed off when READY is turned off.

TABLE 3-4. OPERATOR CONTROL PANEL SWITCH FUNCTIONS (Cont'd)

NAME	FUNCTION	INDICATOR
Start Scan	Gates position of viewer cross-hairs to holding registers to be used as alignment marks	None
Ready	• Enables both film transports to be placed in READY condition if all conditions are met. Conditions: 1) Film tension is on 2) Film is being driven by capstan 3) Transport control is in automatic (computer control) 4) Viewer lights are off 5) Film speed is fixed 6) Buffer loop is not overriding controls • READY condition locks out all operator controls except READY switch, power, master clear, buffer clear, and start scan	Light on when all conditions met off when any condition not met.

TABLE 3-4. OPERATOR CONTROL PANEL SWITCH FUNCTIONS (Cont'd)

NAME	FUNCTION	INDICATOR
Forward Direction/ Reverse Direction	• Forward - Moves film from supply reel to take-up reel (both transports) • Reverse - Rotates capstan in opposite direction (both transports) Cannot be switched when READY	None
Full Speed/ Half Speed	• Full - Enables film to be moved at 14 in/min, nominal, if fixed speed is selected. Moves mirror motor at high speed. • Half - Enables film to be moved at 7 in/min, nominal, under same conditions. Moves mirror motor at slow speed.	None
Tension	Turns on supply and takeup reels to apply tension to film. One switch for each transport. Cannot be switched when READY	None
Capstan Drive/ Reel Drive	• Capstan Drive - Wraps film around the capstan to enable it to move film • Reel Drive - Moves film via the take-up and supply reel motor Can be switched only when	None

TABLE 3-4. OPERATOR CONTROL PANEL SWITCH FUNCTIONS (Cont'd)

NAME	FUNCTION	INDICATOR
Capstan Drive/ Reel Drive (cont'd)	auto/man switch is in manual. • One switch for each transport	
Auto Control/ Manual Control	• Auto Control - Enables computer to control all film motion • Manual Control - Enable operator to control motion • One switch for each transport • Cannot be switched when READY	None
Fixed Speed/ Variable Speed	• Fixed Speed - Enables film to be moved at a fixed speed determined by the setting of the full/half speed switch • Variable Speed - Enable film to be moved at a variable speed determined by the position of the speed control joystick. • One switch for each transport • Cannot be switched when READY	None
Speed Control	• Joystick potentiometer with spring return to center • Provides operation control of both speed and direction of film motion when variable speed and manual control are selected. • One control for each transport • 5K potentiometer	None

functions. These controls are used for loading and positioning the film; the 1700 controls the actual scanning of the film on a scan line basis. A summary of scanner characteristics is given in Table 3-5.

3.2.3 High-Speed Digital Tape Units

Specifications

Type: IBM 3420 (M8)
Actual Density: rated 9042 flux reversals/in.
used at 10,000 flux reversals/in.
Effective Density: rated 6250 bytes/inch
used at 7312 bytes/inch
Media Speed: rated 200 in./sec.
used at 200 in./sec.
Reel Capacity: 2400'

FUNCTIONAL DESCRIPTION

Three separate Tape Unit-Controller pairs are used to interface with a specific Line Buffer Memory and Data Channel Controller. The controller is a specialized 1 x 1 design utilizing a Microprogrammed Sequencer and a Group Coded Recording format.

Eight tracks are used for recorded data and one track is used for control information. The four byte groups are recoded into five bytes and recorded according to the Group Coded Recording method proposed by IBM to the American National Standard for Recorded Magnetic Tape for Information Interchange.

The controller contains a memory for microcontrol (firmware) storage which is 16 bits by 64 words. This memory is loaded by the supervisory computer over a 1700 system A1Q channel under the control of the peripheral software handler package. Separate firmware programs exist for reading and writing tape, for reading and writing the first few feet of the tape with

TABLE 3-5. SUMMARY OF SCANNER CHARACTERISTICS

	PARAMETER	UNITS	SLOW SPEED	FAST SPEED
Photometric	Dynamic range	Optical density	0-2	0-2
	Density levels		64	64
	Density increments	Optical density	0.065	0.065
	Transmission accuracy	Percent of reading	$\pm$ 5	$\pm$ 5
Mechanical	Film size	Inches	2.5 to 9.5	2.5 to 9.5
	Reel size	Inches	1 to 5	1 to 5
	Scan rate	Lines/second	75	150
	Line scan period	Milliseconds	13.3	6.7
	Samples per scan line		6010	6010
	Film speed	Inches/second Inches/min	0.117 7.03	0.234 14.06
	Spot position repeatability	Spot diameters Mils	$\pm$1/6 $\pm$0.25	$\pm$1/6 $\pm$0.25
Optical	Sample Interval	Mils	1.5625	1.5265
	Spot size (diameter @ $I = \frac{1}{2}I_{max}$)	Mils	1.5	1.5
	Target size detected at better than 50% modulation	Mils	1.56	1.56
Electrical	Sample rate	Megasamples/second	0.91	1.82
	Sample time	Microseconds	1.1	0.55
	Analog frequency bandwidth	Megahertz	0.46	0.91

an all ones' pattern, and for rewinding the tape units.

TAPE FORMAT

Each record of recorded data consists of groups of 255 recorded (204 memory) bytes of data separated by 23 bytes of all ones and a single zero character called "resync" bursts. The first group of data is preceded by a preamble consisting of all ones and a single zero character. The preamble of one record and the residual characters (or AGC burst in the case of the first record) of the previous record are separated by a record gap.

PERFORMANCE

A. Lengths on Tape

Automatic Gain Control Burst	14.9 in.
Inter-record Gap	0.3 in.
Preamble (23 T.U. Tachometer pulses)	0.3325 in.
Resync Bursts (23 tape characters)	0.0023 in.
Data Group (204 characters)	0.0256 in.

B. Times

Rewind and unload 2400' tape	51 sec.
Rewind (only)	45 sec.
Load tape	7 sec.
Read Access from stop	2.0 ms.
Read/Write Tape Speed	200 in/sec

C. Data Capacity Calculation

Each Record = Record Gap, Preamble, N·Data Group, N·Resync, Residual where N = Data Groups - record size in Memory/204. Residual = 5/4 (Record length -(N·204)· .001"

Example: Record size = 5120 8-bit characters. N = 5120/204
Data Groups = 25

Record Gap	= 0.3
Preamble	= 0.3325
N· 0.0256	= 0.64
N· 0.0023	= 0.0575
Residual = 5/4 (5120-N·204).001	= 0.025
TOTAL inches/record	1.355
TOTAL records/2400'	21,255

3.2.4 Computer-Compatible Tape (CCT)

A Control Data 1732 Tape Controller and a 609 tape drive are interfaced to the output of the DMCD. This interface does not involve a Data Channel Controller but is connected directly to an AQ channel in the Output Controller A Flexible Processor.

The purpose of this peripheral is to provide an industry standard "computer-compatible" medium for recording DMCD output products.

Table 3-6 and Figure 3-11 describe the data format of magnetic tape. A line or frame of tape data consists of an 8-bit tape word and a parity bit. Tracks 0 through 7 contain the data bits, and track 8 holds the parity bit. Data recorded on the tape is arranged in groups called records and files. A record consists of consecutive frames of information. A minimum of one frame of information constitutes a record. Adjacent records are separated by a 0.6 inch unrecorded area called a record gap. In the 609 tape transport a cyclic code word and a longitudinal parity check character are recorded at the end of each record. A file consists of a group of records. Adjacent files are separated by recording an end-of-file marker six inches from the last record in the file. The load point is a reflective marker indicating the beginning of the usable portion of the

tape. It is located at least 10 feet from the beginning of the tape. The end-of-tape marker is a reflective marker placed not less than 18 feet from the end of the tape. This provides approximately 10 feet of tape trailer and enough tape to hold a record of 96,000 characters after the end-of-tape marker is sensed (See Figure 3-12).

TABLE 3-6. TAPE FORMAT

	608	609
Tracks		nine
Tape Speed		37½ ips
Density (bpi)		800
Parity		
Vertical		odd - placed in ninth track
Longitudinal		even parity check character spaced 4 frames from the CRC code word.
Cyclic Redundancy Code Word		spaced 4 frames from last data character
End-of-File Mark		A 23_8 6 inches from the last record. It is followed by an identical check character.
Initial Gap	3.0 inches minimum for write 0.5 inches for read	same
Record Gap	0.687 inches minimum 0.960 inches maximum 0.750 inches nominal	0.50 inches minimum 0.75 inches maximum 0.60 inches nominal

Two methods of error detection are employed by the 1738 controller: Parity Checks and a Cyclic Redundancy Check (CRC).

During a Write, the read heads of the tape transport transfer the newly written character to the controller. The controller performs a parity

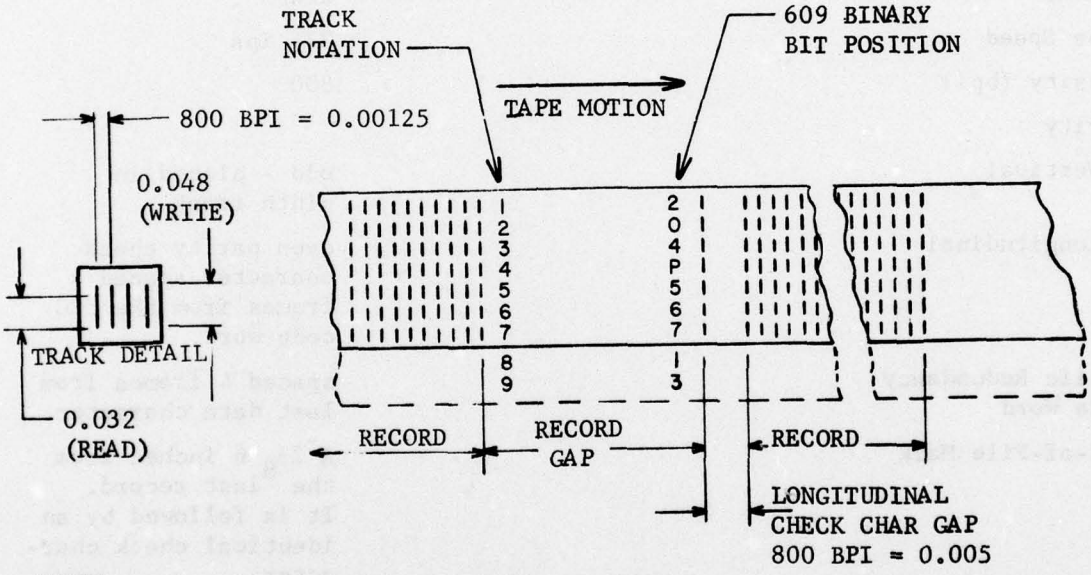

NOTES:

1. OXIDE SIDE UP ON DIAGRAM, RECORDING HEAD ON SAME SIDE AS OXIDE.
2. WRITE FREQUENCY 30 kC ±1%.
3. AVERAGE STEADY STATE TAPE SPEED 37.5 ips.

D3979

Figure 3-11. Tape Format

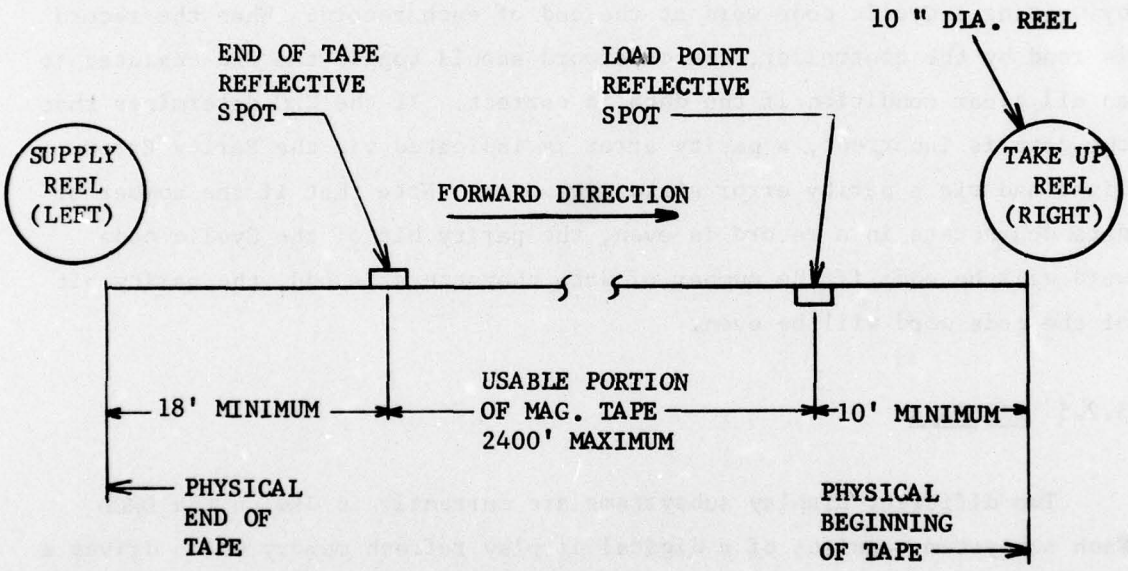

Figure 3-12. Physical Layout of Tape

check and sets the Parity Error status bit if an error has occurred. If the Alarm interrupt has been selected, an interrupt occurs.

During a Read, the parity bit recorded on the tape is checked against the character. The Parity Error status bit sets if an error occurs. If the Alarm interrupt has been selected, an interrupt occurs.

The Cyclic Redundancy feature is an additional check of the accuracy of data transmission and reception between the controller and the tape unit. The CRC, used by the 1732 only in conjunction with the 609, is accomplished by writing a cyclic code word at the end of each record. When the record is read by the controller, the code word should toggle the CRC register to an all clear condition if the data is correct. If the CRC determines that the data is incorrect, a parity error is indicated via the Parity Error light and via a parity error status response. Note that if the number of data characters in a record is even, the parity bit of the Cyclic code word will be odd; if the number of data characters is odd, the parity bit of the code word will be even.

3.2.5 Displays

Two different Display subsystems are currently in use on the DMCD Each subsystem consists of a digital display refresh memory which drives a standard RGB color TV monitor. As mentioned in other sections of this report the DMCD can provide output for up to eight such displays.

The first display subsystem was constructed by Philco-Ford, and is referred to as the Image Storage and Display Unit (ISDU). This display is intended for on-line image viewing and presents a scrolling or "waterfall" image consisting of a black and white background image with change events superimposed in color. The display refresh memory holds 485 scan lines with each line having 640, 6-bit bytes of storage. Each byte can be coded to store either 32 gray levels or eight different colors at four intensity levels. This display accepts data from the DMCD at 150 lines per second.

Each incoming line is added to the top of the displayed image and the whole image is moved down one line. Scan lines are presented from left to right.

The second display subsystem was constructed by Control Data under a separate contract and is referred to as the CDC Digital Scan Converter and Interactive Display. This display is intended for use as either a second on-line display or as an off-line image analysis system. The major components of this display subsystem are:

- Display refresh memory (640 x 490 x 8 bits)
- Color monitor
- "Graph Pen" sonic digitizer and light table
- Keyboard and track ball
- Display console

This display subsystem, shown in Figure 3-13 (the 609 tape drive is also shown), uses the Output Controller A (OCA) Flexible Processor (See block diagram Figure 3-14) as a system controller and interface to the DMCD and is a fully programmable image handling system.

A summary of the capabilities of the software provided for this application is given in Table 3-7.

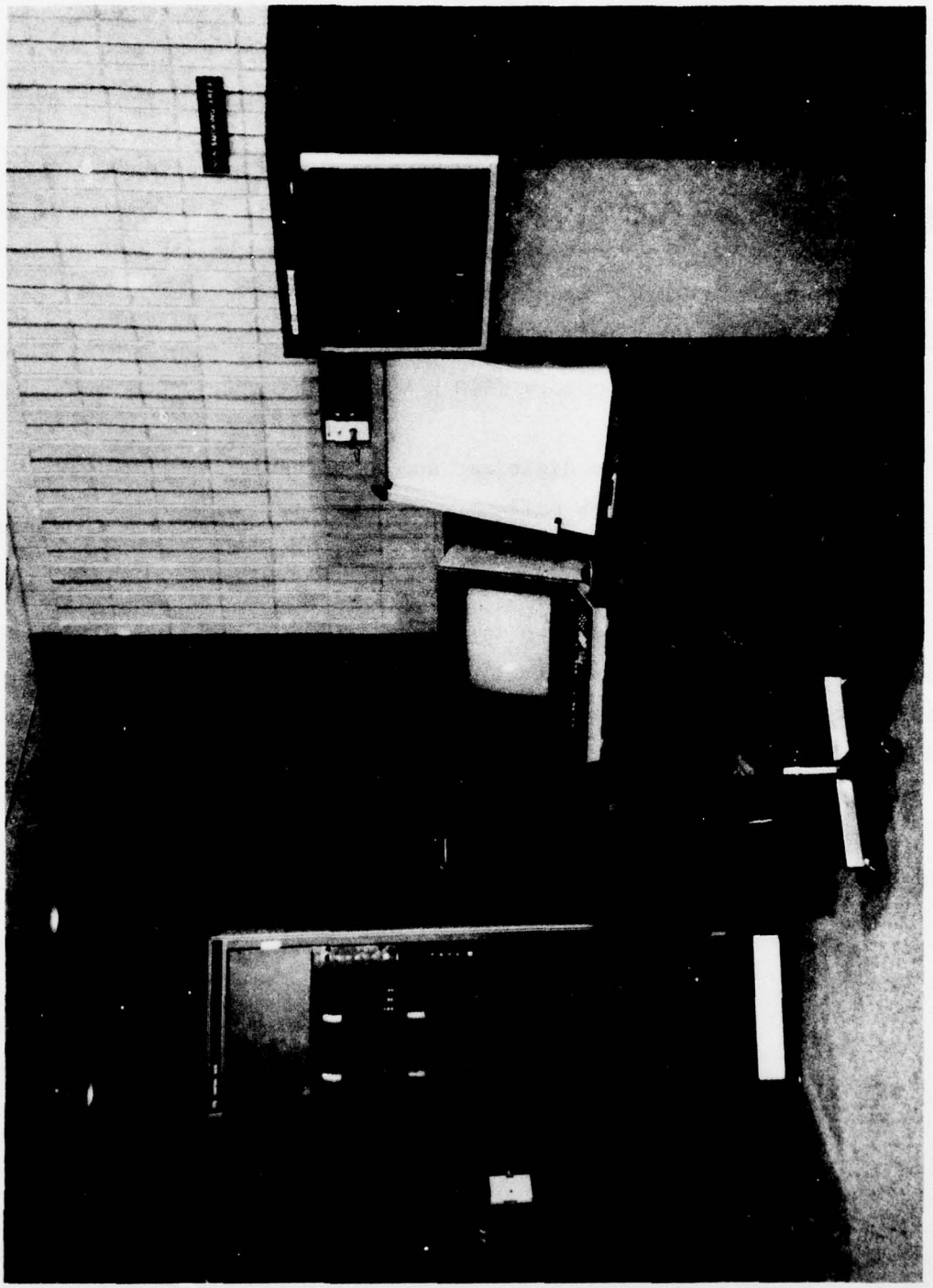

Figure 3-13. CDC Digital Scan Converter and Interactive Display Subsystem

Figure 3-14. Block Diagram of Image Display Station

AD-A056 953 CONTROL DATA CORP MINNEAPOLIS MINN F/G 17/9
DIGITAL MODULAR CHANGE DETECTOR.(U)
MAY 78 R DENNY, M BAYNES, W MCLURE F30602-73-C-0141
UNCLASSIFIED RADC-TR-78-104 NL

2 OF 3
AD
A056953

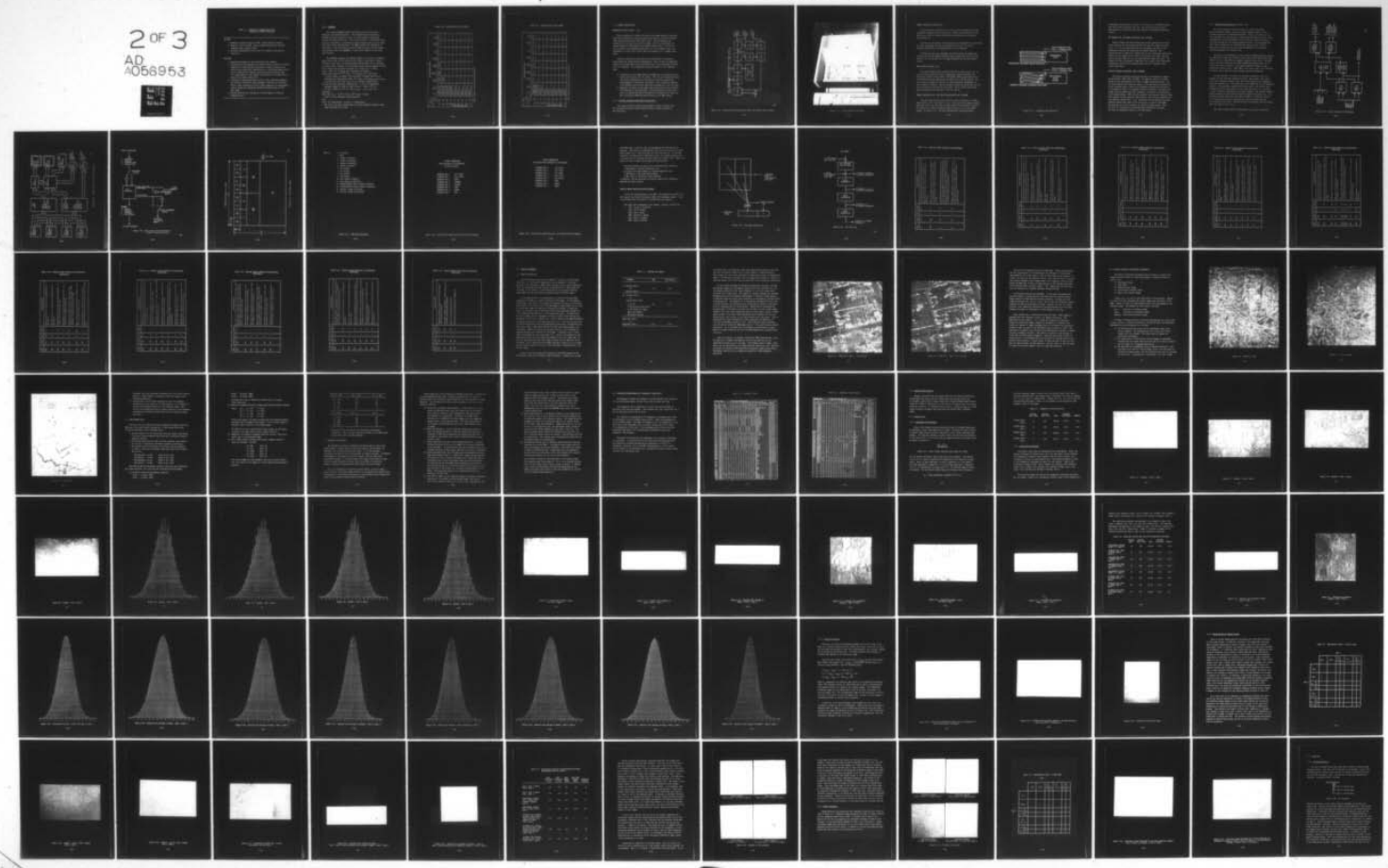

TABLE 3-7. SUMMARY OF CAPABILITIES OF CDC INTERACTIVE DISPLAY SUBSYSTEM

ON-LINE

- Presents scrolling display of DMCD change detection results
- Operator control of DMCD system through keyboard and composite image/character display format
- Provides programmable function keys for commonly used operator directives

OFF-LINE

- Statistical analysis of full-resolution 8-bit imagery
- Classification and evaluation of change detection results including: capability of relating map coordinates to image coordinates for ground truth change event identification; classifying change events into 4 categories of validity; maintaining classification logs on a large number of test flights for evaluation of probability of detection and false alarm rates.
- Interactive image manipulation such as, zoom, windowing, graphics and character annotation using keyboard, trackball and cross-hair cursor, image orientation (X and Y FLIP), selection of programmable look-up tables for displaying different interpretations of the same image.
- Utility functions for loading and storing imagery on computer-compatible tape.

3.2.6 SAPPHIRE

The acronym SAPPHIRE stands for Synthetic Aperture Precision Processor with High Reliability. This equipment was constructed by Goodyear Aerospace Corporation and is a high resolution multi-mode digital SAR processing system. This system includes: airborne SAR data-collection equipment, a ground-based digital doppler phase history correlator and a laser beam recorder. The DMCD includes two interfaces to this system. These interfaces allow the DMCD to receive digital imagery and auxiliary data from SAPPHIRE, or pass output products to the laser beam recorder.

The SAPPHIRE equipment can produce imagery in a variety of different modes and can also be run either at full speed or half speed. Tables 3-8 and 3-9 show that, in some speed/mode combinations, it is necessary to process only a portion of the available swath width of imagery in order not to exceed the available processor (P) or tape unit (T) bandwidth. The P and T numbers were calculated as follows:

P) Line Time (sec)=1 x 10^{-3} (sec) + # of pixels (P) x 10^{-6} (sec)
In other words, the number P is the number of pixels which can be processed (at 1 μsec/pixel) after the 1 msec inter-record gap has been subtracted from the line time, up to a maximum of 8192 pixels.

T) 7312 effective pixels/in. @200 in./sec. = 1.46 x 10^{6} pixels/sec.
Preamble length is .2185 in. @200 in./sec. = 1.09 x 10^{-3} sec.
Gap (est. time) is .3 in. @ $\approx$ 100 in./sec. = 2.55 x 10^{-3} sec.

Therefore:

Line Time (sec) - (1.09 + 2.55) x 10^{-3} (sec) = N (sec)
where N = Time available for writing data

And:

1.46 x 10^{6} (pixels/sec) = N (sec) = T (pixels/sec)
The value T was then rounded down to the next smaller character group (204 pixels/group) on tape.

TABLE 3-8. CAPABILITIES AT FULL SPEED

RANGE RESOLUTION MODES: Pixels \ MSEC / Line	Line	AZIMUTH RESOLUTION MODES: AA 3.28	AB BA 6.57	AC CA 9.85	AD BB DA 13.13	BC CB 19.70	BD DB 26.27	CC 29.55	CD DC 39.40	DD 52.53
AA	12288	P 2280 T-None	P 5570 T-1224	P 8192 T-5916	P 8192 T-10812	P 8192 T-Full	P 8192	P 8192	P 8192	P 8192
AB BA	6144	P 2280 T-None	P 5570 T-4284	P-Full T-Full						
AC CA	4096	P 2280 T-None	P-Full T-Full							
AD BB DA	3072	P 2280 T-None	P-Full T-Full							
BC CB	2048	P-Full T-None	T-Full							
BD DB	1536	P-Full T-None	T-Full							
CC	1366	P-Full T-None	T-Full							
CD DC	1024	P-Full T-None	T-Full							
DD	768	P-Full T-None	T-Full							

NOTE: An empty box implies full processing capability.

TABLE 3-9. CAPABILITIES AT HALF SPEED

RANGE RESOLUTION MODES	MSEC / Line	AZIMUTH RESOLUTION MODES								
Pixels / Line		AA	AB BA	AC CA	AD BB DA	BC CB	BD DB	CC	CD DC	DD
		6.56	13.14	19.70	26.26	39.40	52.54	59.10	78.80	105.06
AA	12288	P-5560 T-4080	P-8192 T-Full	P-8192	P-8192	P-8192	P-8192	P-8192	P-8192	P-8192
AB BA	6144	P-5560 T-4030	P-Full T-Full							
AC CA	4096	P-Full T-4080	T-Full							
AD BB DA	3072	P-Full T-Full								
BC CB	2048	P-Full T-Full								
BD DB	1536	P-Full T-Full								
CC	1366	P-Full T-Full								
CD DC	1024	P-Full T-Full								
DD	768	P-Full T-Full								

NOTE: An empty box implies full processing capability.

3.3 CHANNEL ORGANIZATION

PROCESSOR SECTION (Figure 3-15)

Nine processors per channel constitute one Change Detection Processor (CDP) which performs the change detection and feature oriented processing tasks described previously (See Figure 3-16). These processors are connected for one channel as shown in Figure 3-15 via a high speed I/O channel capable of 256 megabits per second transfer rates. Five of the nine processors are performing computation on a "per element" basis, two processors on a "per strip" basis, and two processors on a "change event" basis.

Software flexibility within each of the processors is obtained by using read/write random access micromemories. Each of these micromemories contain the instructions for the particular part of the algorithm that each unit is to perform. This capability has proven useful in the following ways:

- In addition to the change detection algorithm, an automatic lock-on feature was required for the system. This was not considered during the initial configuration of the system, but only required the reprogramming of the present processors. With a hardwired machine, a new hardware section would have been necessary for just this task.
- Diagnostic routines can be loaded and executed within each processor for isolation of failing modules. This capability has shown that even in a system this size, the mean-time-to-repair can be kept low and a nine-minute MTTR has been achieved on the DMCD system.

3.3.1 Flexible Processor Functional Descriptions

The change detection process flow diagram is shown in Figure 3-15. The following discussion breifly describes each of these processor's main functions.

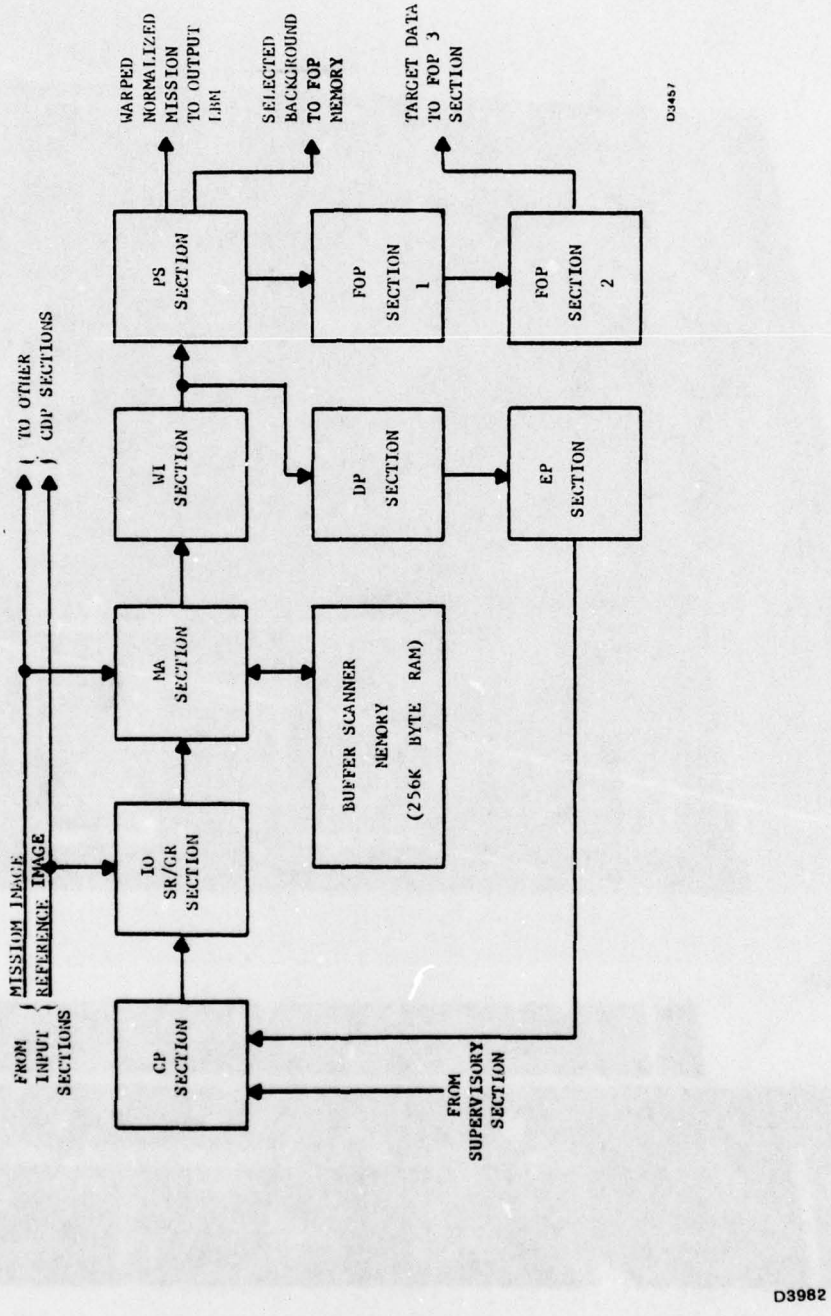

Figure 3-15. Change Detection Processor (Four Per System) Block Diagram

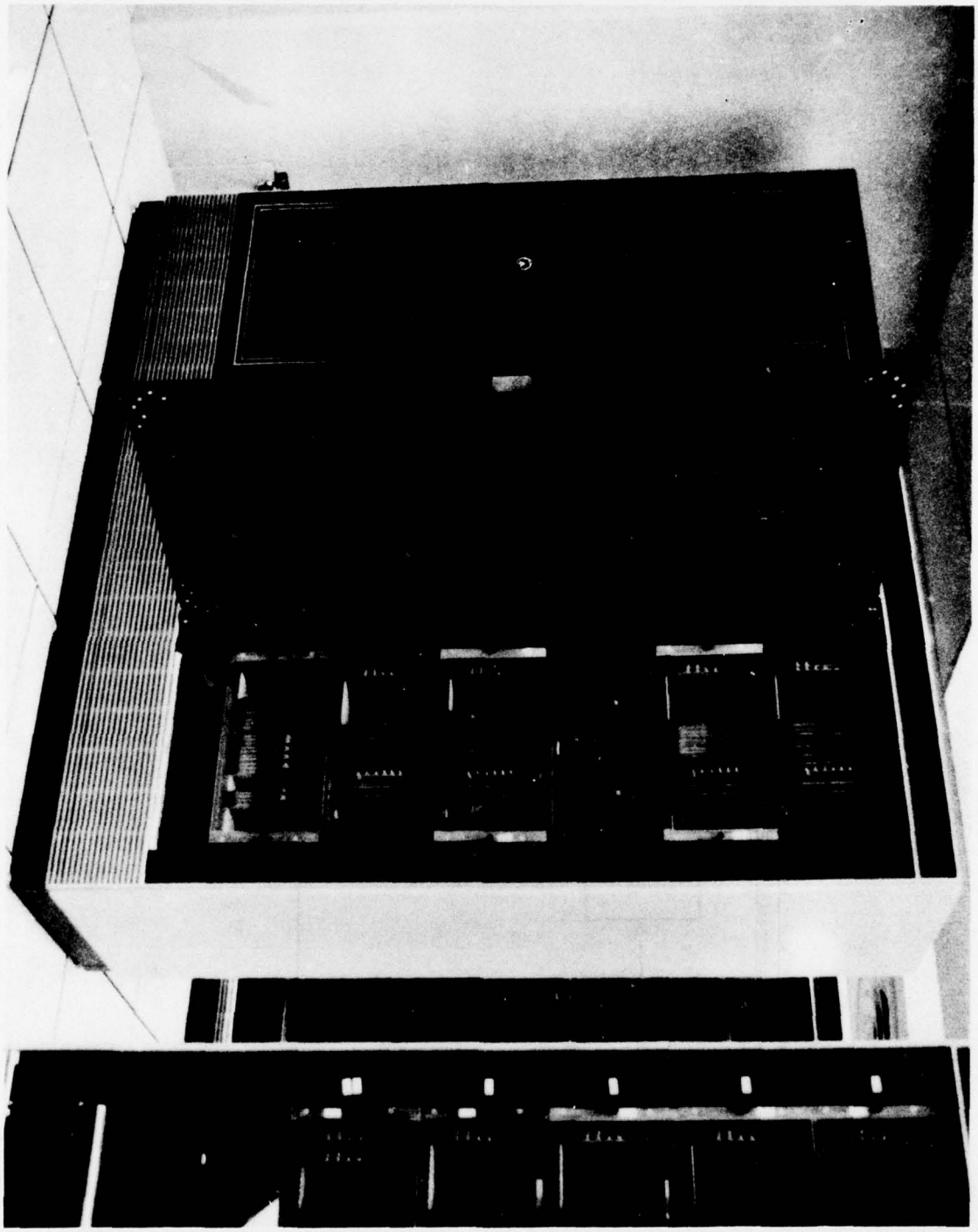

Figure 3-16. Change Detection Processor

CONTROL PROCESSOR SECTION (CP)

The CP Flexible Processor acts as the system interface between the supervisory computer and the correlator. During initialization, the CP section will load the other sections with microsequences and operator input parameters

The CP will also update starting position and photodensity corrections and their increments for each strip which will be sent to the I/O Flexible Processor via the high-speed FP to FP I/O channel.

Calculations are also performed in the CP section for harnessing, sliding mission, and window centering; these results are sent to the SP computer for calculations used in these functions for the four channel system.

INPUT/OUTPUT SECTION (I/O)

For each reference pixel received from the scanner (every 4.4 μ s), the I/O section sends the X and Y coordinates identifying where the collateral element can be found in the buffer memory to the MA section. The photoequalization corrections are also sent to the MA section. All of the above operands are updated by their respective increments and each element is counted. When the center of strip or end of line occurs, the I/O section interrupts the CP section. The CP section then sends another package of the operands to the I/O section.

MEMORY ADDRESSING (MA) AND WARP INTERPOLATION (WI) SECTIONS

The data from the collateral (mission) film is stored in a buffer memory that is 65K 6-bit bytes in size. Since the buffer memory contains many scan lines, the data from a single scan on the reference film can be matched to a curved (piecewise linear) scan of data in the buffer memory, see Figure 3-17. The Warp Interpolation section performs

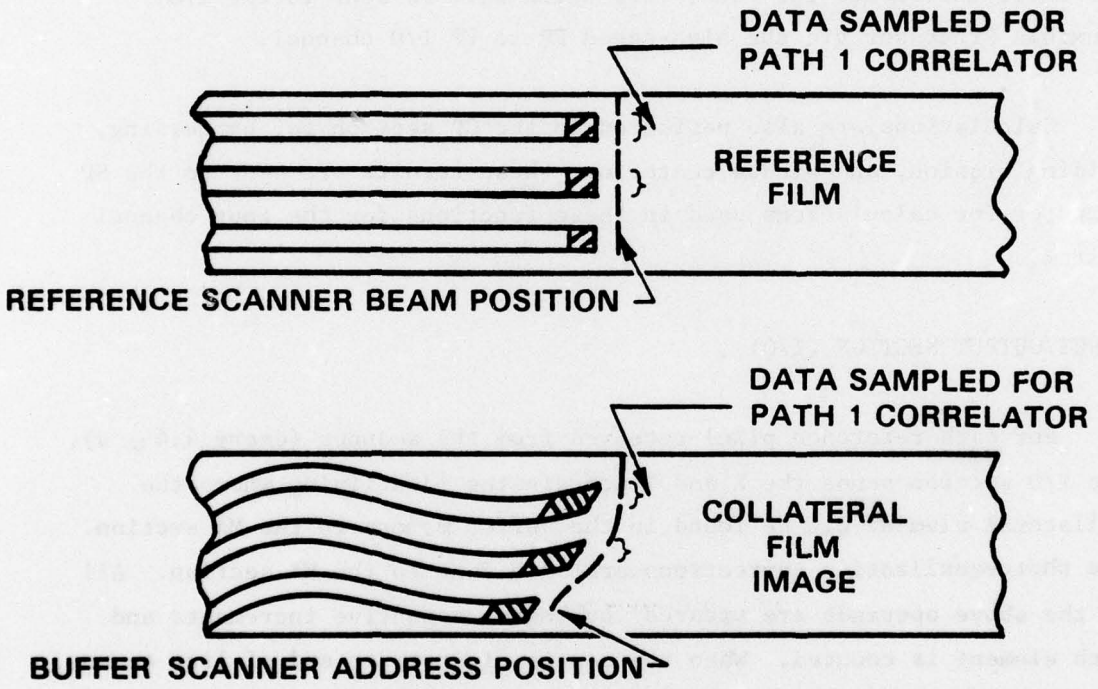

Figure 3-17. Correlator Data Extraction

a four-point interpolation to arrive at a value for a collateral element that lies on the predicted scan line. The four pixels used in the interpolation are read from the buffer memory by the Memory Addressing section.

DOT PRODUCT (DP) AND ERROR PROCESSING (EP) SECTIONS

The Dot Product and Error Processing sections perform the calculations necessary for determining how well the two film images are correlated, i.e., the misregistration of the two images, and some of the operations necessary for harnessing and window centering. The misregistration is computed by examination of the correlation coefficients between the two images at five sites - the present scan path, and four other scan paths that are one cell away from the center scan path. The method of finite differences, using these five values of the correlation coefficient, will give the misregistration in the X (azimuth) and Y (range) directions.

FEATURE ORIENTED PROCESSING (FOP) SECTIONS

The Feature Oriented Processing sections are designated PS (photonormalization), FOP1, FOP2, and FOP3. In addition, there is a buffer memory to hold approximately 25 lines of tagged background pixels. The PS section adjusts the collateral pixel to the same density distribution as the reference pixel, looks at the difference between the two pixels to determine if there is a possible target at this point, and stores the tagged selected background pixel (reference, collateral, or difference) in the buffer memory. FOP1 receives possible target pixels from PS, links them together to form possible change events, and collects statistics for each possible change event. FOP2 calculates various measures for each possible change event based on the statistics it receives from FOP1. The measures are used to classify the possible change events. FOP3 receives the classifications and positional information from FOP2 and tags the appropriate pixels in the FOP memory.

3.3.2 Output Processor Section (Figure 3-18)

The output processor section consists of Feature Orientated Porcessing Memory (FOPM), Output Line Buffer Memory (OLBM), and two flexible processors designated OCB and OCA. Figure 3-19 shows the data paths through the output section to the various peripheral devices. Both the OLB Memory and the FOP Memory serve as buffers between the Change Detection Section and the Output Processor Section. The OLB Memory has four lines of delay and the FOP Memory has sixteen lines of delay. Image data is placed in the Output Section Memories by the four P/S flexible processors (See Figure 3-20).

The data in the OLB Memory is 8-bit warped normalized mission imagery. The W/N mission image can be routed to the output high-speed digital tape (HSDT) or to a 9 track 800 bpi computer-compatible tape (CCT). The HSDT unit is used for storage of the warped normalized mission image or, in an off-line mode, can store a four channel mosaicked image or a pre-normalized filtered image. These HSDT's then can be used as the reference or mission input image for further change detection processing.

The OCB processor can output 15 selectable different images to a maximum of eight displays connected on-line. These images range from eight full resolution images to one full swath (5120 pixels) compressed image (See Figure 3-21). The image data in the FOPM that the OCB processor outputs to the displays is packed into 16-bit words. Each 16-bit word contains two 6-bit image pixels and one 4-bit tag field. The tag field is used to indicate which pixels are strong changes, weak changes, shadow-induced changes and scintillation-induced changes (See Figure 3-22). As the OCB processor reads this data from the FOPM, it translates the two 6-bit pixels and the 4-bit tag field into two 5-bit pixels and two 3-bit priority tag fields. Associated with each priority tag is an output mode (See Figures 3-23, 3-24).

The output associated with each priority tag and the translation

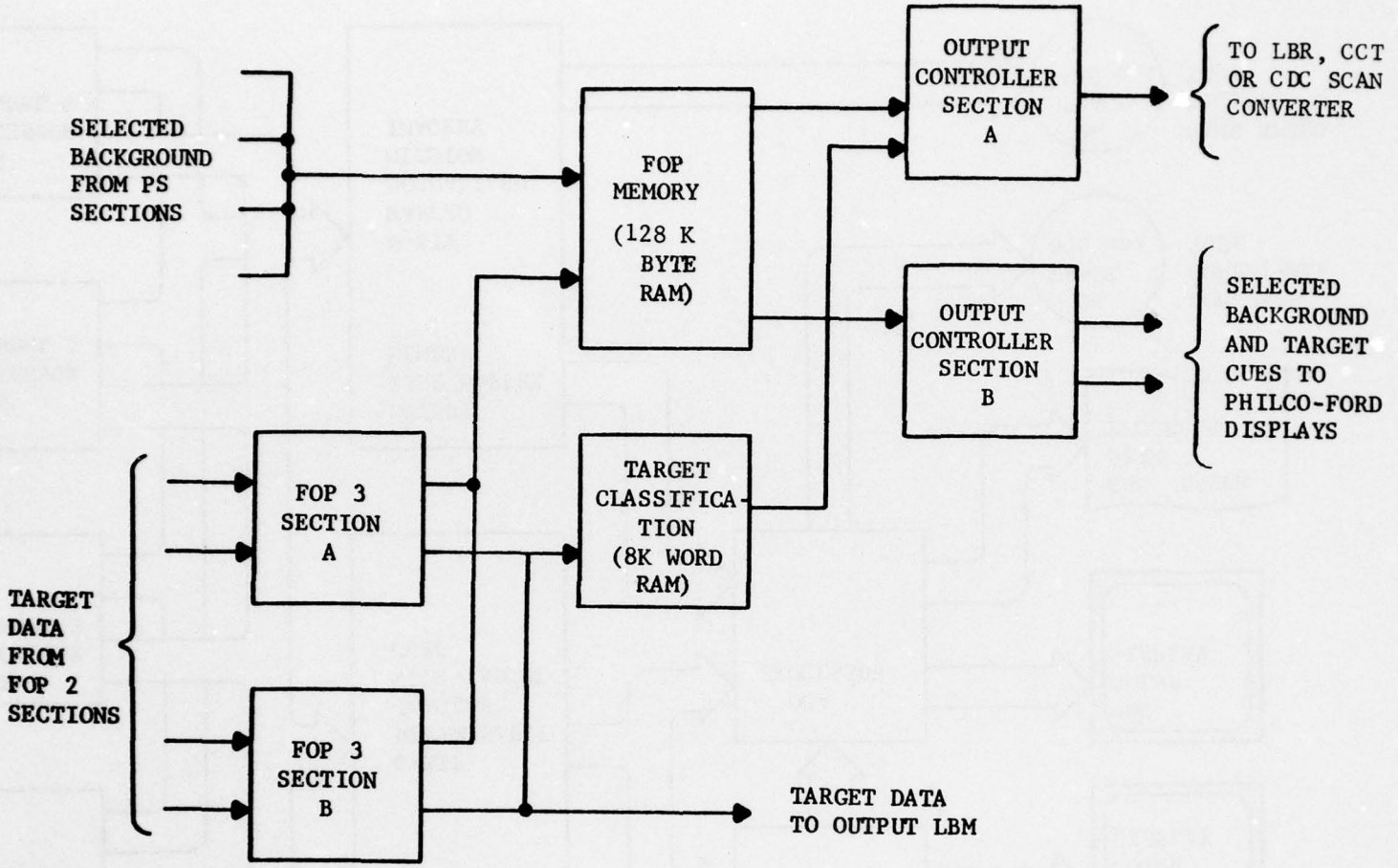

Figure 3-18. Output Processor Block Diagram

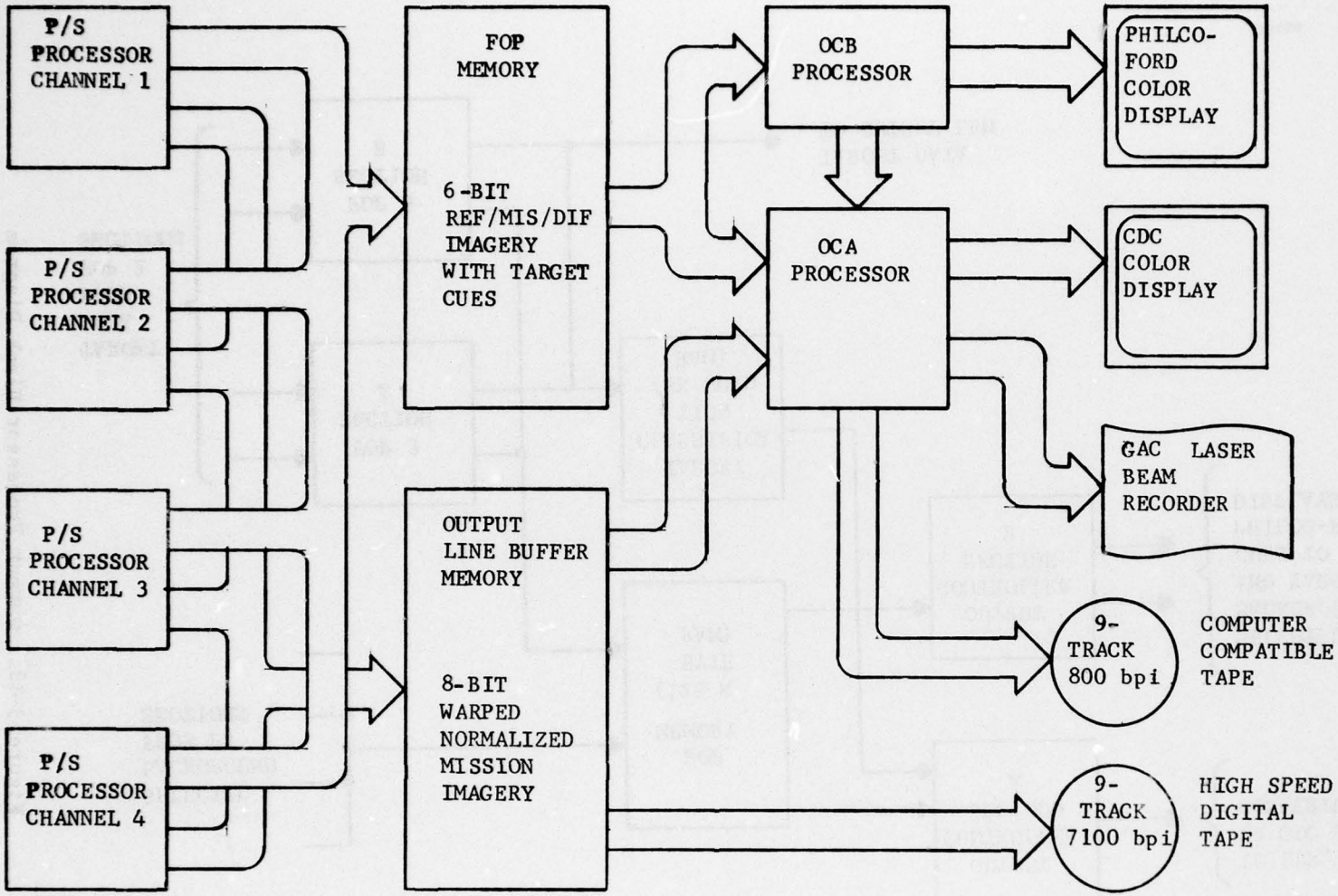

Figure 3-19. Output Processor Section Data Paths

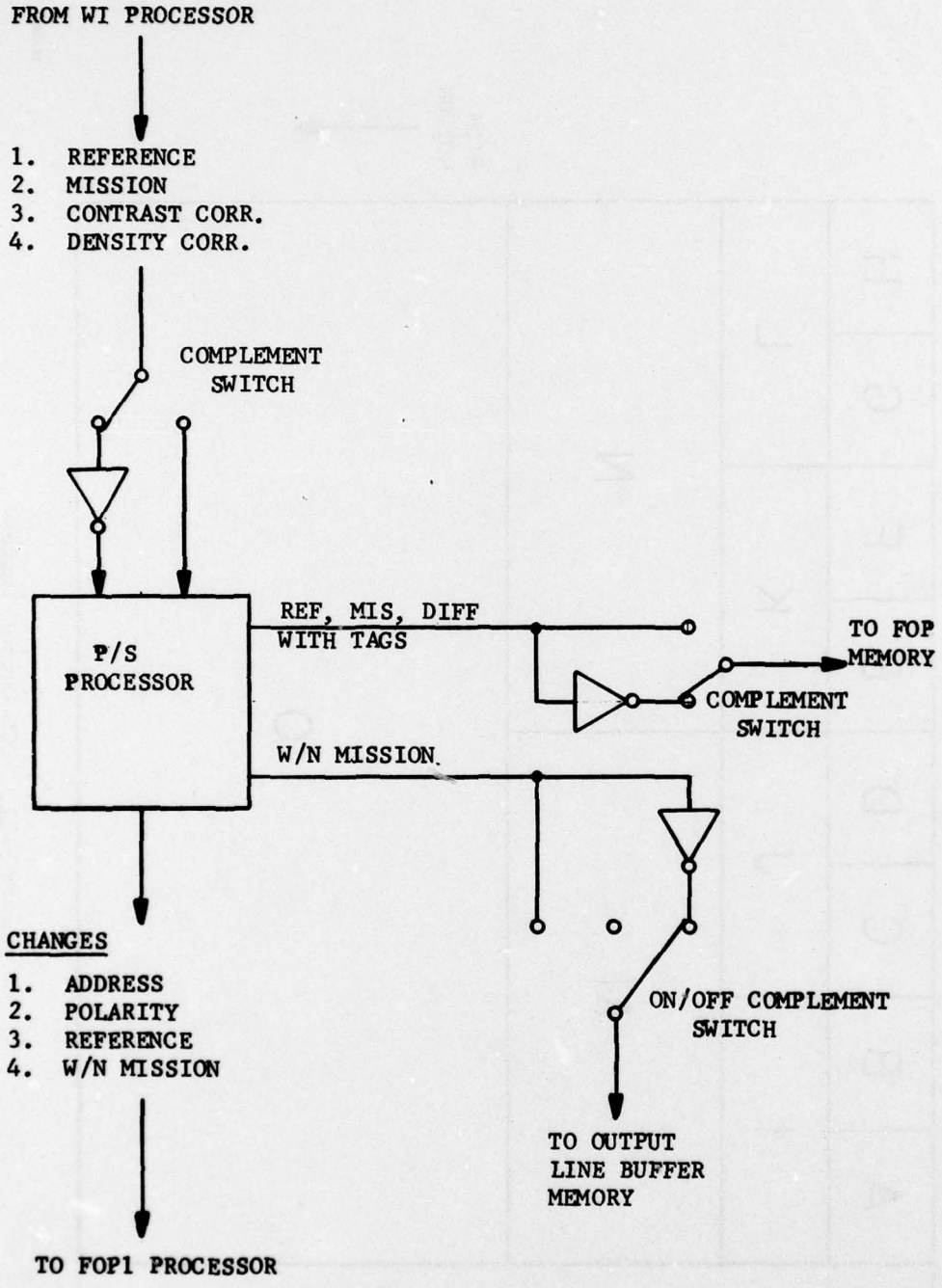

Figure 3-20. Data Paths from P/S Processors to Output Processing Section

D3985

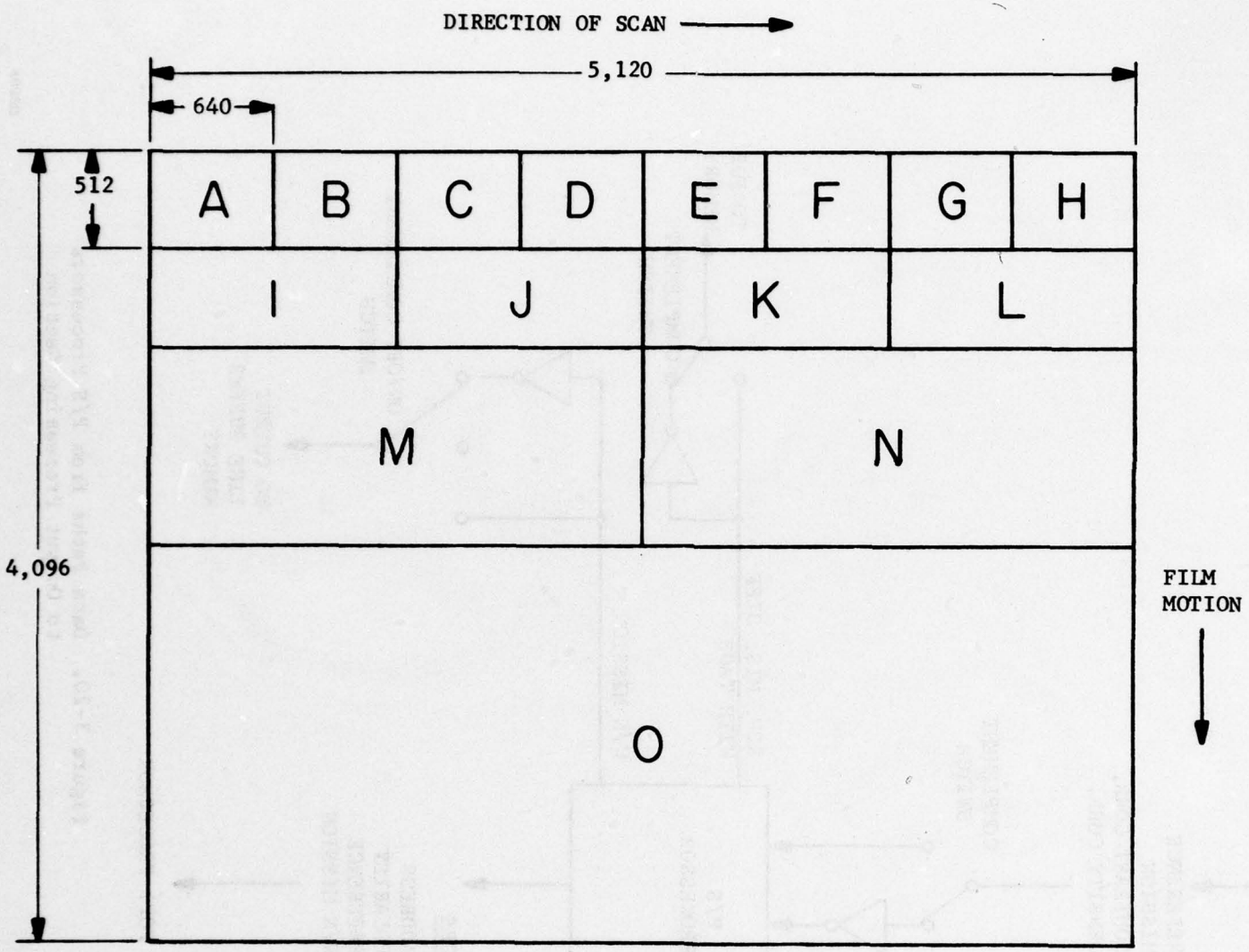

Figure 3-21. OCB Output Images

FOP TAG		
	0	no change
	1	GRID
	2	change on Mission
	3	change on Reference
	4	shadow on Reference
	5	shadow on Mission
	6	not defined
	7	not defined
	8	not defined
	9	not defined
	10	weak change on Mission
	11	weak change on Reference
	12	SCINTILLATION induced change on Mission
	13	SCINTILLATION induced change on Reference
	14	possible change on Mission
	15	possible change on Reference

Figure 3-22. FOPM Tag Definitions

OUTPUT CONVERSION

COLOR PRIORITY TAG DEFINITION

(32 GRAY LEVELS)

PRIORITY TAG 0	K=1.0 M=16
PRIORITY TAG 1	K=0.5 M=08
PRIORITY TAG 2	CYAN
PRIORITY TAG 3	MAGENTA
PRIORITY TAG 4	YELLOW
PRIORITY TAG 5	BLUE
PRIORITY TAG 6	GREEN
PRIORITY TAG 7	RED

Figure 3-23. OCB Priority Tag Definitions for Color Displays

OUTPUT CONVERSION

BLACK AND WHITE PRIORITY TAG DEFINITION

PRIORITY TAG 0	K=.25 M=16
PRIORITY TAG 1	K=.5 M=16
PRIORITY TAG 2	K=.5 M=08
PRIORITY TAG 3	K=1.0 M=16
PRIORITY TAG 4	K=2.0 M=16
PRIORITY TAG 5	GRAY
PRIORITY TAG 6	BLACK
PRIORITY TAG 7	WHITE

Figure 3-24. OCB Priority Tag Definitions for Black and White Displays

from FOPM tags to priority tags is programmable and selected by the operator. This system of programmable tags allows the operator to select which target cues to view and also the color for each cue. As the OCB processor is generating the compressed images, the highest priority tag is selected for the compressed output pixel (See Figure 3-25). Figure 3-26 shows the flow of image data through the OCB processor.

The OCA processor can perform the following output functions:

- FOP Memory to computer-compatible tape
- Output Line Buffer Memory to computer-compatible tape
- FOP Memory to GAC Laser Beam Recorder
- OCB output to CDC Digital Scan Converter

In addition, the OCA processor can receive inputs from a TRAK-Ball, GRAF-PEN and ASCII Keyboard.

MODULAR CHANGE DETECTION MICRO-PROGRAMS

All of the micro-programs in the DMCD are summarized in Table 3-10 with respect to author*, processor number and micromemory length. Also, a brief functional description is included for each program.

The names that correspond to the authors' initials in Table 3-10

* VCF - Victor C. Froehlich
RVR - Ray V. Rigles
RRD - Ron R. Denny
MEM - Michael E. Murphy
MLS - Mike L. Sandahl
BDB - Bruce D. Becker

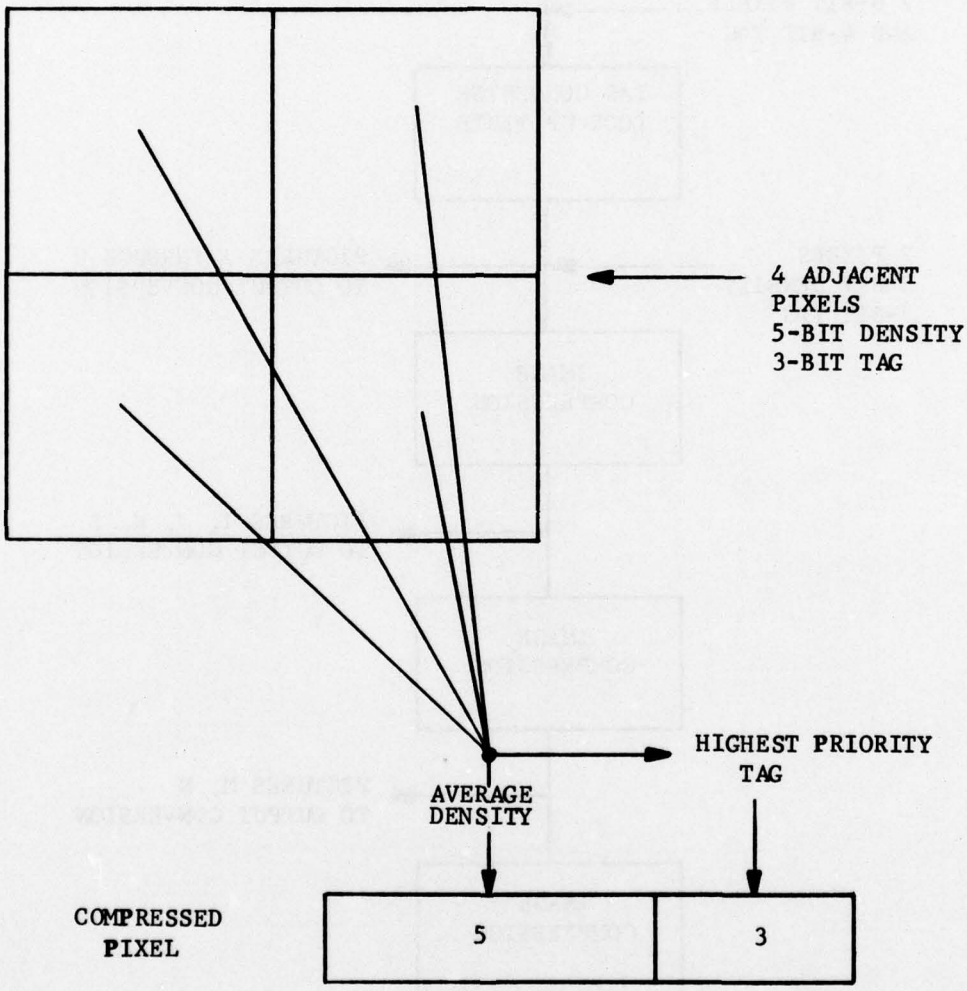

Figure 3-25. OCB Image Compression

D3987

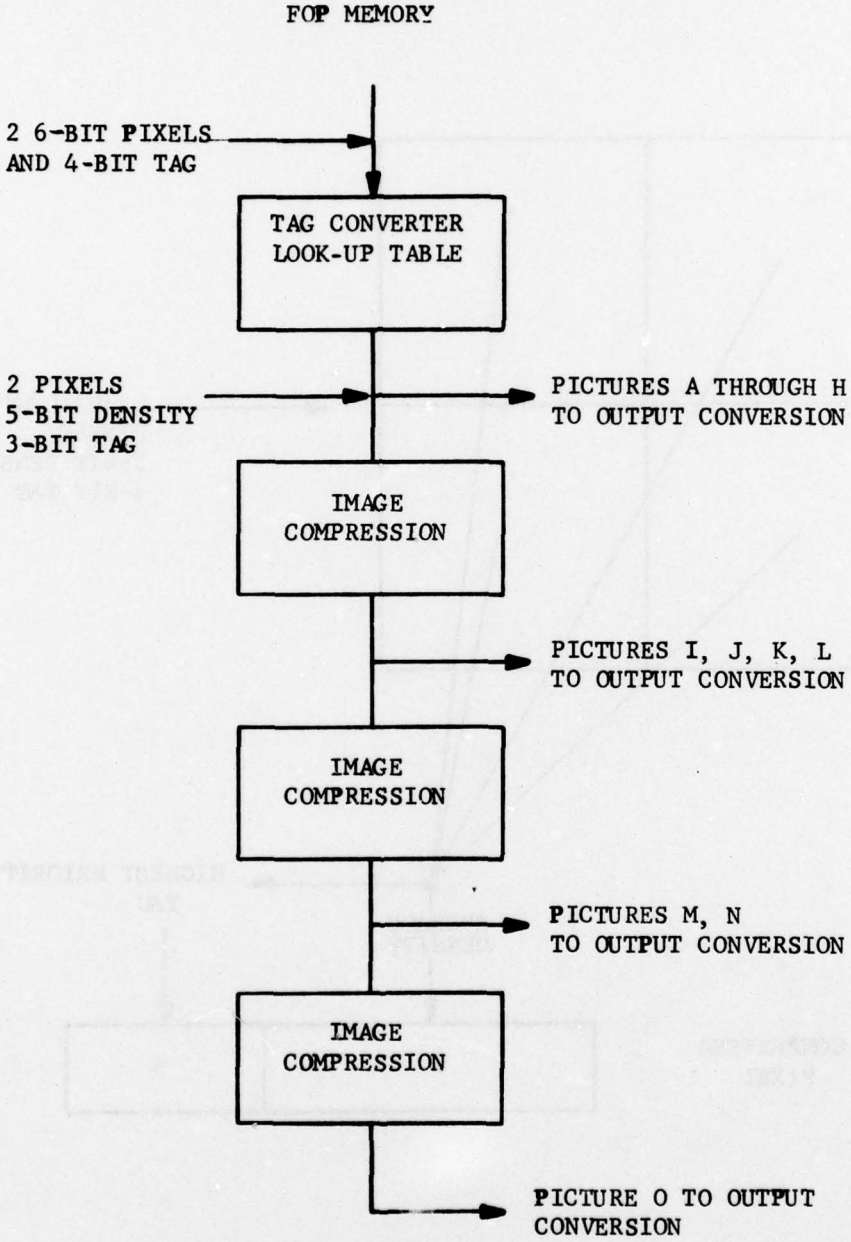

Figure 3-26. OCB Data Flow

D3988

TABLE 3-10. MODULAR CHANGE DETECTION MICROPROGRAMS

Name	Author	FP	Length	General Description
CP	VCF	1	465	CP (Control Processor) provides a link between the SC1700 and other FPs in the CDP. It updates the warp and photonormalization predictions at strip centers based on error estimates from EP calculations.
HRNS	MEM	1	494	HRNS (Strip harness) provides a weighted, linear least squares fit to the warp positions. The weight is determined by the center correlation coefficient. Strips too far from fit are pulled back into line.
IO	VCF	2	215	IO (Input/Output) performs SR/GR (slant range/ground range) corrections to the reference image. It also provides element synchronization to MA, WI, DP, PS and line synchronization to SC1700 and PS. It updates warp and photonormalization corrections for each element and calculates numerical scan memory address.
MA	VCF	3	215	MA (Memory Addressing) moves the mission image elements from the mission line buffer memory to the numerical scan memory. For each reference element, MA receives four mission elements from the numerical scan memory.

TABLE 3-10. MODULAR CHANGE DETECTION MICROPROGRAMS (CONTINUED)

Name	Author	FP	Length	General Description
WI	VCF	4	189	WI (Warp Interpolation) interpolates between the four mission elements from MA for the fractional warp. It also keeps a two line history of the warped mission image to send.
DP	VCF	5	211	DP (dop product) calculates the sums which are used by EP in determining the correlation coefficient.
EP	RVR	6	521	EP (error processing) filters the dot products, calculates correlation coefficients and performs a parabolic fit to determine error offset.
EPL	RVR	6	197	EPL contains the standard multiply, divide and square root routines used by EP.
PS	RVR	7	217	PS (photonormalization section) applies radiometric corrections to mission pixels and performs differencing and background threshold testing.
PNPS	RVR	7	16	PNPS (positive imagery) is a function code loader for PS which sets up for no inversion of input imagery.

TABLE 3-10. MODULAR CHANGE DETECTION MICROPROGRAMS (CONTINUED)

Name	Author	FP	Length	General Description
PNNG	RVR	7	16	PNNG (negative imagery) is a function code loader for PS which sets up for an inversion of input imagery.
OMON	RVR	7	4	OMON (output memory on) is a function code loader for PS which selects mission imagery to the output line buffer memory.
OMOF	RVR	7	4	OMOF (output memory off) is a function code loader for PS which selects no output for the output line buffer memory.
OMCP	RVR	7	4	OMCP (output memory compliment) is a function code loader for PS which sends the compliment of the mission imagery to the output line buffer memory.
FMRF	RVR	7	4	FMRF (FOP memory reference) is a function code loader for PS which selects reference imagery to the FOP memory.
FMDF	RVR	7	4	FMDF (FOP memory difference) is a function code loader for PS which selects difference imagery to the FOP memory.
FMMS	RVR	7	4	FMMS (FOP memory mission) is a function code loader for PS which selects mission imagery to the FOP memory.

TABLE 3-10. MODULAR CHANGE DETECTION MICROPROGRAMS (CONTINUED)

Name	Author	FP	Length	General Description
FCTR	RVR	7	4	FCTR (FOP compliment, true) sets the target polarity for the FOP memory.
FCCP	RVR	7	4	FCCP (FOP compliment, compliment) sets the compliment of the target polarity for the FOP memory.
G000	RVR	7	6	G000 (no grid) is a function code loader for PS which sets up no grid on the output imagery.
G032	RVR	7	6	G032 (32 x 32 grid) is a function code loader for PS which superimposes a 32 x 32 element grid onto the output imagery.
G034	RVR	7	6	G064 (64 x 64 grid) is a function code loader for PS which superimposes a 64 x 64 element grid onto the output imagery.
G100	RVR	7	6	G100 (100 x 100 grid) is a function code loader for PS which superimposes a 100 x 100 element grid onto the output imagery.
G128	RVR	7	6	G128 (128 x 128 grid) is a function code loader for PS which superimposes a 128 x 128 element grid onto the output imagery.

TABLE 3-10. MODULAR CHANGE DETECTION MICROPROGRAMS (CONTINUED)

Name	Author	FP	Length	General Description
G256	RVR	7	6	G256 (256 x 256) is a function code loader for PS which superimposes a 256 x 256 element grid onto the output imagery.
FOP1	RVR	8	681	FOP1 (feature oriented processing # 1) links the elements within a target, accumulates statistics over the targets and throws out small targets.
FOP2	RVR	9	460	FOP2 (feature oriented processing # 2) classifies the targets.
FOP3	MLS	A&B	112	FOP3 (feature oriented processing # 3) writes the classification information into the FOP memory.
TAG 1	RVR	D	16	TAG 1, TAG 2, TAG 3, and TAG 4 are function code loader programs for
TAG 2	RVR	D	16	the OCB program. They are FOP tag to priority tag look-up tables
TAG 3	RVR	D	16	which assign display format for the FOP tagged pixels.
TAG 4	RVR	D	16	
HIST	RVR	8	303	HIST (histogram) is a program which generates reference, mission, and difference histograms.
DMP1	RVR	ANY	43	DMP1 (dump channel 1) is a program used to dump MOS memory from DSA channel 1.

TABLE 3-10. MODULAR CHANGE DETECTION MICROPROGRAMS (CONTINUED)

Name	Author	FP	Length	General Description
DMP2	RVR	ANY	43	DMP2 (dump channel 2) is a program used to dump MOS memory from DSA channel 2.
DMP3	RVR	ANY	43	DMP3 (dump channel 3) is a program used to dump MOS memory from DSA channel 3.
SCIN	RVR	9	32	SCIN (scintillation) is a function code loader program FOP2. It is a decision table for scintillation tests.
SHAD	RVR	9	32	SHAD (shadow) is a function code loader program for FOP2. It is a decision table for shadow/weak target tests.
OCB	RRD	D	959	OCB (output controller B) controls the display output, image compression and tag interpretation (i.e. valid targets, shadows, weak targets, scintillation and/or possible targets).
OCS1	RRD	D	500	OCS1 is a function code loader for OCB which initializes the tags and sets up a cross reference for them.
ALBK	RRD	D	14	ALBK (all background) is a function code loader for OCB which displays only the existing background, ignoring any tag the elements carry.

TABLE 3-10. MODULAR CHANGE DETECTION MICROPROGRAMS (CONTINUED)

Name	Author	FP	Length	General Description
TRRG	RRD	D	2	TRRG (valid targets, red and green) is a function code loader for OCB which displays the valid targets as either red (positive target) or green (negative target).
TRBK	RRD	D	2	TRBK (valid targets, background) is a function code loader for OCB which displays the background for the valid targets.
SHCY	RRD	D	2	SHCY (shadows, cyan) is a function code loader for OCB which displays all shadows with the color cyan.
SHBK	RRD	D	2	SHBK (shadows, background) is a function code loader for OCB which displays the background of all the shadows.
SHRG	RRD	D	2	SHRG (shadows, red and green) is a function code loader for OCB which displays the shadows as either red (positive shadow) or green (negative shadow).
WTCY	RRD	D	2	WTCY (weak targets, cyan) is a function code loader for OCB which displays all weak targets with the color cyan.
WTBK	RRD	D	2	WTBK (weak targets, background) is a function code loader for OCB which displays the background of all weak targets.

TABLE 3-10. MODULAR CHANGE DETECTION MICROPROGRAMS (CONTINUED)

Name	Author	FP	Length	General Description
WTRG	RRD	D	2	WTRG (weak targets, red and green) is a function code loader for OCB which displays the weak targets as either red (positive weak targets) or green (negative weak targets).
SCMG	RRD	D	2	SCMG (scintillation, magenta) is a function code loader for OCB which displays all scintillation with the other magenta.
SCBK	RRD	D	2	SCBK (scintillation, background) is a function code loader for OCB which displays the background of all scintillation.
SCRG	RRD	D	2	SCRG (scintillation, red and green) is a function code loader for OCB which displays the scintillation as either red (positive scintillation) or green (negative scintillation).
PTBL	RRD	D	2	PTBL (possible targets, blue) is a function code loader for OCB which displays all possible targets as blue.
PTBK	RRD	D	2	PTBK (possible targets, background) is a function code loader for OCB which displays the background of all possible targets.

TABLE 3-10. MODULAR CHANGE DETECTION MICROPROGRAMS (CONTINUED)

Name	Author	FP	Length	General Description
PTRG	RRD	D	2	PTRG (possible targets, red and green) is a function code loader for OCB which displays the possible targets as either red (positive possible targets) or green (negative possible targets).
BCP	BDB	1	495	BCP controls all input from and output to the SC 1700 during auto-acquisition.
BCPI	BDP	1	9	BCPI is a function code loader program for BCP which initializes all data sent to BCP.
BIO	BDB	2	254	BIO controls the compressions of the input data and maintains a histogram of this compressed data, (used only during auto-acquisition).
BMA	BDB	3	244	BMA makes the accesses to the numerical scan memory for any programs requiring its use , (used only during auto-acquisition).
BWI	BDB	4	212	BWI computes the error functions for each candidate window, (used only during auto-acquisition).
BDP	BDB	5	219	BDP is the controller for both the coarse and fine searches during auto-acquisition.

TABLE 3-10. MODULAR CHANGE DETECTION MICROPROGRAMS (CONTINUED)

Name	Author	FP	Length	General Description
BEP	BDB	6	462	BEP makes calculations to determine the best reference window, (used during auto-acquisition).
BSP	BDB	7	255	BPS provides a quadratic approximation to estimate the best fit for the images, (used during auto-acquisition).
MMA	BDB	3	217	MMA is the off-line mosaicking controller.
MMI	BDB	4	17	MMI transfers off-line mosaicking data from MMA to PS.

4.0 SYSTEM PERFORMANCE

4.1 IMAGE REGISTRATION

Accurate spatial registration of images is essential to good change detection. The accuracy of registration can be measured in two ways: by using a Root Mean Square (RMS) error technique and by visual examination. These two techniques and some results of applying them to DMCD output are discussed in this section. Both techniques use the original reference image (REF) and the warped/photonormalized mission (W/N MIS) image.

In the RMS technique, the registration is checked (using the WECK program on the 6600) at a number of points in the image. In the examples given below, nine sites in one channel are examined at each of 34 locations along track. For a given site on the REF image, a small number (5) of sites on the W/N MIS image are examined, including the "warped" or predicted site. The distance from the W/N MIS site which best matches the REF site to the predicted W/N MIS site is the residual RMS error. The RMS errors for all the REF sites are averaged to produce a number which reflects the "goodness of warp" for a complete run. By this measure, the DMCD performance of spatial correction is very good (See Table 4-1). Even for the case with the artificially severe warp and photodensity distortions, the RMS error is less than a pixel. RMS errors typical of "real" data range between .5 to 2.0 pixels. Results are not quite so good, however, if one examines the maximum residual error instead of the average. A maximum of up to three times the average can occur (See Table 4-1). However, the maximum or near maximum must occur at a very small percentage of the total image area, or the site sampling would find more large residuals and the RMS error would be larger. So, it appears that the DMCD registers "nearly all" of an image pair to within a pixel or two with "very occasional" misregistration of up to four pixels.

However, both the registration process and the WECK program use the correlation coefficient to measure image similarity. Knowing this, we must

TABLE 4-1. SELECTED RMS ERRORS

IMAGERY	RMS	MAX RESIDUAL
1) Gallant Hand A vs Gallant Hand B	.79	2.47
2) Gallant Hand B vs Gallant Hand B with $\pm 2^{o}$ yaw $\pm$ 25% stretch along track $\pm$ 5% stretch in range mean and standard deviations reduced	.81	1.77
ERIM 350-2 Pass 1 vs ERIM 352-2 Pass 3	1.61	4.54

not assume that a low RMS error means good registration unless we also know that the correlation coefficient is a good measure of image similarity. This brings us to the visual technique for measuring accuracy of registration. NOTE: A low RMS error does mean that the registration process is capable of removing "almost all" of the warp as perceived by the correlation coefficient.

In the visual technique for measuring registration accuracy, the REF and W/N MIS images are superimposed using the CDC scan converter or, as in the example included in this report (Figures 4-1 and 4-2), using transparencies and a light table. The images are aligned assuming zero residual misregistration and the apparent displacement of selected strong features is measured using the cursor (scan converter) or estimated by counting pixels (transparencies). The emphasis is on the maximum misregistration but with a little practice, one becomes good at estimating the percent of the scene which is misregistered by a given amount. Examining the transparencies included (Pair 3 from Table 4-1) with this in mind, we find a small region ($\approx$10%) in the lower right registered very well (less than a pixel), a small region ($\approx$15%) in the upper right registered poorly (between two and four pixels error), and the rest of the scene within one to two pixels. This is essentially the same information as that conveyed by the RMS error of 1.61 and the maximum residual of 4.54. (Note that the visual technique could be used to produce an RMS measure but that this would require several man-hours.) So, we conclude that the correlation coefficient is a good measure of image similarity and that the DMCD registration algorithm works very well.

There is, however, an apparent problem with DMCD registrations: when the same pair of images from HSDT are run with the same set-up, the registration results are not the same. The residual errors, though still small, are not necessarily in the same direction from run to run. This has the effect of causing the FOP algorithm to classify a given strong return differently from run to run, making the selection of FOP parameters impossible.

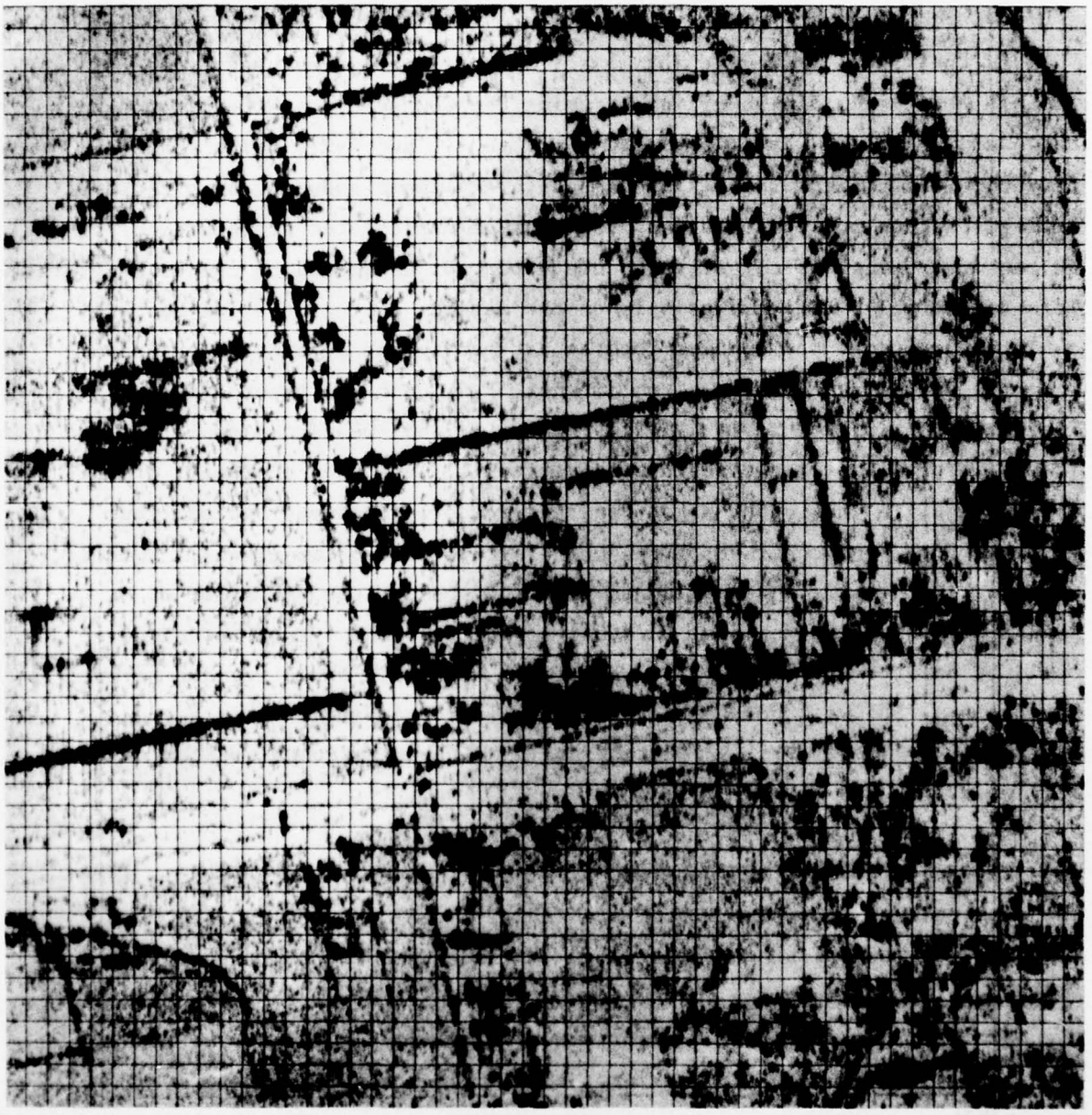

Figure 4-1. ERIM 350-2 Pass 1 20 x 20 Grid

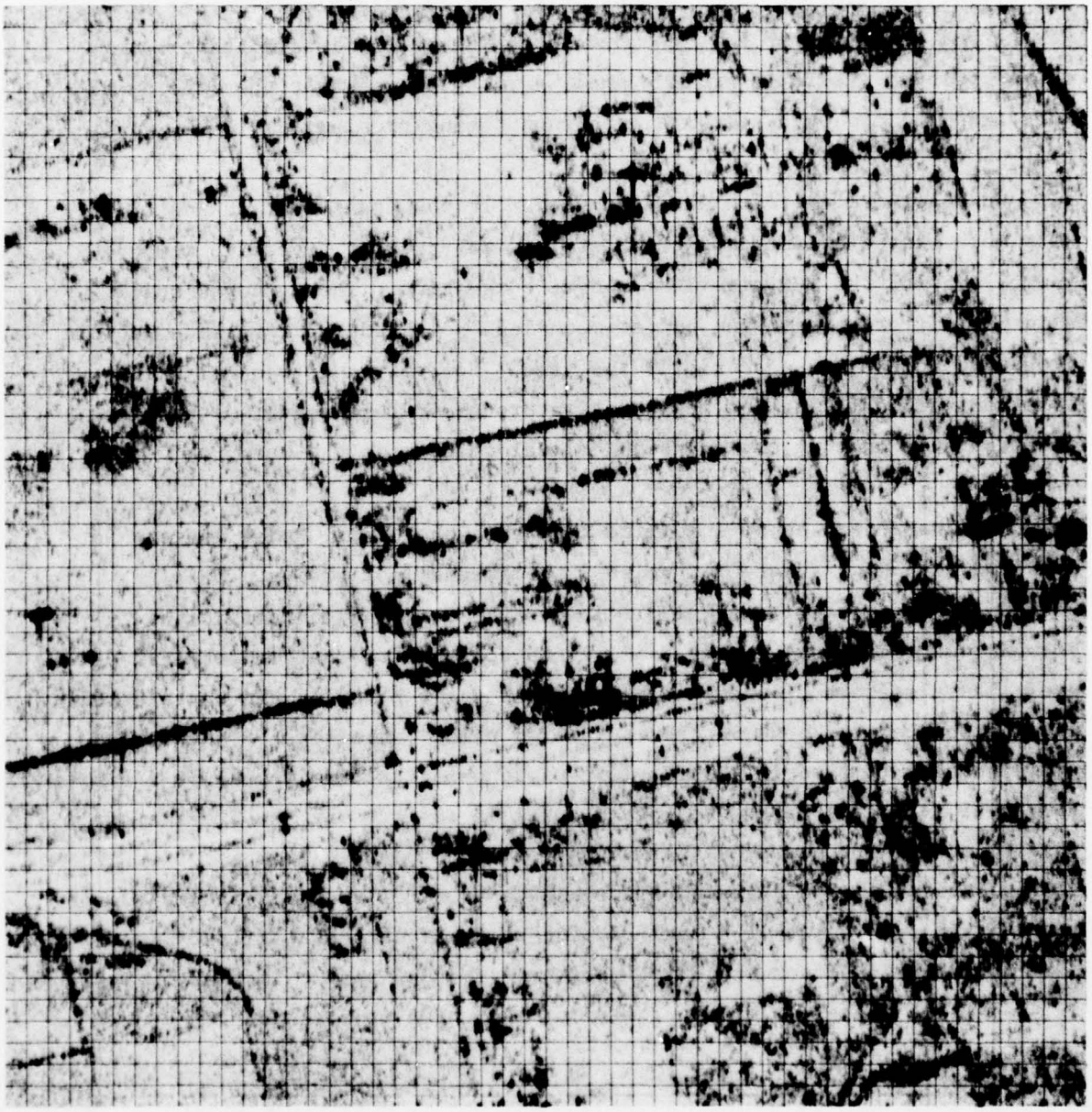

Figure 4-2. ERIM 352-2 Pass 3 20 x 20 Grid

How can an all digital system be inconsistant? After many man-months and much investigation it was determined that randomly and occasionally (approximately one in 500 lines) a line of input image would disappear, as though the tape unit had skipped a record. This had the effect of presenting slightly different input images which led to slightly different warps. Fixing the HSDT has, so far, not been done due to the intermittent nature of the problem (there is still a small - .5% - chance that the line dropouts are produced by a software interrupt timing problem).

An alternate approach was attempted. It was found that making the warp more stable by increasing the strip width and the recursive memory length enabled the FOP algorithm become consistent. The warp was still slightly different each run but so much less so that the difference picture presented to FOP was essentially the same. However, this was not a good solution, since making the registration process unresponsive to the line dropouts also made it unresponsive to real changes in the warp.

Still another way to stabilize the warp was found. Radar imagery is peppered with high frequency "noise", the images look grainy. This graininess has two effects: 1) it lowers the correlation coefficient between two registered images, making the correlation coefficient less useful as a measure of image similarity and 2) it broadens the correlation surface so that the peak at the registered point is harder to "see". The graininess is removed in the off-line photonormalization process by a simple four-cell averaging technique. Each pixel is replaced by the average of itself and its three nearest neighbors. Note that positional accuracy of strong returns is not degraded since the centroid of a strong return is not moved by this technique. A small amount of image contrast is lost but this does not seem to affect the FOP algorithm. The net result is that the warp is stable for filtered imagery, thereby making FOP consistent.

4.2 FEATURE ORIENTATED PROCESSING PERFORMANCE

The Feature Orientated Processing section attempts to improve the change detection output by classifying changes to determine whether a feature is a:

1) Legitimate change
2) Weak target
3) Shadow-induced change
4) Scintillation-induced change
5) Small noise-induced change

Figures 4-3, 4-4, and 4-5 show some output of this process. Figures 4-3 and 4-4 are the reference and mission images that were input to the DMCD. Figure 4-5 shows the FOP processed color cues superimposed on the reference image. The changes are color coded as follows:

Red: additions to reference image
Green: deletions from reference image
Magenta: scintillation-induced change

Although a thorough analysis of the FOP algorithm was not in the scope of this contract, a number of qualitative conclusions about the algorithm's implementation and performance can be stated:

1) The FOP algorithm does a good job of suppressing small noise-induced changes. The implementation has a limit of 50 active change events per channel. This limit does not affect the algorithm's performance.
2) The suppression of scintillation-induced changes is acceptable provided that the change events have an area of at least 10 pixels and the images are in precise registration.
3) The algorithm was implemented using 10 flexible processors. Four processors were used for linking change events, four were used for classifying change events, and two processors were used for applying the color cues. By merging the classification and color cueing

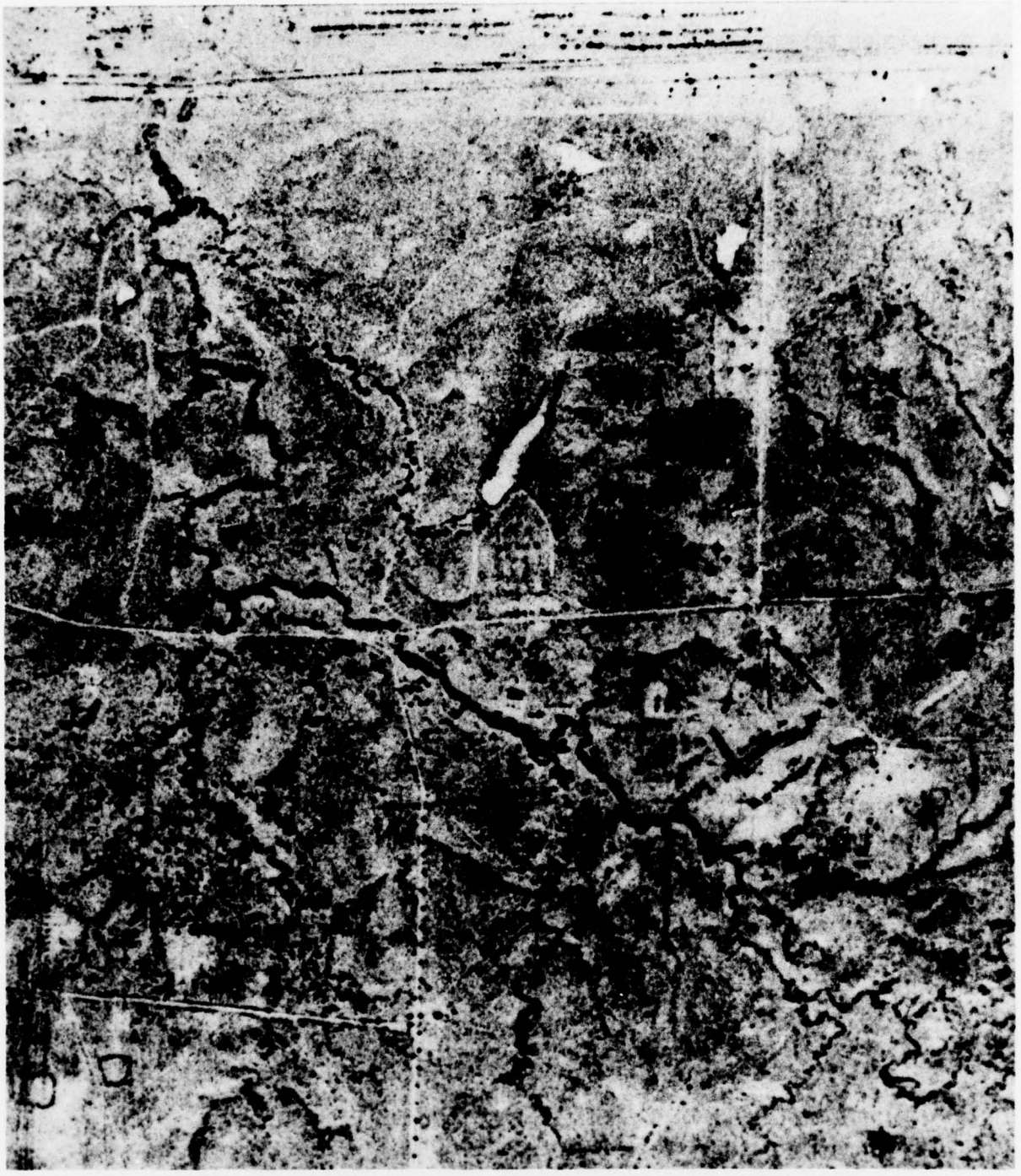

Figure 4-3. Reference Image

Figure 4-4. Mission Image

Figure 4-5. FOP Output

processes into four processors instead of six, this total could be reduced to eight flexible processors without any change in the processing capability.

4) A major fault in the current algorithm is that the parameter thresholds are very sensitive to image quality, i.e. a function of the mean and standard deviation of the reference image. The utility of the algorithm would be greatly improved if the parameter thresholds were computed automatically from the reference image statistics.

4.3 FOUR CHANNEL FILM

Three sets of four channel film were available for checkout while the DMCD was in the DISD research laboratory: 1) Paul Murphy UPD-6 film, 2) Gallant Hand UPD-4, and 3) Reforger UPD-4.

- The Paul Murphy film was effectively only one channel film because there were missing channels, and there was no continuity between adjacent channels.
- The Gallant Hand film was used on initial checkout, but proved to be too low in contrast for consistent automatic acquisition.
- The Reforger film was the best of the three, and was evaluated in detail. Two pairs of Reforger films were used, herein called RF1 and RF4:

RF1 Reference	= B-22A	Dated 12 Oct. 1974
RF1 Mission	= B-24A	Dated 17 Oct. 1974
RF4 Reference	= B-35A	Dated 11 Oct. 1974
RF4 Mission	= B-88A	Dated 13 Oct. 1974

Both RF1 and RF4 had acceptable contrast values for auto acquisition and change detection, but still had the following notable problems:

a) Excessive shear between adjacent channels:
   B-22A - 4 lines (RF1)
   B-24A - 12 lines (RF1)

B-35A - 26 lines (RF4)

B-88A - 22 lines (RF4)

The DMCD has no way to remove this shear while it is doing change detection.

b) Means and standard deviations change significantly between channels:

B-24A	Ch. 1	$\mu = 170$	$\sigma = 30.0$
	Ch. 2	$\mu = 174$	$\sigma = 26.5$
	Ch. 3	$\mu = 184$	$\sigma = 32.0$
	Ch. 4	$\mu = 164$	$\sigma = 40.0$

Within each channel, the mean increased and the standard deviation decreased near the edges of the channel. On the outside edges of channels 1 and 4 this was a very steep change.

The DMCD has no way to smooth these abrupt changes at the mosaic boundary at the same time as doing a change detection.

c) Sometimes, two adjacent channgels would not overlap. This would cause a gap in the mosaicked image.

d) The X offset between reference and mission changes rapidly as lines are advanced. For RF1:

X = 384	$\Delta X = 48$
X = 704	$\Delta X = 56$
X = 1408	$\Delta X = 72$
X = 1472	$\Delta X = 76$
X = 1872	$\Delta X = 84$

The Y warp changes as lines advance, and across a given channel. Also, the nature of the change in Y warp changes between adjacent channels.

RFI, X = 896	Ch. 1 ΔY	Ch. 2 ΔY
Y = 80	42	34
Y = 400	40	20
Y = 720	40	12
Y = 1040	36	6
(X = 1472)	Ch. 1	Ch. 2
Y = 160	52	38
Y = 480	50	26
Y = 800	48	18
Y = 1120	44	10

Because of this, the warp is not continuous across mosaic boundaries. Also, the auto acquisition offset is not predictable either down track or across channels.

4.4 AUTOMATIC ACQUISITION

The Automatic Acquisition algorithm has been proven to work on all sample imagery - Senior Lance, Ft Sill, Paul Murphy, Gallant Hand, and Reforger. But a certain sensitivity exists: 1) A true standard deviation of at least 30 (on a 0-255 scale) is usually required. 2) Numerous shortcomings in the quality of the four channel film can cause auto acquisition failure. 3) Certain areas of an image, urban areas or those without a large definitive feature, just do not take to acquisition. Usually, choosing a different search area solves the last problem.

But, even though auto acquisition usually works, it has not been a useful tool for initiating change detection on the sample four channel films. A discussion of the problems encountered in transferring an auto acquisition result to Four Channel Change Detection follows.

Three categories of auto acquisition problem areas exist: 1) Selection of a bad Reference Window (RW), 2) Search algorithm fails to find the mission window, and 3) Mission window found but not close enough for change detection. The following list defines these problems, their causes, and possible solutions.

a) RW contains prominent false features. A false feature is a very bright or dark area which is on the film but not on the image. This could be caused by a film imperfection (see film problem d for example) or a range mark. A solution for bright false features is to complement the input image, since the Range Mark Remover works on dark features only. The only other solution is to adjust the RW selection area so the false feature is not included.

b) Random RW Selection. This is caused by featureless terrain or very low standard deviation. Very low standard deviation can sometimes be improved by adjusting the scanner gain and bias. If the image is featureless then a new or larger RW selection area could be tried.

c) Search algorithm fails due to low standard deviation. A mission standard deviation of 30 to 40 is needed for the search algorithm to be consistent. If gain and bias can not be adjusted to put the standard deviation in this range, than auto acquisition is unlikely.

d) Search algorithm fails due to varying mean and standard deviation. (See film problems b and c.) Unless the Y offset between reference and mission is close to zero, the mission fit window will fall on a different part of the four-channel swath than the RW (perhaps covering the end of one channel and the beginning of the next). The contrast and density corrections would then be based on invalid data for part of the window, and the mission window would not be found. Off-line photonormalization successfully solved this problem on the RF1 films.

e) From 1000 to 3000 lines of image are needed to perform an Automatic Acquisition. The result is a ΔX and ΔY offset pair from a point on the reference film to the mission film. ΔX and ΔY vary

so much along the film, that an offset pair can only be a valid input to change detection at or near the point where it was computed (See film problems e and f). This means that change detection can only be done from auto acquisition results, when both films are repositioned to the line where the result was found. Note that this warp prediction problem exists with SAPPHIRE data also and that the SAPPHIRE input cannot be repositioned automatically.

f) When change detection is attempted following an auto acquisition, with ΔY not close to zero, portions of two mission channels will be registered against one reference channel. The change detection program will remove the interchannel gap, but it cannot correct for the shear (See film problem a). Image continuity will be lost at the channel separation line, and registered values of ΔX for each strip will differ markedly on each side of the line. The Harness program cannot handle the discontinuity in ΔX and will try to make ΔX smooth across the channel, pulling some strips out of registration. This problem can be eliminated by doing off-line mosaicking before auto acquisition.

g) The Reference Window and the Reference Window Selection area are identical on all four CDP's. The mission search areas cover all four film channels and are all different. The mission fit window is found on exactly one CDP. Change detection can normally be started from auto acquisition on the film channel which contains the matching windows, but not on the other channels.

This problem is caused by the difference in the Y-warp between film channels (See film problem f). If it is an inherent problem with the four channel film, then it cannot be solved. A combination of off-line mosaicking, off-line photonormalization, and SR/GR corrections can be used to raise the probability of successful Four Channel Change Detection.

4.5 RELIABILITY/MAINTAINABILITY (DIAGNOSTIC CAPABILITY)

The diagnostic system was designed to provide modular fault isolation in a pre-determined amount of time, this allows minimum down time.

The diagnostics are a combination of tests done by the SC1700 and microcode, self-testing programs. Each hardware unit (FP, tape drive, etc.) has an individual test or set of tests.

If a failure is encountered by the diagnostic, a message will be sent to the operator via the standard output device. These vary depending on the unit being tested. The types of messages are, 1) an explanation of the error and a card replacement slot, or slots, 2) only the slot or slots 3) an explanation of the error. The replacement card slots are all pre-determined (See Table 4-2) by using failure probability tables and diagnostic failure modes.

The method of testing may vary depending on the operator's knowledge of the failure. If the specific area to test cannot be determined from the information available testing may be conducted on all FP's in a correlator, executing tests in all FP's simultaneously. If the failure can be isolated to an individual unit, testing may be done by using a group of tests or an individual test.

TABLE 4-2. DIAGNOSTIC TABLE

PROGRAM NAME		FP NAME AND EQUIPMENT CODE													REPLACEMENT CARD SLOT BY PROBABILITY RATE AND TEST AREA	CARD SLOT NUMBER AND NAME	
CARD LEVEL	ERROR LEVEL	CP 1-(E)	IO 2	MA 3	WI 4	DP 5	EP 6	PS 7	FOP 1 8	FOP 2 9	FOP 3A A	FOP 3B B	OCA C	OCB D			
BDIAG		X	X	X	X	X	X	X	X	X	X	X	X	X	Z	1	DATCH
T001	TBUS	X	X	X	X	X	X	X	X	X	X	X	X	X	31-22-33-26-24	2	DAQCH
T002	RTF1		X	X	X	X		X			X	X	X		21-22	3	CQTCH
T003	RTF2									X					23-22	4	OPEN
T004	RTF3						X		X						25-22	5	DATCH
T005	RTF4	X												X	27-22	6	DAQCT
T006	RTF8	X	X	X	X	X	X	X	X	X	X	X	X	X	22-21	7	CQTCH
T007	INDX	X	X	X	X	X	X	X	X	X	X	X	X	X	31-33	8	OPEN
T008	CND3	X	X	X	X	X	X	X	X	X	X	X	X	X	31-33-29	9	DATCH
T009	AL2A	X	X	X	X	X	X		X	X			X	X	28-30-32	10	DAQCT
T010	AL2B	X	X	X	X	X	X		X	X			X	X	28-30-32	11	CQTCH
T011	AL2C	X	X	X	X	X	X		X	X			X	X	28-30-32	12	OPEN
T012	AL2D	X	X	X	X	X	X		X	X			X	X	28-30-32	13	DATCH
T013	AL2E	X	X	X	X	X	X		X	X			X	X	28-30-32	14	DAQCT
T014	AL2F	X	X	X	X	X	X		X	X			X	X	28-30-32	15	CQTCH
T015	AL1A							X			X	X			28-30	16	MULTY
T016	AL1B							X			X	X			28-30	17	IRPT1
T017	AL1C							X			X	X			28-30	18	TMPFLØ
T018	AL1D							X			X	X			28-30	19	IRPT2
T019	CND0	X	X	X	X	X	X	X	X	X	X	X	X	X	28-30-29	20	TMPFL1
T020	CND1	X	X	X	X	X	X	X	X	X	X	X	X	X	31-33-29	21	MINEM
T021	CND2	X	X	X	X	X	X		X	X			X	X	28-30-32-29	22	MCNT1
T022	EXPN	X	X	X	X	X	X	X	X	X	X	X	X	X	16	23	MINEM
T023	TRAP	X	X	X	X	X	X	X	X	X	X	X	X	X	17-19	24	MCNT2
T024	TM0A	X	X		X	X	X	X	X	X	X	X	X	X	18	25	MINEM
T025	TM0B	X	X		X	X	X	X	X	X	X	X	X	X	18	26	MCNT3
T026	TM1A	X	X			X	X		X	X			X	X	20	27	MINEN
T027	TM1B	X	X			X	X		X	X			X	X	20	28	FRACK
T028	LR0A	X	X		X		X		X	X	X	X	X	X	34-36	29	MASK
T029	LR0B	X	X		X		X		X	X	X	X	X	X	34-36	30	ARILUØ
T030	LR1A	X	X		X		X		X	X				X	38-40	31	INDX1
T031	LR1B	X	X		X		X		X	X				X	38-40	32	ARILU1
T032	DSA1													X	MA	33	INDX2
T033	DSA2										X				MA	34	LRGFLØ
T034	DSA3												X		MA	35	OUTREGØ
T035	DS11													X	MA	36	LRGFLØ
T036	DS32														MA-OP	37	OUTREG1
T037	Q108														M-OP	38	LRGFL1
T038	Q116		X												M	39	INPFLØ
T039	Q132													X	M	40	LRGFL1
	Q164														M-OP	41	INPFL1
T041	Q208							X							M		
	Q216														M-OP		
T043	Q232										X				M		
T044	Q264			X											M		
	Q308														M-OP		
	Q316														M-OP		
T047	Q332												X		M		
T048	Q364			X											M		
T049	Q118													X	M		
T050	INPE	X	X	X	X	X	X	X	X	X					NONE		
T051	INPI		X												39-41-35 IP		
T052	INPL			X											39-35 IP		
T053	INPW				X										39-35-37 IP		

TABLE 4-2. DIAGNOSTIC TABLE (CONTD.)

PROGRAM NAME		FP NAME AND EQUIPMENT CODE													REPLACEMENT CARD SLOT BY PROBABILITY RATE AND TEST AREA		CARD SLOT NUMBER AND NAME	
CARD LEVEL	ERROR LEVEL	CP (-E)	IO 2	MA 3	WI 4	DP 5	EP 6	PS 7	FOP 1 8	FOP 2 9	FOP 3A A	FOP 3B B	OCA C	OCB D				
T054	INPD					X									39-41-35-37	IP	1	DATCH
T055	INPX						X								39-41-35-37	IP	2	DAQCH
T056	INPA							X							39-41-35	IP	3	CQTCH
T057	INPB								X						39-35-37	IP	4	OPEN
T058	INPC									X					39-41-35		5	DATCH
T059	INPS															OP	6	DAQCT
T060	INPT															OP	7	CQTCH
T061	INPF												X		39		8	OPEN
T062	INPG													X	39	IP	9	DATCH
T063	OUTC														39-41-35-37	IP	10	DAQCT
T064	D108															OP	11	CQTCH
	D132															OP	12	OPEN
	D208															OP	13	DATCH
	D232															OP	14	DAQCT
	D264															OP	15	CQTCH
	D332															OP	16	MULTY
	D318															OP	17	IRPT1
	D328															OP	18	TMPFLØ
	D118															OP	19	IRPT2
	D364															OP	20	TMPFL1
T074	Q318												X		M		21	MIMEM
T075	Q328														M	OP	22	MCNT1
T076	(DSA2)											X			MA		23	MIMEM
T077	(Q232)											X			M		24	MCNT2
T078	LROC	X	X		X		X		X	X	X	X	X	X	34-36		25	MIMEM
T079	(DSA1)							X							MA		26	MCNT3
T080	(Q132)							X							M		27	MIMEN
T081	LR1C	X	X		X		X		X	X				X	38-40		28	FRACK
T082	DS31												X		MA		29	MASK
T083	(DS11)										X	X			MA		30	ARILUØ
T084	(Q118)										X	X			M		31	INDX1
T085	(Q108)										X	X			M		32	ARILU1
T086	(DSA2)			X											MA		33	INDX2
T087	(DSA1)										X	X			MA		34	LRGFLØ
T088	(DSA3)			X											MA		35	OUTREGØ
T089	(Q116)			X											M		36	LRGFLØ
T090	(DSA1)		X												MA		37	OUTREG1
T091	(DSA2)							X							MA		38	LRGFL1
T092	(DSA1)			X											MA		39	INPFLØ
T093	(Q108)														M		40	LRGFL1
	EXP3	X	X	X	X	X	X	X	X	X	X	X	X	X		OP	41	INPFL1
	HSCC	X														OP-IP		
	HSCA		X	X	X	X	X	X	X	X	X	X	X	X		OP-IP		
	D116															OP		

5.0 DIGITAL RADAR ANALYSIS

Imagery utilized by CDC for change detection and feature oriented processing algorithm definition and testing came from sampled radar film. If the DMCD System was to receive data from a digital doppler phase history correlator (DPHC), a determination of the effect of digital data on the algorithm was necessary. To determine these effects, a study was done on the CDC change detection simulator using data from two digital DPHC, HIRSADAP, FLAMR.

5.1 HIRSADAP DATA

5.1.1 Conversion To Gray Scale

Prior to any change detection processing using the HIRSADAP Radar Data, a conversion to gray scale data had to be made. The range bin data received by Digital Image Systems Division consisted of 11-bit binary floating point numbers. The data was recorded in 12-bit fields with the mantissa contained in the lower 8 bits, 1 bit of zero and the exponent found in the upper 3 bits as shown in Figure 5-1.

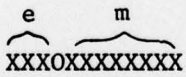

Figure 5-1. 11-Bit Binary Floating Point Range Bin Format

For the initial conversion, 8-bit gray values were desired. This implies $0 \leq g_i \leq 2^8 - 1$, where g_i represents the amplitude of the range bin in gray scale. Since $0 \leq \log_2$ (mantissa) < 8 and $0 \leq$ exponent ≤ 7, this implies $0 \leq [\log_2$ (mantissa) + exponent$] < 15$ or $0 \leq [\log_2$ (mantissa) + exponent$] < 2^4 - 1$. By multiplying this output by $2^4 + 1$, the desired range of values is obtained. The conversion formula takes the following form, therefore:

$$g_i = [\log_2 \text{ (mantissa)} + \text{exponent}] [2^4 + 1]$$

The four resulting images, azimuth look 1 and azimuth look 2 from pass 1, along with azimuth look 1 and azimuth look 2 from pass 2 are found in Figures 5-2, 5-3, 5-4, and 5-5, respectively. Figures 5-6, 5-7, 5-8, and 5-9 are the corresponding histograms. Table 5-1 is a summary of the statistical data related to each of the images.

TABLE 5-1. SUMMARY OF STATISTICAL DATA

	MINIMUM GRAY VALUE	MAXIMUM GRAY VALUE	MEAN	STANDARD DEVIATIONS	ENTROPY
AZIMUTH LOOK 1 PASS 1	44	252	150.53	12.86	4.74
AZIMUTH LOOK 2 PASS 1	44	252	148.79	12.76	4.74
AZIMUTH LOOK 1 PASS 2	77	230	150.88	12.70	4.74
AZIMUTH LOOK 2 PASS 2	71	230	147.79	12.55	4.73

5.1.2 Integration Techniques

Essentially three forms of integration were investigated. First, noncoherent averaging of azimuth look 1 and 2 for each pass; second, adjacent cell averaging in range for each azimuth look; and third, adjacent cell averaging in azimuth for each azimuth look. The resulting images for each of the integration techniques for pass 1 are as follows: Figure 5-10, noncoherent average, looks 1 and 2; Figure 5-11, adjacent cell average in range, look 1; Figure 5-12, adjacent cell average in range, look 2; and Figure 5-13, adjacent cell average in azimuth, look 2.

The resulting images for each of the integration techniques for pass 2 are as follows: Figure 5-14, noncoherent average, looks 1 and 2; Figure 5-15,

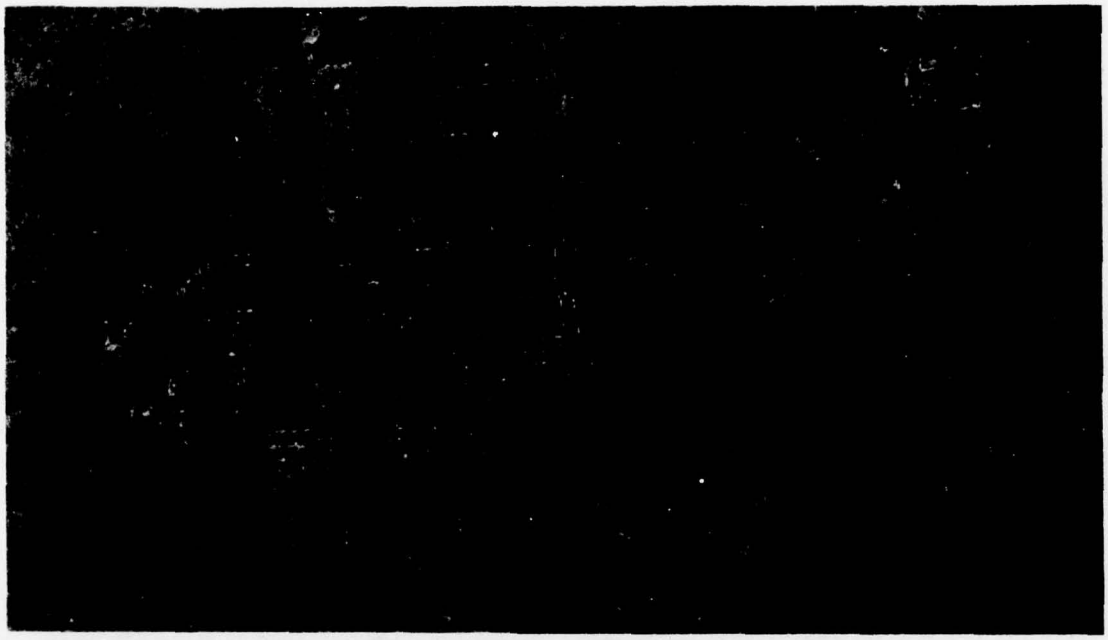

Figure 5-2. Azimuth - Look 1, Pass 1

Figure 5-3. Azimuth - Look 2, Pass 1

Figure 5-4. Azimuth - Look 1, Pass 2

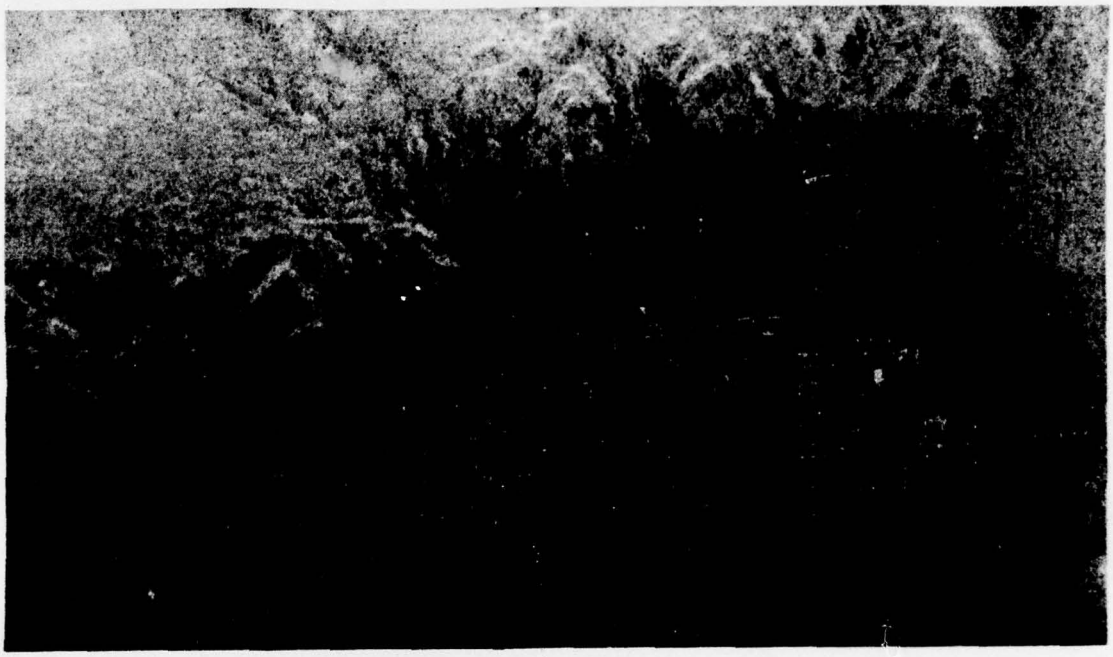

Figure 5-5. Azimuth - Look 2, Pass 2

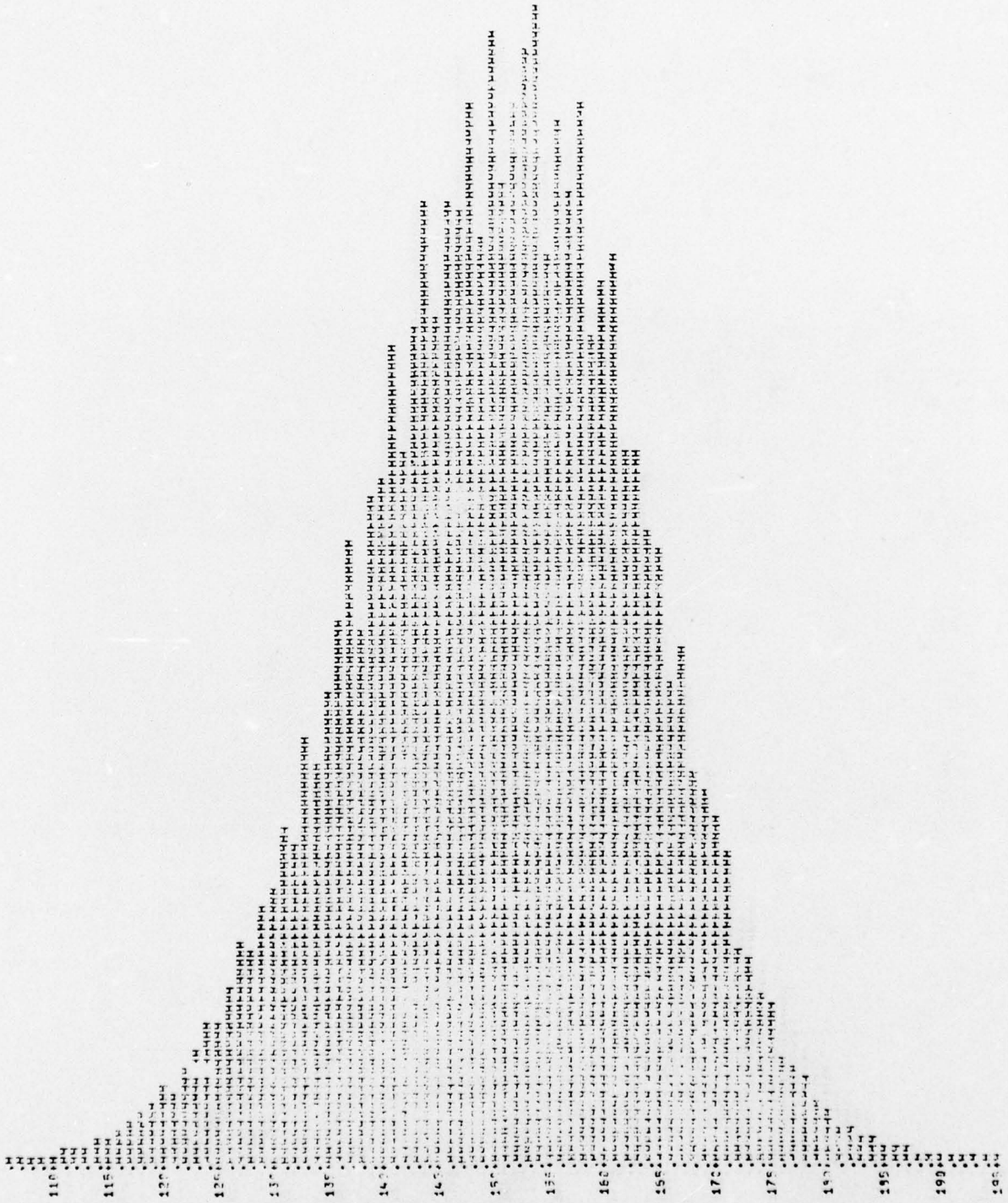

Figure 5-6. Azimuth - Look 1, Pass 1

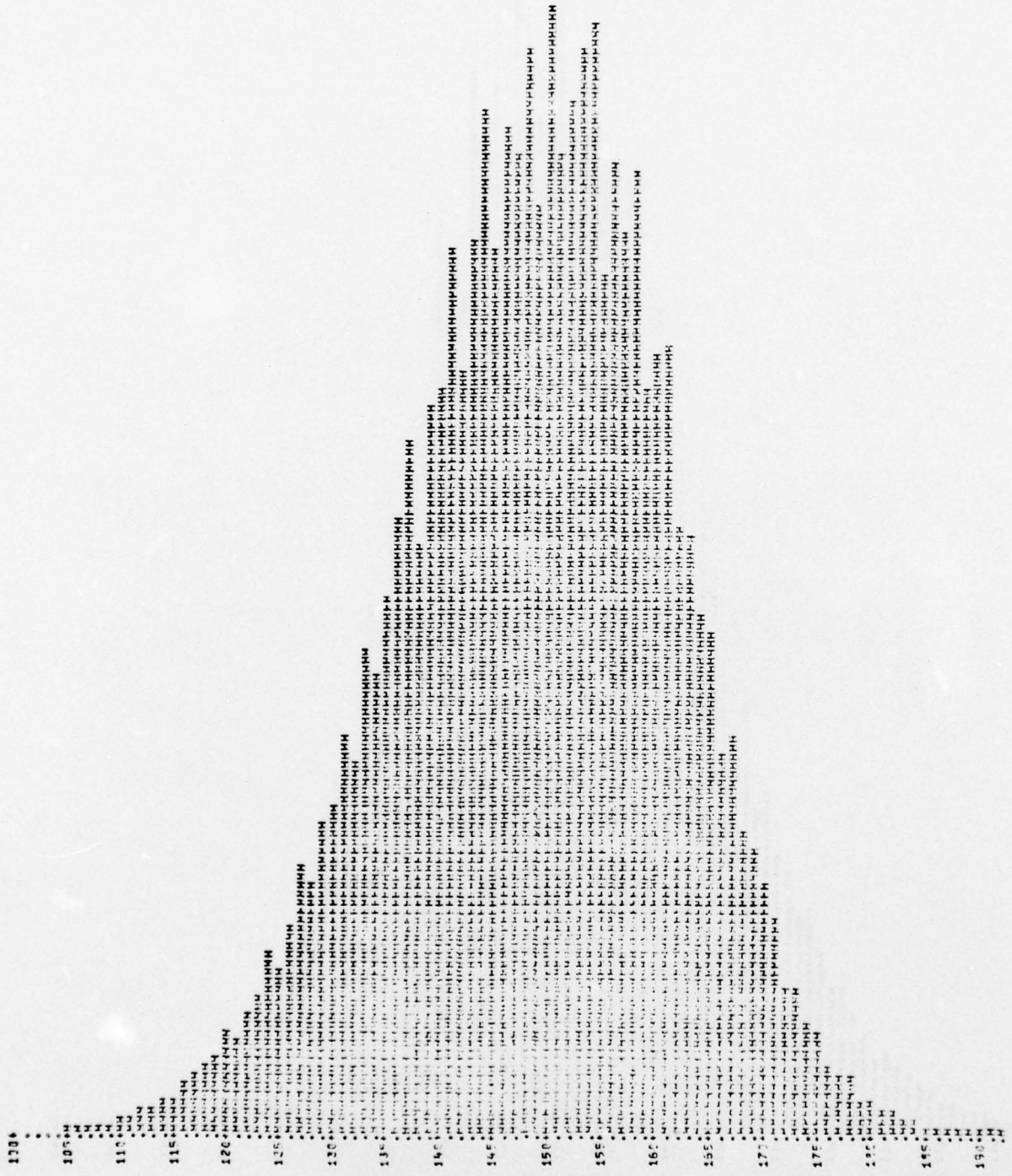

Figure 5-7. Azimuth - Look 2, Pass 1

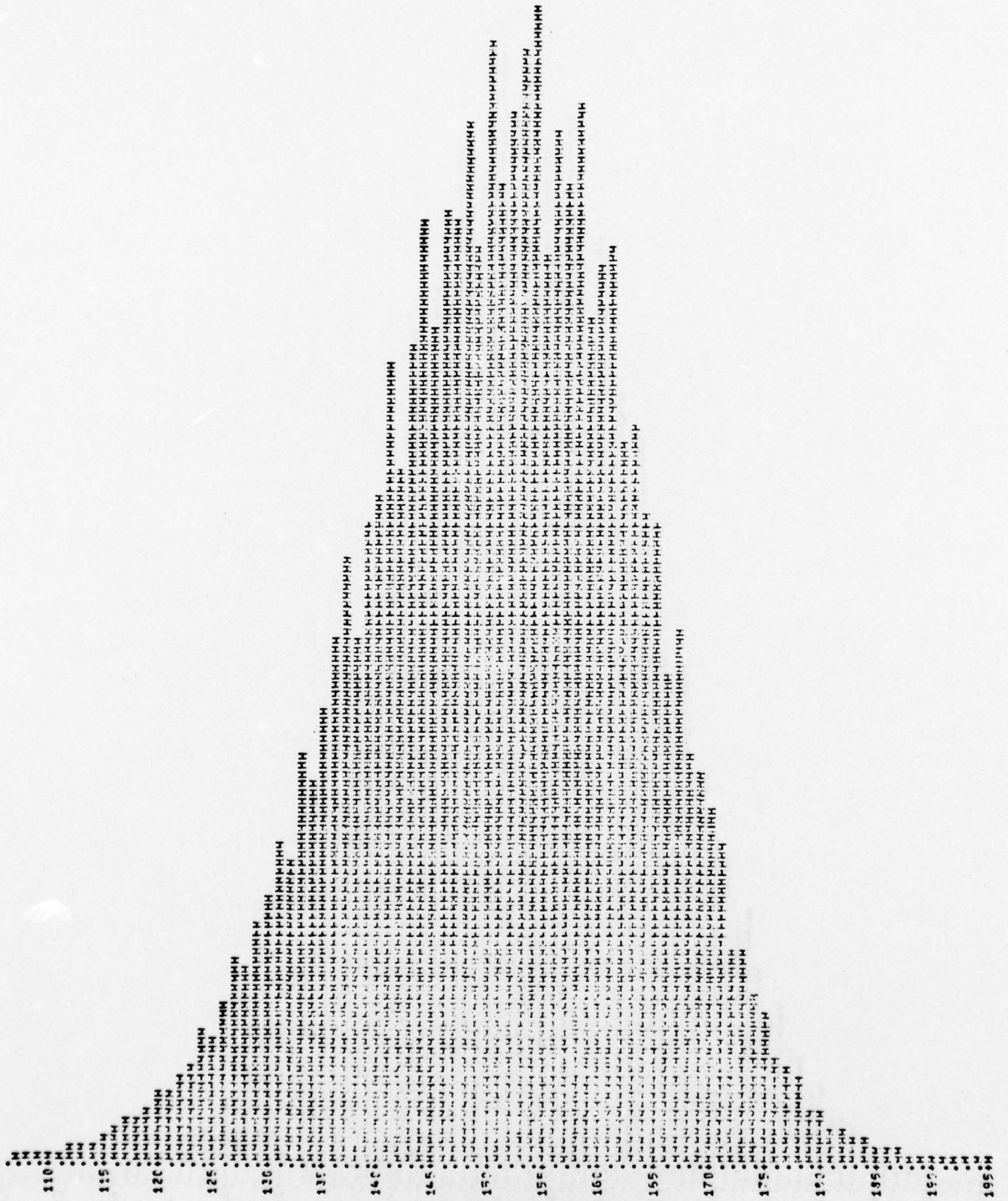

Figure 5-8. Azimuth - Look 1, Pass 2

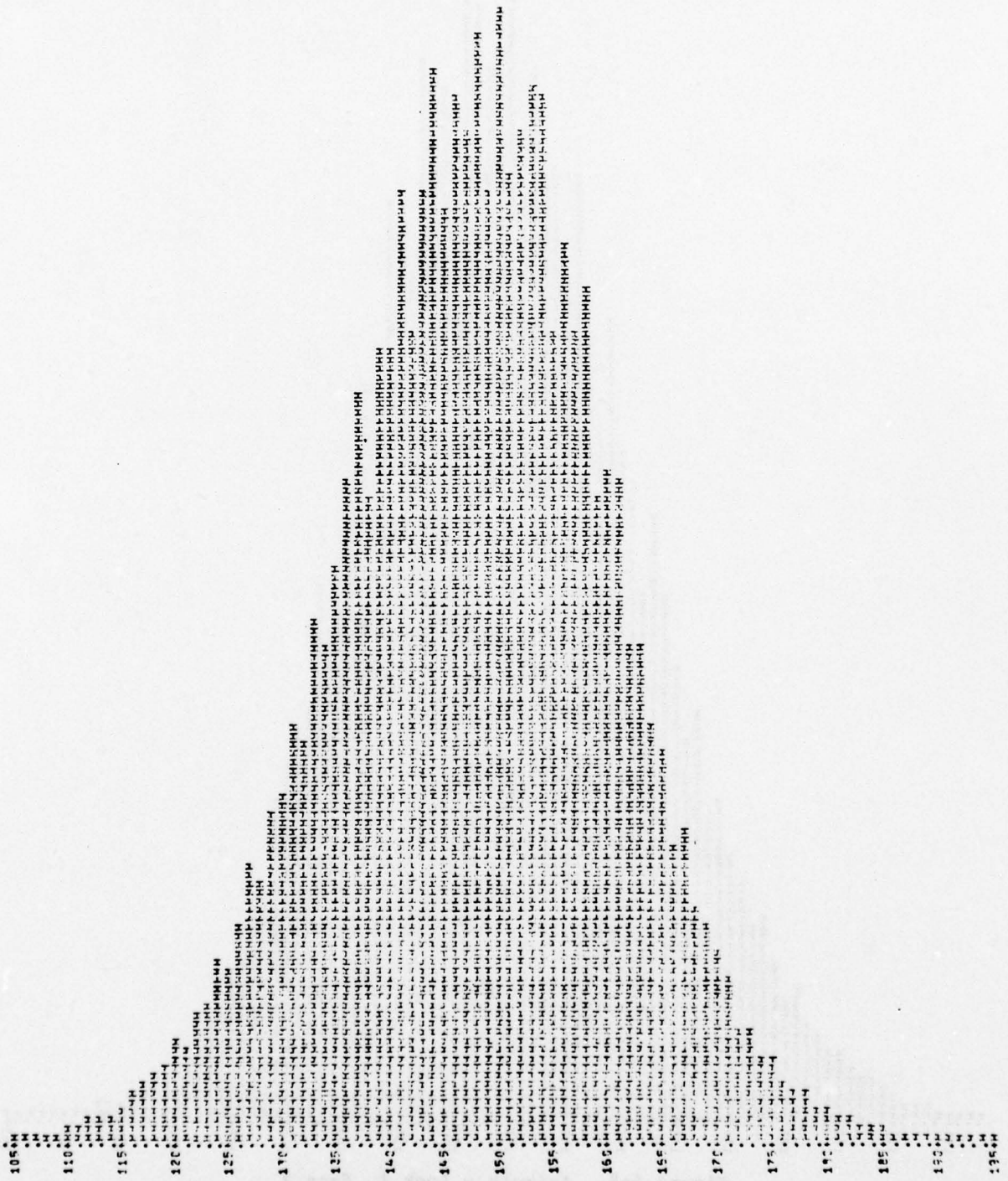

Figure 5-9. Azimuth - Look 2, Pass 2

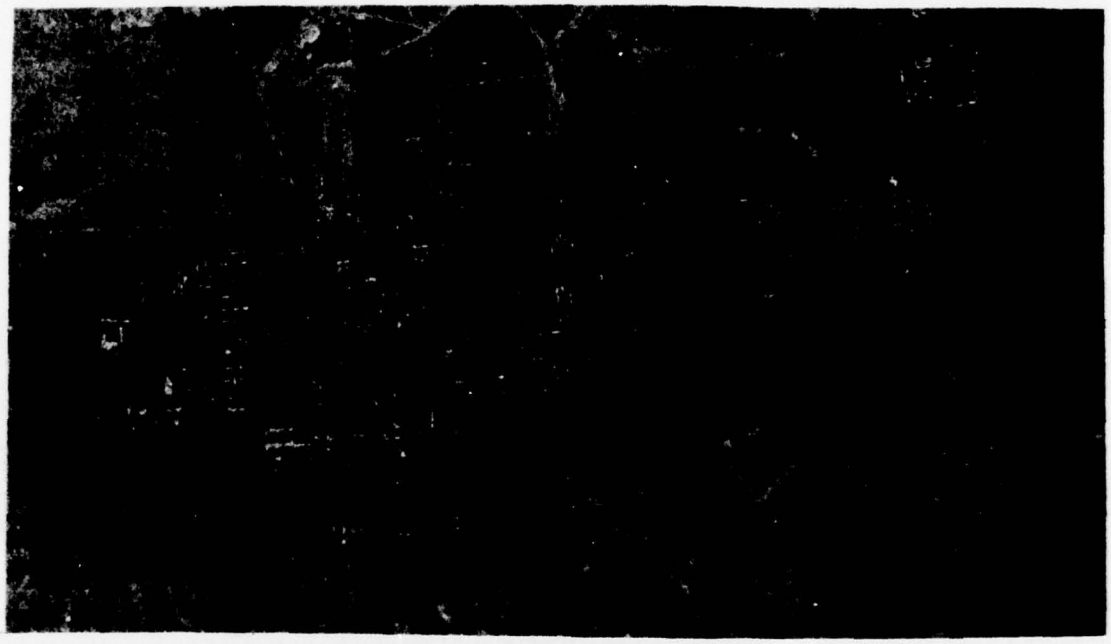

Figure 5-10. Noncoherent Average - Look 1
and Look 2, Pass 1

Figure 5-11. Adjacent Cell Average in Range - Look 1, Pass 1

Figure 5-12. Adjacent Cell Average in Range - Look 2, Pass 1

Figure 5-13. Adjacent Cell Average in Azimuth - Look 2, Pass 1

Figure 5-14. Noncoherent Average - Look 1 and Look 2, Pass 2

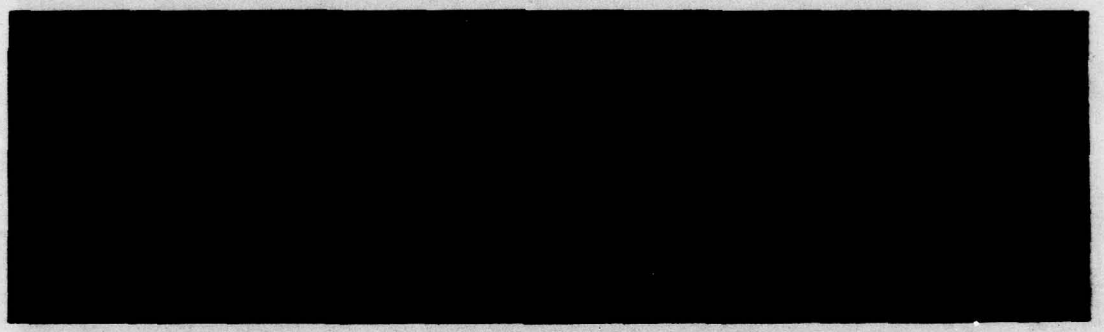

Figure 5-15. Adjacent Cell Average in Range - Look 1, Pass 2

adjacent cell average in range, look 1; Figure 5-16, adjacent cell average in range, look 2; and Figure 5-17, adjacent cell average in azimuth, look 2.

The resulting histograms corresponding to the images for pass 1 are found in Figures 5-18, 5-19, 5-20, and 5-21, respectively. The resulting histograms corresponding to the images for pass 2 are found in Figures 5-22, 5-23, 5-24, and 5-25, respectively. Table 5-2 provides a summary of the resultant statistical data for each of the integration techniques.

TABLE 5-2. RESULTANT STATISTICAL DATA FOR INTEGRATION TECHNIQUES

	MINIMUM GRAY	MAXIMUM GRAY VALUE	MEAN	STANDARD DEVIATION	ENTROPY
NONCOHERENT AVERAGE LOOKS 1 & 2 PASS 1	86	229	149.40	10.21	4.59
ADJACENT CELL AVER. IN RANGE LOOK 1 PASS 1	52	243	150.29	12.07	4.70
ADJACENT CELL AVER. IN RANGE LOOK 2 PASS 1	65	246	148.51	11.96	4.70
ADJACENT CELL AVER. IN AZIMUTH LOOK 2 PASS 1	93	228	147.72	11.97	4.70
NONCOHERENT AVERAGE LOOKS 1 & 2 PASS 2	96	229	149.08	9.94	4.57
ADJACENT CELL AVER. IN RANGE LOOK 1 PASS 2	87	229	150.66	11.94	4.69
ADJACENT CELL AVER. IN RANGE LOOK 2 PASS 2	82	229	147.49	11.76	4.68
ADJACENT CELL AVER. IN AZIMUTH LOOK 2 PASS 2	99	227	149.82	11.53	4.67

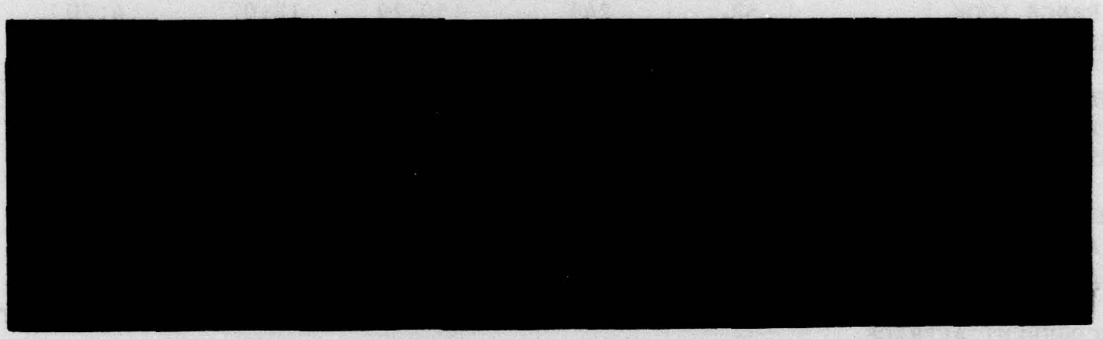

Figure 5-16. Adjacent Cell Average in Range - Look 2, Pass 2

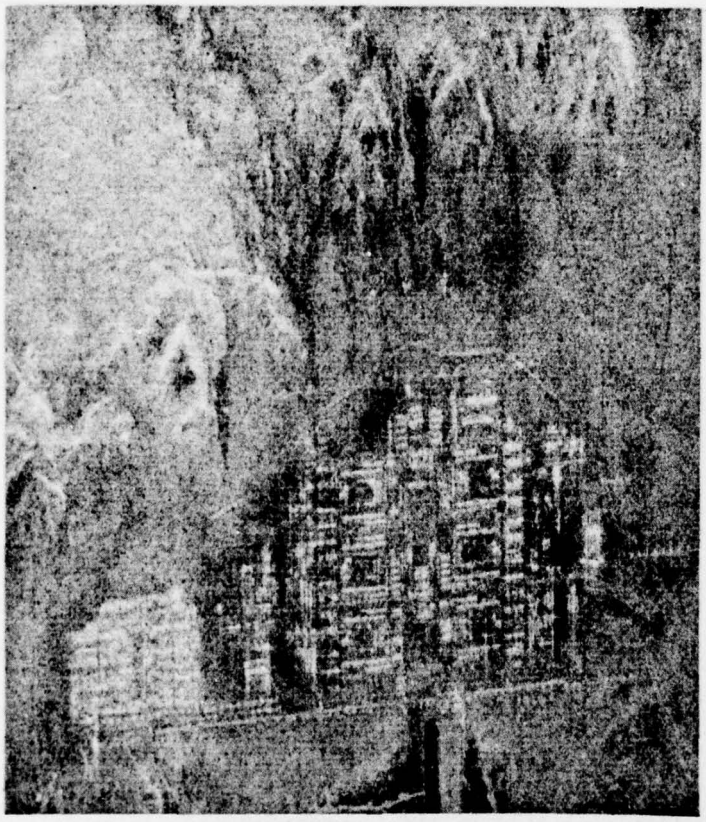

Figure 5-17. Adjacent Cell Average in Azimuth - Look 2, Pass 2

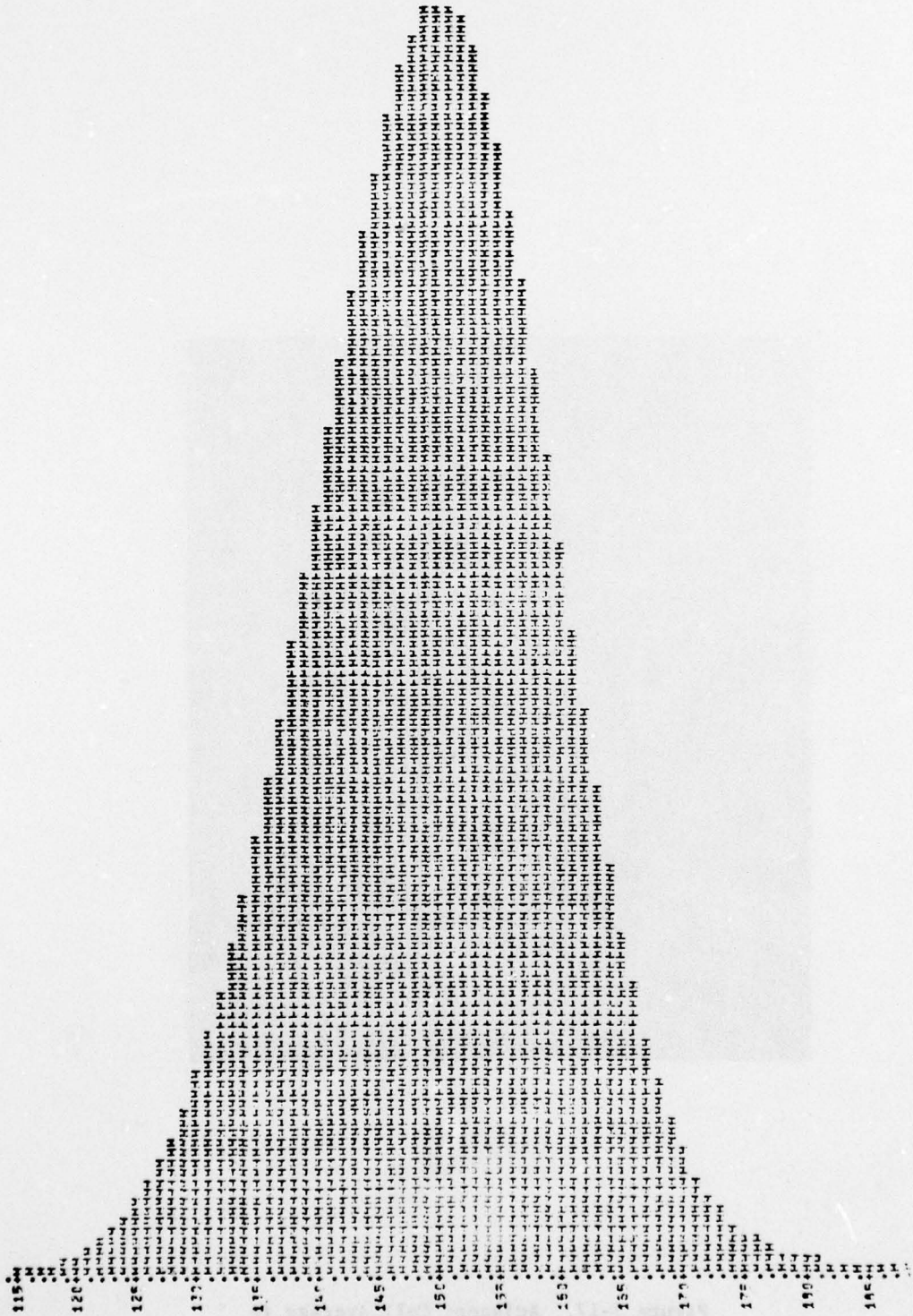

Figure 5-18. Noncoherent Average - Look 1 and Look 2, Pass 1

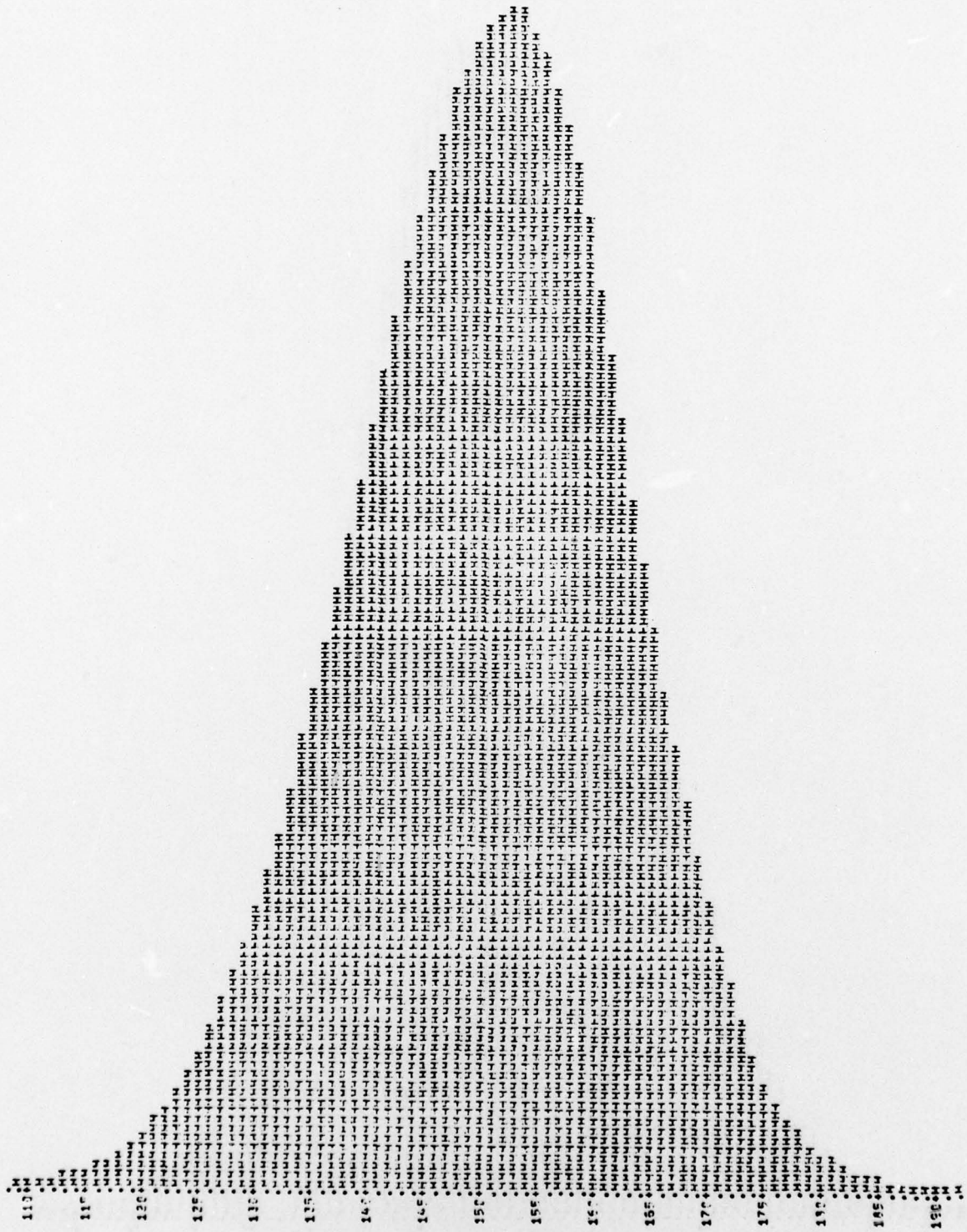

Figure 5-19. Adjacent Cell Average in Range - Look 1, Pass 1

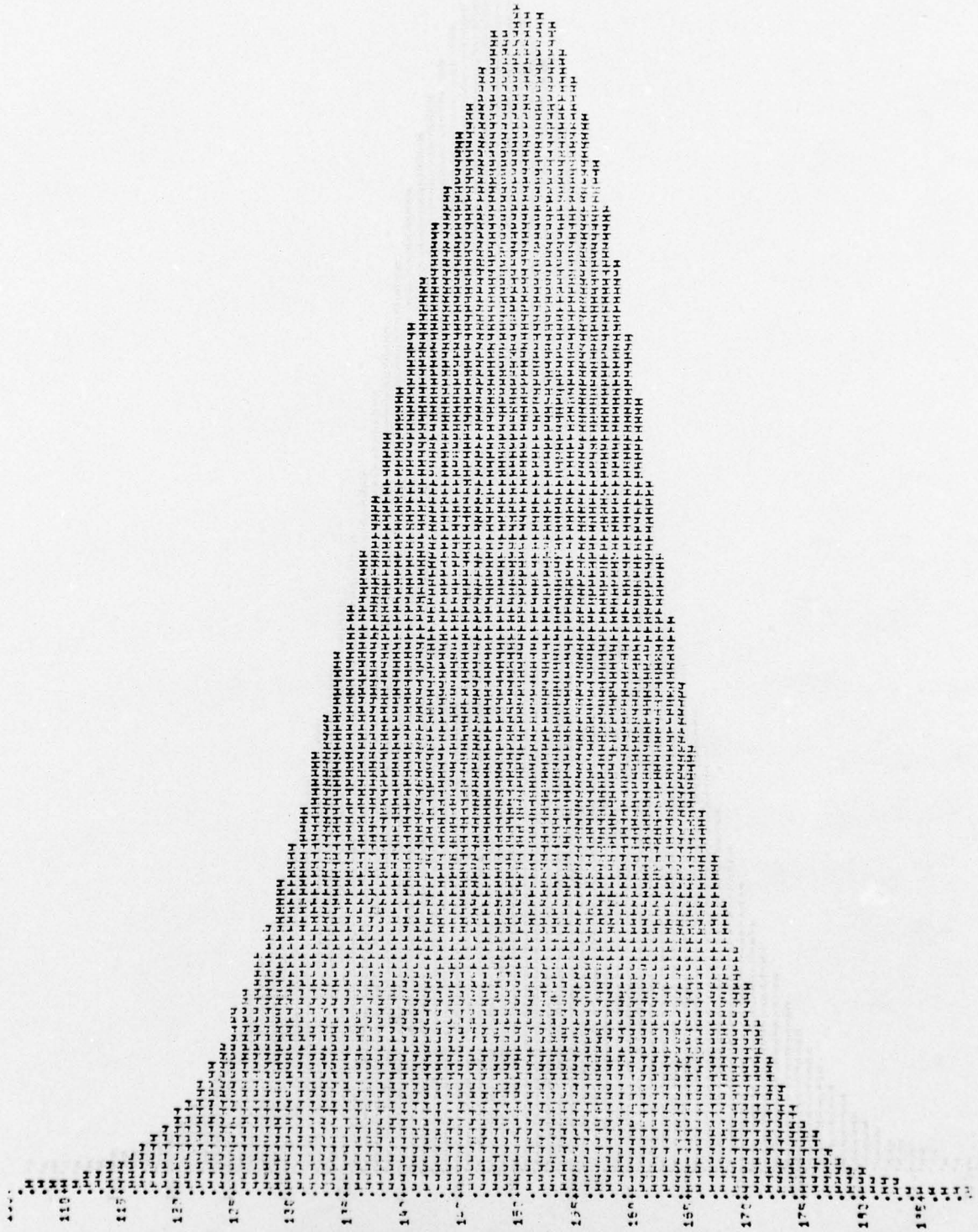

Figure 5-20. Adjacent Cell Average in Range - Look 2, Pass 1

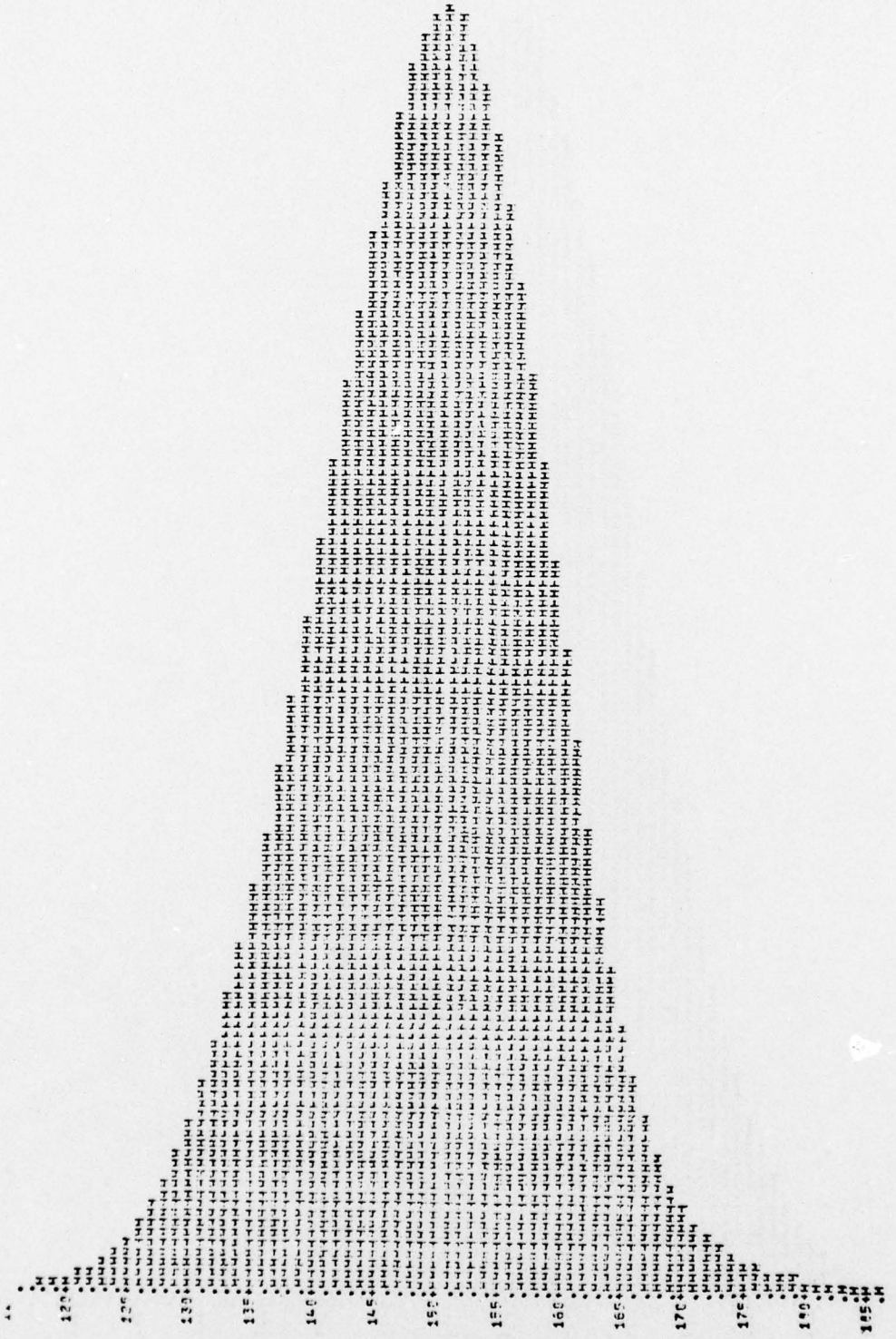

Figure 5-21. Adjacent Cell Average in Azimuth - Look 2, Pass 1

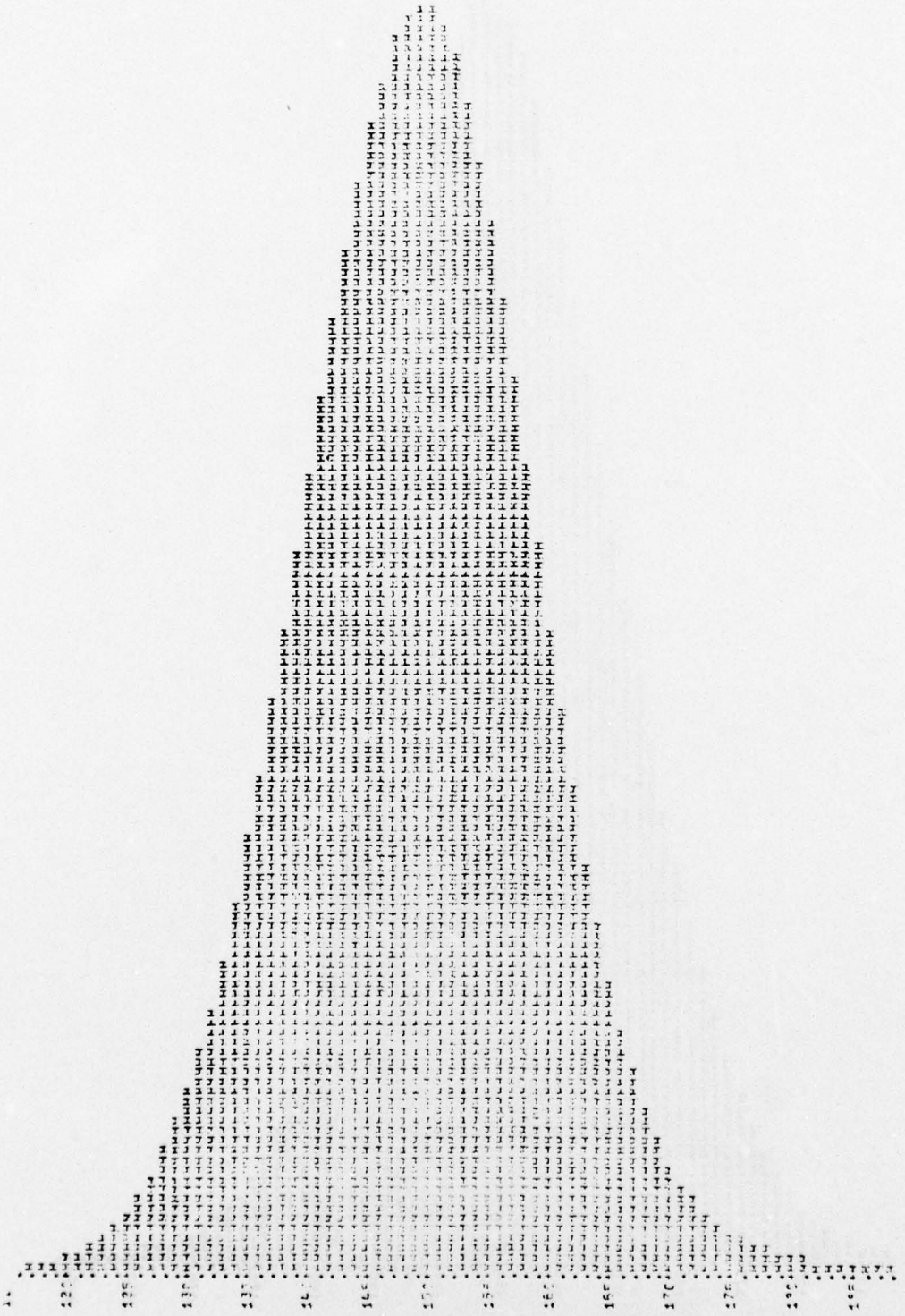

Figure 5-22. Noncoherent Average - Look 1 and Look 2, Pass 2

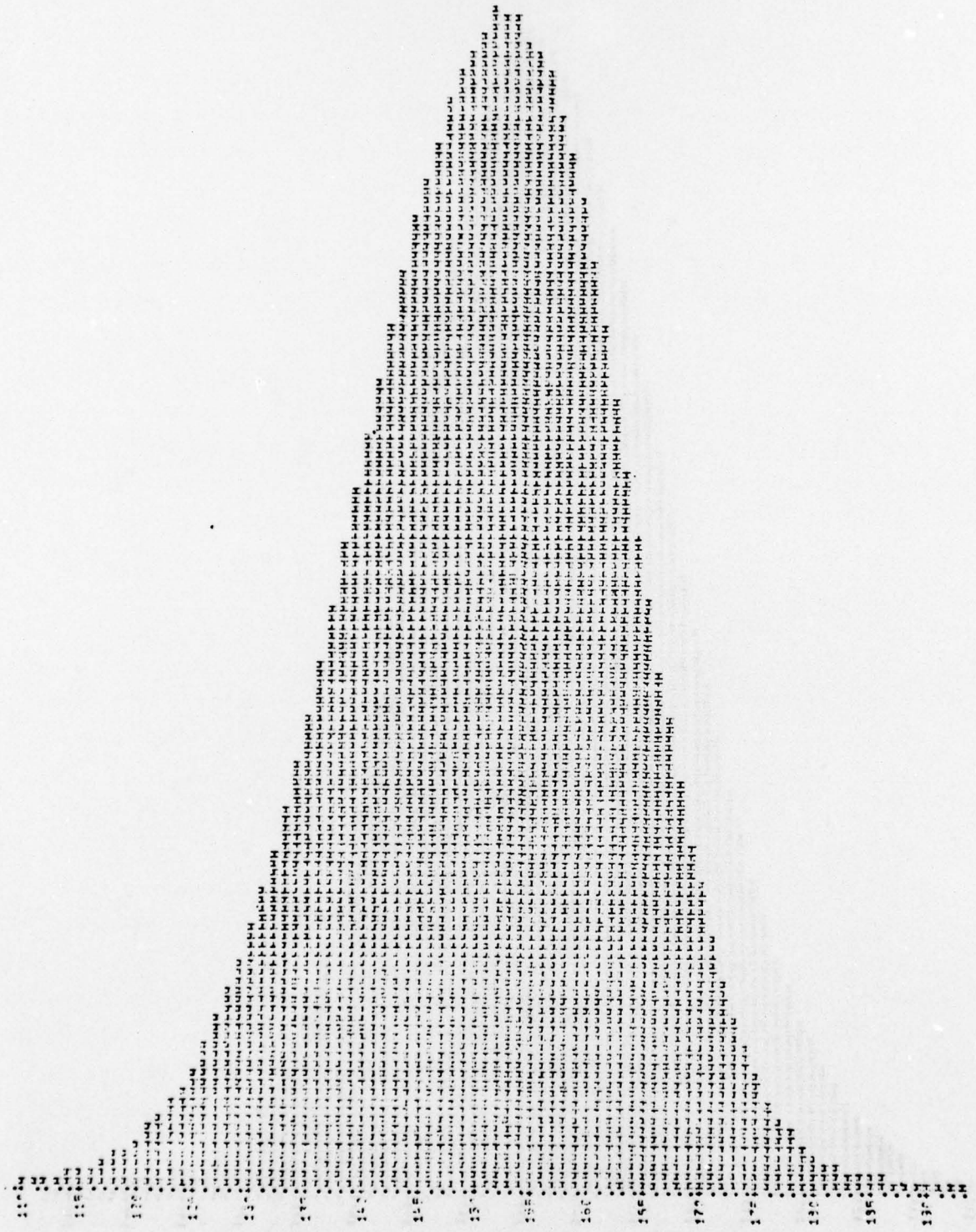

Figure 5-23. Adjacent Cell Average in Range - Look 1, Pass 2

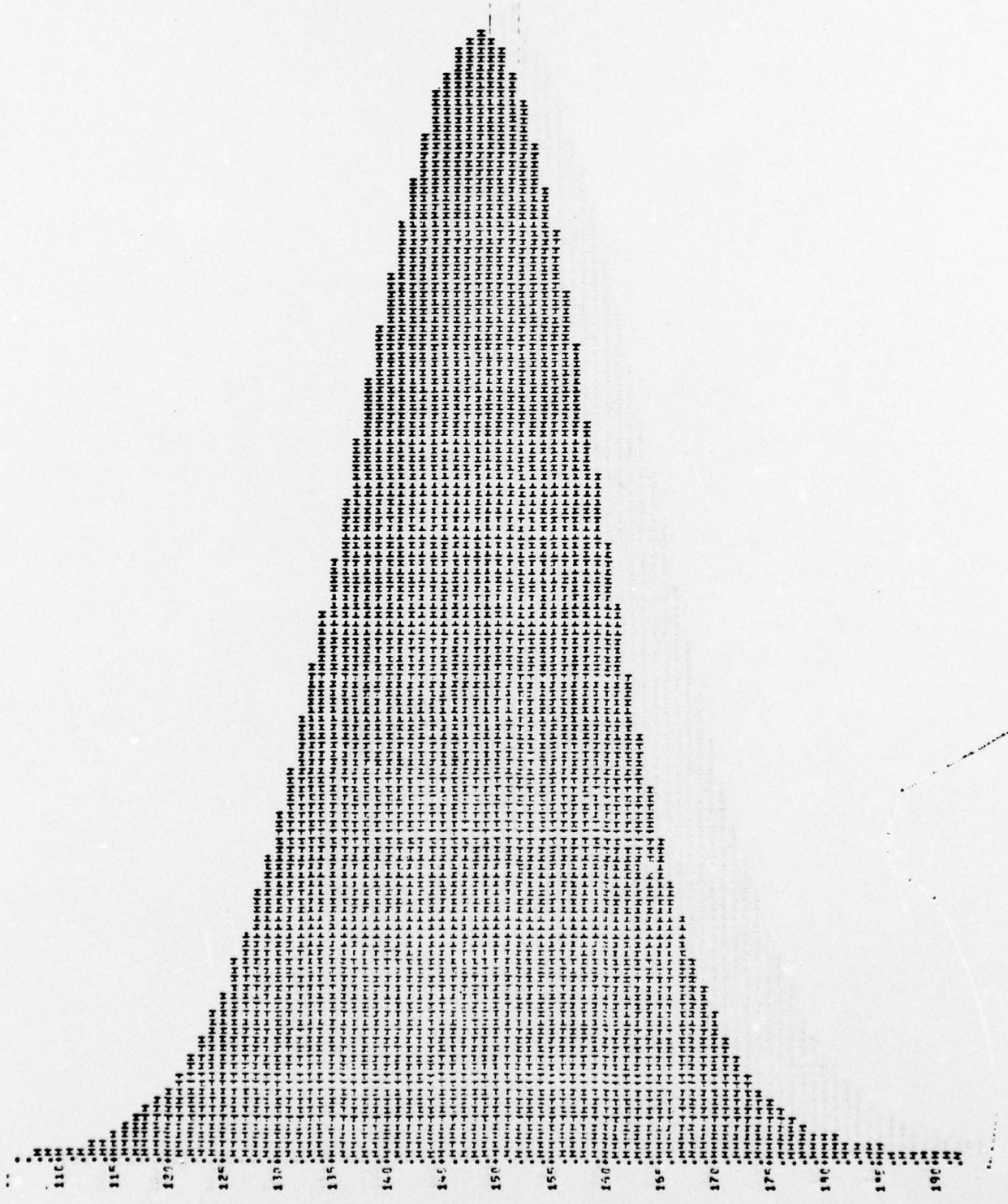

Figure 5-24. Adjacent Cell Average in Range - Look 2, Pass 2

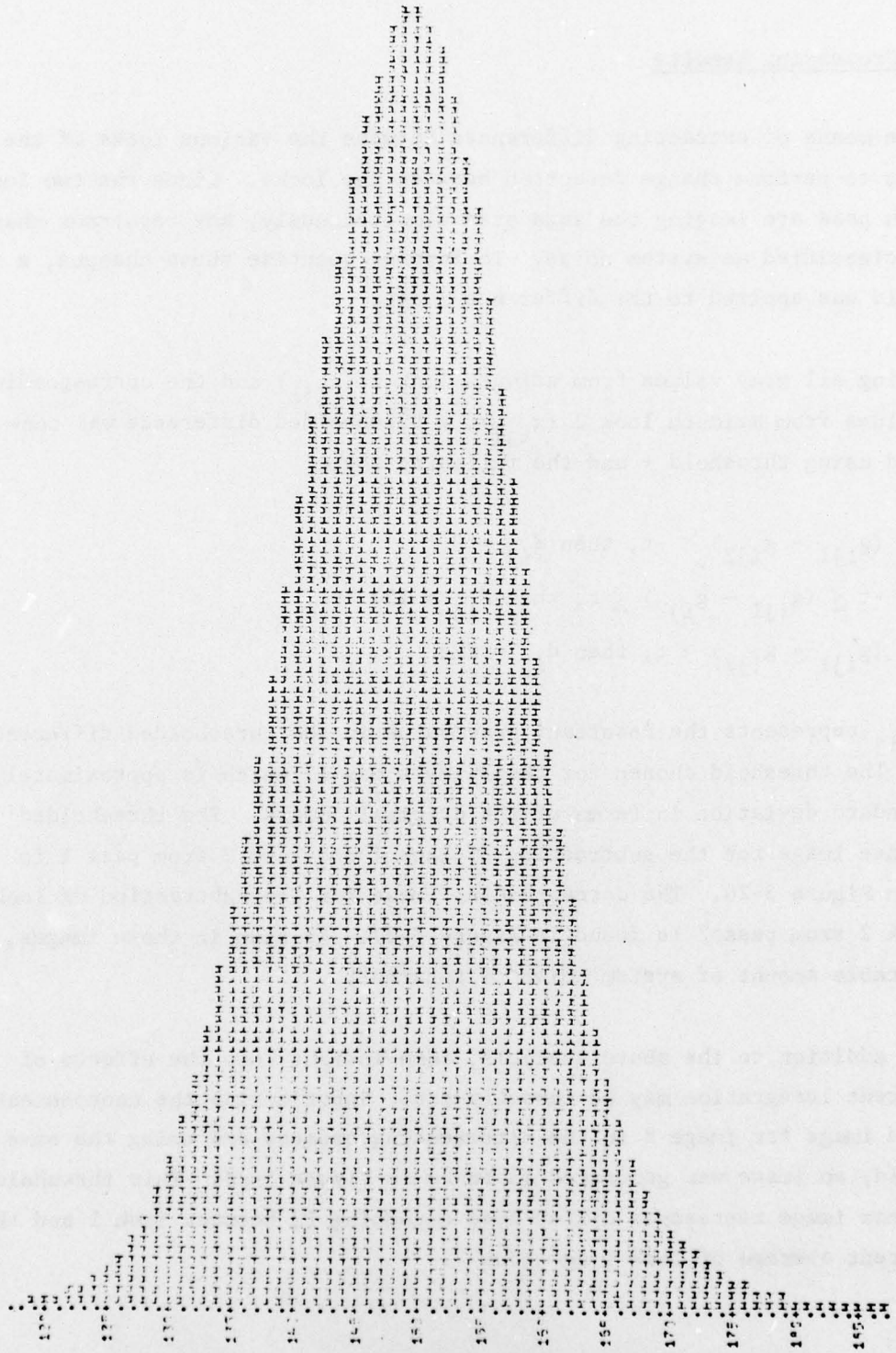

Figure 5-25. Adjacent Cell Average in Azimuth - Look 2, Pass 2

5.1.3 Processing Results

One means of extracting differences between the various looks of the radar is to perform change detection between the looks. Since the two looks for each pass are imaging the same area simultaneously, any resultant changes can be classified as system noise. To further quantize these changes, a threshold was applied to the difference image.

Using all gray values from azimuth look 1 (g_{ij1}) and the corresponding gray values from azimuth look 2 (g_{ij2}), a thresholded difference was constructed using threshold + and the following logic:

$$\text{if } (g_{ij1} - g_{ij2}) < -t, \text{ then } d_{ij} = 0$$

$$\text{if } -t \leq (g_{ij1} - g_{ij2}) \leq t, \text{ then } d_{ij} = 127$$

$$\text{if } (g_{ij1} - g_{ij2}) > t, \text{ then } d_{ij} = 225$$

where d_{ij} represents the resultant gray value in the thresholded difference image. The threshold chosen for these tests was 12 which is approximately one standard deviation in terms of the original images. The thresholded difference image for the subtraction of look 1 and look 2 from pass 1 is found in Figure 5-26. The corresponding image for the subtraction of look 1 and look 2 from pass 2 is found in Figure 5-27. As seen in these images, a considerable amount of system noise is apparent.

In addition to the above analysis, some insight into the effects of noncoherent integration may be investigated. Substituting the noncoherently averaged image for image 2 in the differencing process and using the same threshold, an image was generated as found in Figure 5-28. This thresholded difference image represents differences exceeding 12 between look 1 and the noncoherent average of look 1 and look 2.

Figure 5-26. Thresholded Difference Image for the Subtraction of Look 1 and Look 2 from Pass 1.

Figure 5-27. Thresholded Difference Image for the Subtraction of Look 1 and Look 2 from Pass 2.

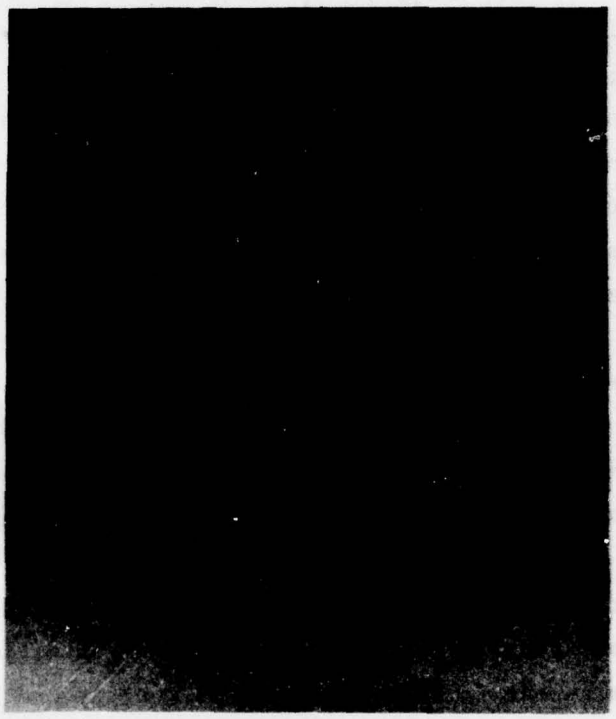

Figure 5-28. Thresholded Difference Image

5.1.4 Change Detection Between Passes

Prior to actual change detection processing, all files were truncated to 6-bit gray values. In addition, sections of the images were extracted which provided representative ground coverage. Using the files created in this manner, Table 5-3 depicts the possible combinations which were available for processing. A * indicates those combinations for which registration runs using the automatic strip processor program TRAK were made. Qualitative analysis of the registration accuracy is available in the tonal difference image which is available as a by-product of the process. Tonal difference images for the runs made, as found in Table 5-3, are as follows: Figure 5-29, azimuth look 2 pass 1 versus look 2 pass 2; Figure 5-30, azimuth look 2 pass 1 versus look 1 pass 2; Figure 5-31, noncoherent average pass 1 versus noncoherent average pass 2; Figure 5-32, adjacent cell average in range look 2 pass 1 versus adjacent cell average in range look 2 pass 2; and Figure 5-33, adjacent cell average in azimuth look 2 pass 1 versus adjacent cell average in azimuth look 2 pass 2. In addition, a statistical analysis of the registration accuracy is available via program WECK. Using the synthetic dependent image resulting from the registration process and the original dependent image, this program essentially places square patches down on a user-specified grid, and using the correlation coefficient as its discriminating metric computes the magnitude of mismatch remaining between the two images. A summary of this analysis for the files processed is found in Table 5-4.

Up to this point in our analysis, no integration technique has demonstrated any obvious superiority in terms of the change detection process. All difference images appear to be a nearly equal quality and statistical analysis of the registration accuracy does not single out any particular combination as causing extreme difficulty for the automatic registration process. This analysis does seem to indicate that combination 5, adjacent cell average in range look 2 pass 1 versus look 2 pass 2, and combination 6, adjacent cell average in azimuth look 2 pass 1 versus look 2 pass 2, are not viable ways to process the data. The automatic process becomes particularly unstable in hard-to-match areas, and due to the scale difference, results could be unreliable.

TABLE 5-3. REGISTRATION TESTS - SIX-BIT FILES

PASS 1		PASS 2: AZL1	AZL2	ACA in R: 1	ACA in R: 2	NCA (1 & 2)	ACA in A: 1	ACA in A: 2
AZL1								
AZL2		*	*					
ACA in R	1							
	2		*		*			
NCA (1 & 2)			*			*		
ACA in A	1							
	2		*					*

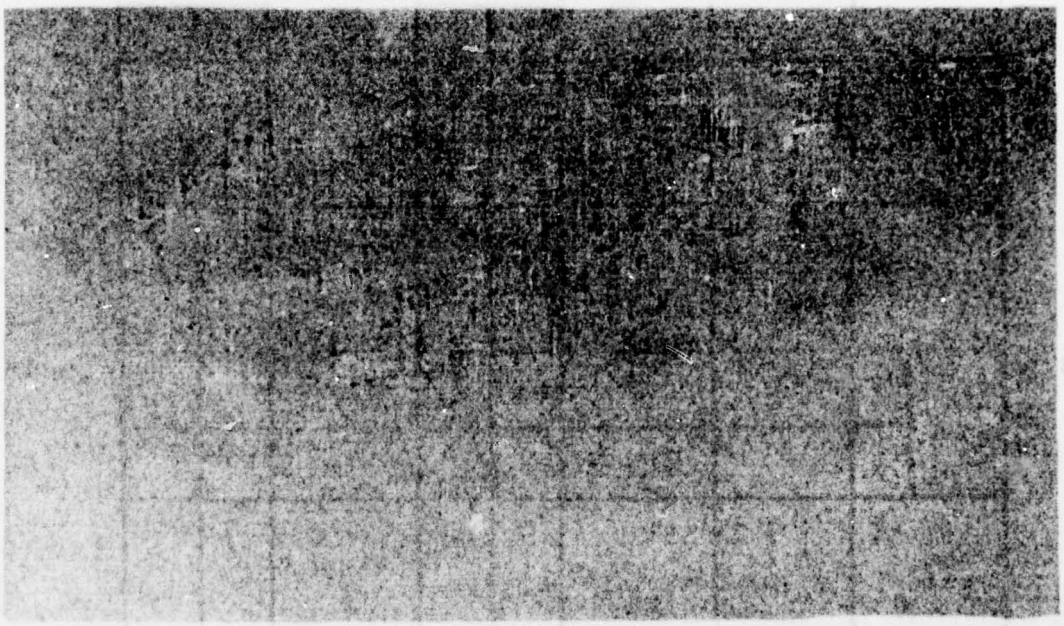

Figure 5-29. Azimuth - Look 2, Pass 1 Versus Look 2, Pass 2

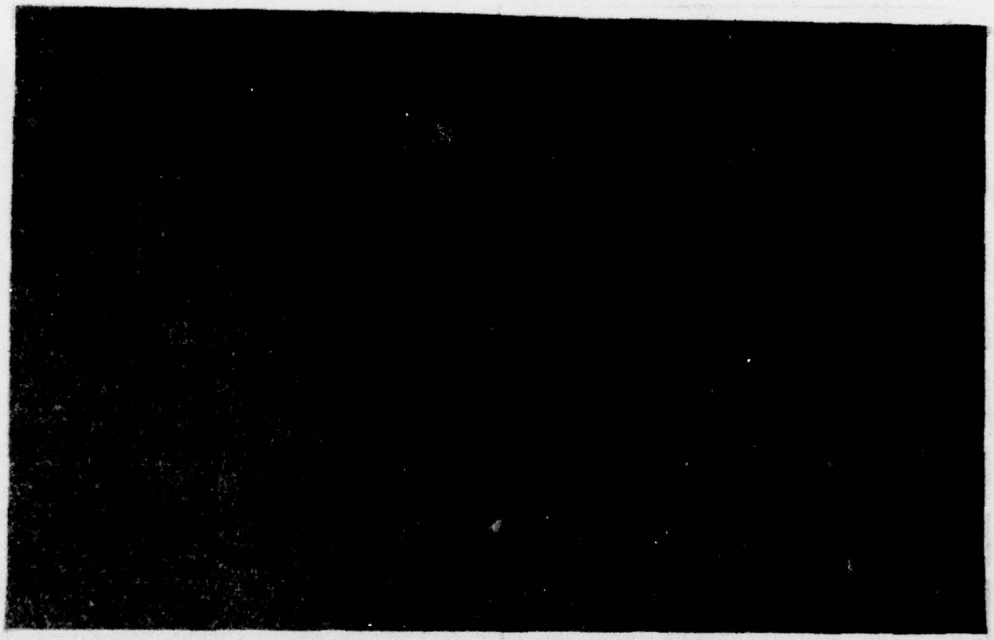

Figure 5-30. Azimuth - Look 2, Pass 1 Versus
Look 1, Pass 2

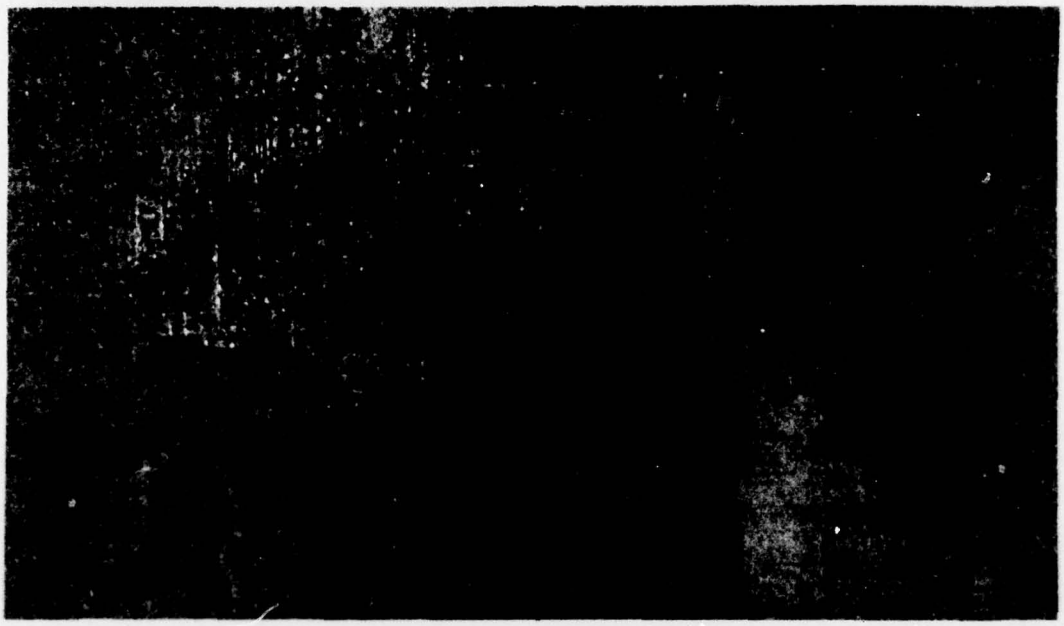

Figure 5-31. Noncoherent Average Pass 1 Versus
Noncoherent Average Pass 2

Figure 5-32. Adjacent Cell Average in Range - Look 2, Pass 1 Versus Adjacent Cell Average in Range - Look 2, Pass 2

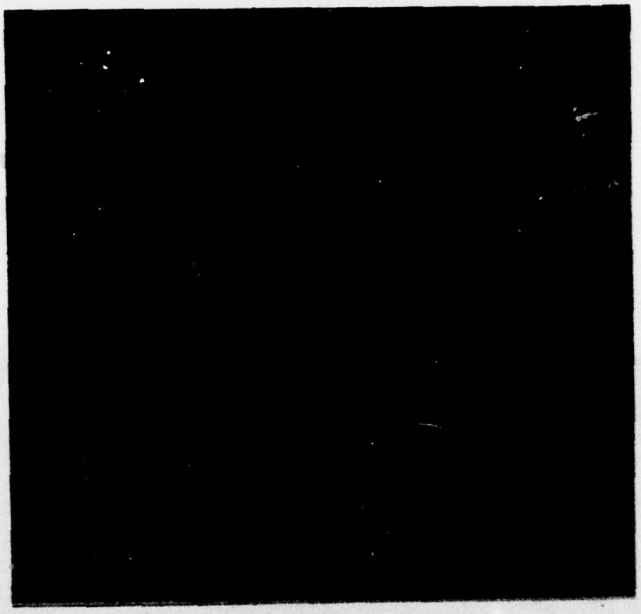

Figure 5-33. Adjacent Cell Average in Azimuth - Look 2, Pass 1 Versus Adjacent Cell Average in Azimuth - Look 2, Pass 2

TABLE 5-4. STATISTICAL ANALYSIS OF REGISTRATION ACCURACY (MEASUREMENTS ARE IN PIXELS)

	MEAN DEVIATION X-AXIS	MEAN DEVIATION X-AXIS	MEAN RADIAL ERROR	ROOT MEAN SQUARE ERROR	NUMBER OF SAMPLES
LOOK 2 PASS 1 VERSUS LOOK 2 PASS 2	-.08	-.05	.63	.85	59
LOOK 2 PASS 1 VERSUS LOOK 1 PASS 2	.06	.11	.84	1.16	79
NONCOHERENT AVERAGE PASS 1 VERSUS NON-COHERENT AVERAGE PASS 2	-.13	-.22	.87	1.03	117
NONCOHERENT AVERAGE PASS 1 VERSUS LOOK 2 PASS 2	-.11	-.04	.85	1.03	124
ADJACENT CELL AVERAGE IN RANGE LOOK 2 PASS 1 VERSUS ADJACENT CELL AVERAGE IN RANGE LOOK 2 PASS 2	-.32	-.02	.84	1	70
ADJACENT CELL AVERAGE IN AZIMUTH LOOK 2 PASS 1 VERSUS ADJACENT CELL AVERAGE IN AZIMUTH LOOK 2 PASS 2	.09	-.17	.68	.83	82
ADJACENT CELL AVERAGE IN RANGE LOOK 2 PASS 2 VERSUS LOOK 1 PASS 1	-.27	-.21	1.01	1.31	90

Having obtained these results, additional analysis via program FOP (Feature Oriented Processing) was initiated. Four sets of the files which were now registered, those being: 1) look 2 pass 1 versus look 2 pass 2, 2) noncoherent average pass 1 versus noncoherent average pass 2, 3) adjacent cell average in azimuth look 2 pass 1 versus adjacent cell average in azimuth look 2 pass 2, and 4) adjacent cell average in range look 2 pass 1 versus adjacent cell average in range look 2 pass 2, were analyzed. The same area, equivalent to 800 lines by 850 cells, was analyzed for each set of files. The results of that analysis are depicted in Figure 5-34. The images in this figure present only those events which were classified as real changes between the original independent and dependent files. As is apparent, many of the change events are common to all of the processed pairs. There are, however, many events classified as changes from a particular pair that are not common to all of the remaining pairs. It becomes an extremely difficult task, at best, to determine which pair of original images processed produced the file of change events with highest probability of detection along with lowest false alarm rate. To do this would require, not only two controlled passes over an area with known ground truth, but also a certification of the radar image collected verifying that all returns expected are actually present on both images.

In this study, however, all but one of the original dependent and independent images used for change detection processing differ only by the integration technique used in their creation; the one exception being when the original data from look 2 of each pass was used for the mission and reference images in processing. This being the case, it appears obvious that either final results are being influenced by the integration, or FOP processing parameters must be altered in view of the fact that integration has been done on the original files. To investigate the second of these possibilities, an examination of the thresholded difference image created in FOP processing is in order.

Program FOP is essentially a two-pass system. Pass one detects all events for which classification as real changes, false alarms, shadows, etc. is necessary. This is, in essence, a thresholded difference image. In the

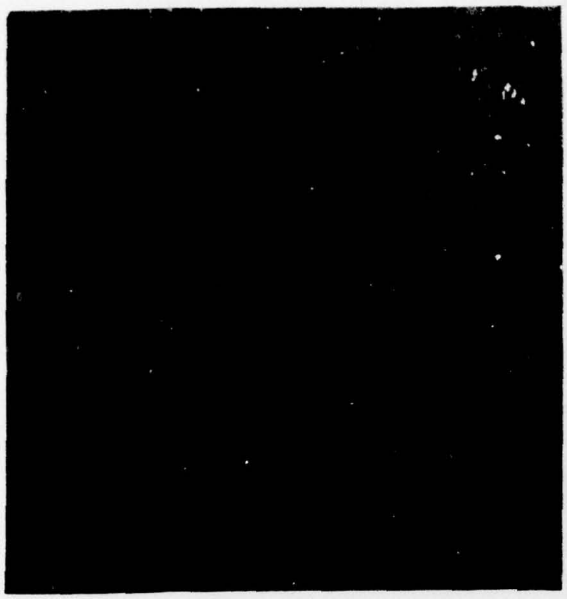

FINAL CHANGES
ACAA L2 PASS 1 vs ACAA L2 PASS 2

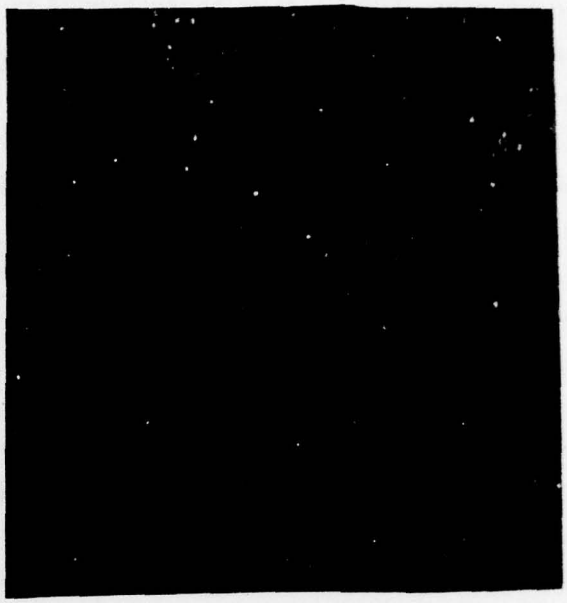

FINAL CHANGES
ACAR L2 PASS 1 vs ACAR L2 PASS 2

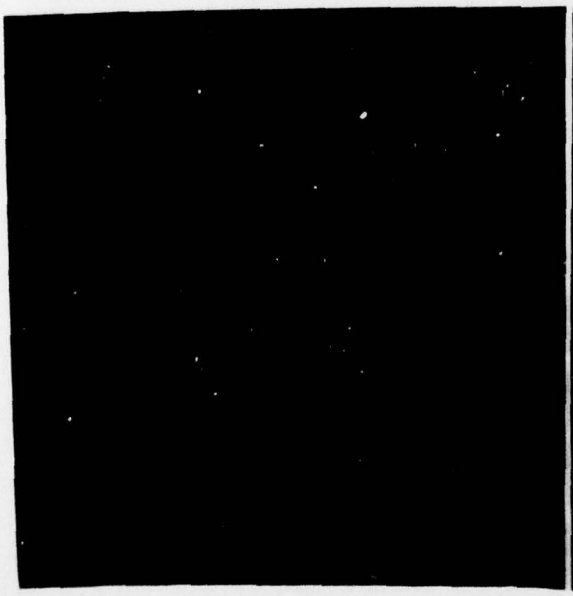

FINAL CHANGES
L2 PASS 1 vs L2 PASS 2

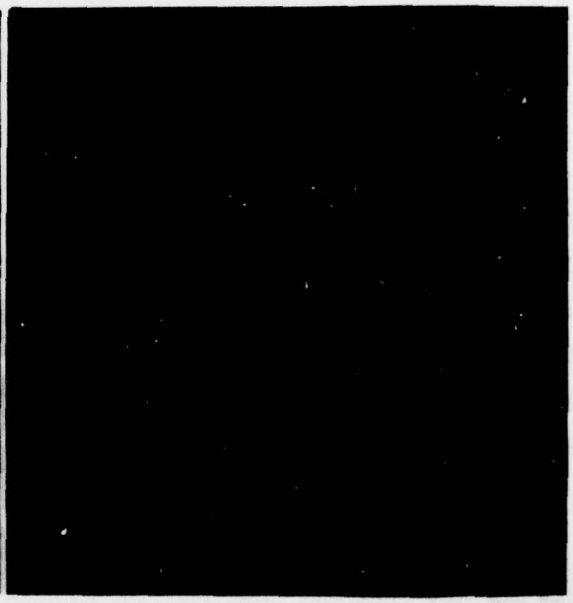

FINAL CHANGES
NCA L1+L2 PASS 1 vs NCA L1+L2 PASS 2

Figure 5-34. Results of FOP Analysis

second pass, FOP deletes those events not meeting all criteria of real changes. Output from the pass one was as examined in Figure 5-35. For all those events classified as real changes for a particular pair of original files but not common to another pair, it must first be established that the event in question appeared on the thresholded difference image in both cases. In all but a very few cases, this appears to be true. This being true, the constitution of the event must differ enough to cause final classification to change. This would seem a reasonable assumption. The effects of the integration would be to lower the magnitude of all boundary cells of an event. This could well be enough to diminish the size of the change event proper. Since the ERASE logic in FOP tests for a minimum event size, many of the differences in classification are results of this conditional logic. The important consideration, however, is that even though the event was of a different constitution, it did exist and could have been retained by altering process parameters. Whether the adjustment of parameters to force inclusion or deletion of events significantly raises the false alarm rate can only be determined by an in-depth analysis of controlled passes as discussed earlier.

5.1.5 8-Bit Processing

Change detection processing was also completed using the 8-bit files as shown in Table 5-5. Difference images generated are found in Figure 5-36 for the run comparing azimuth look 2 pass 1 to azimuth look 2 pass 2, and Figure 5-37 for the run comparing the noncoherent average of looks 1 and 2 for pass 1 to the noncoherent average of looks 1 and 2 from pass 2. These difference images show registration to be of an equal quality with results generated from the six-bit files. It appears no distinct advantage has been gained with the inclusion of the additional two bits.

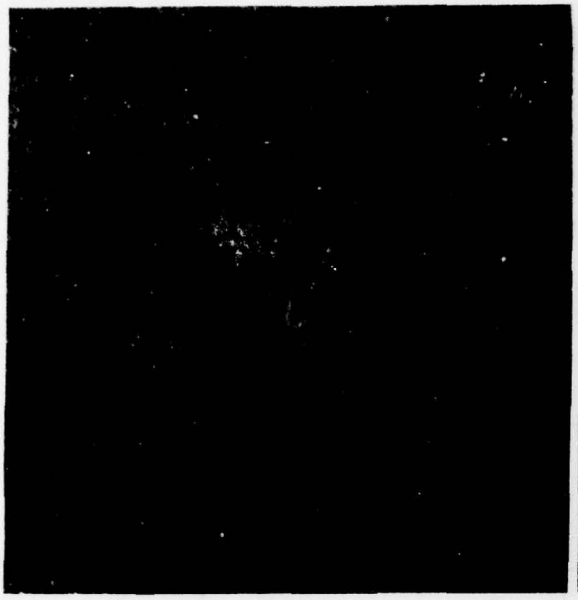

CANDIDATE CHANGES
ACAA L2 PASS 1 vs ACAA L2 PASS 2

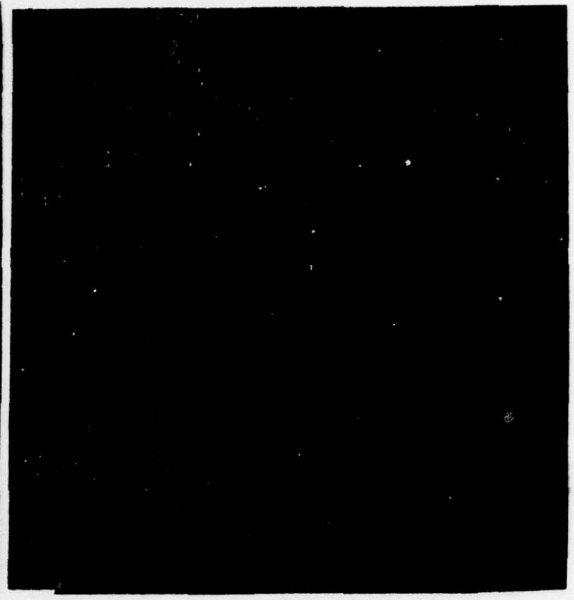

CANDIDATE CHANGES
ACAR L2 PASS 1 vs ACAR L2 PASS 2

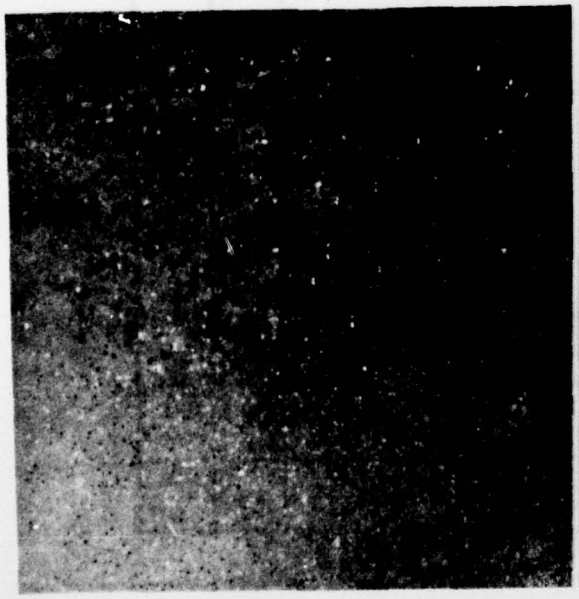

CANDIDATE CHANGES
L2 PASS 1 vs L2 PASS 2

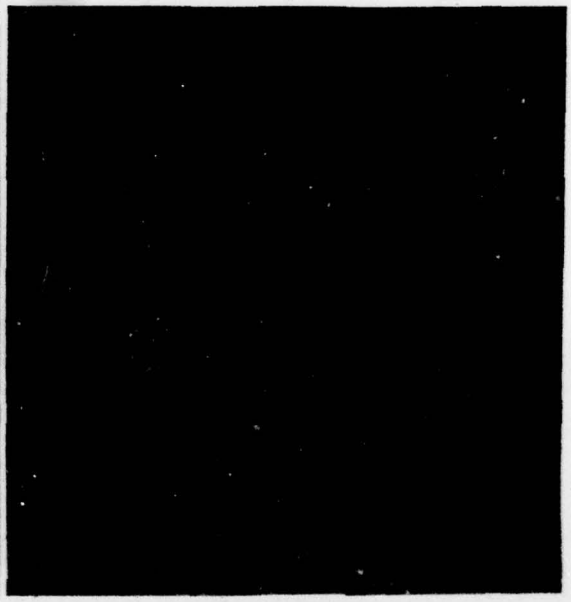

CANDIDATE CHANGES
NCA L1+L2 PASS 1 vs NCA L1+L2 PASS 2

Figure 5-35. FOP Output from Pass 1

TABLE 5-5. REGISTRATION TESTS - 8-BIT FILES

PASS 2

PASS 1		AZL1	AZL2	ACA in R 1	ACA in R 2	NCA (1 & 2)	ACA in A 1	ACA in A 2
AZL1								
AZL2			*					
ACA in R	1							
	2							
NCA (1 & 2)						*		
ACA in A	1							
	2							

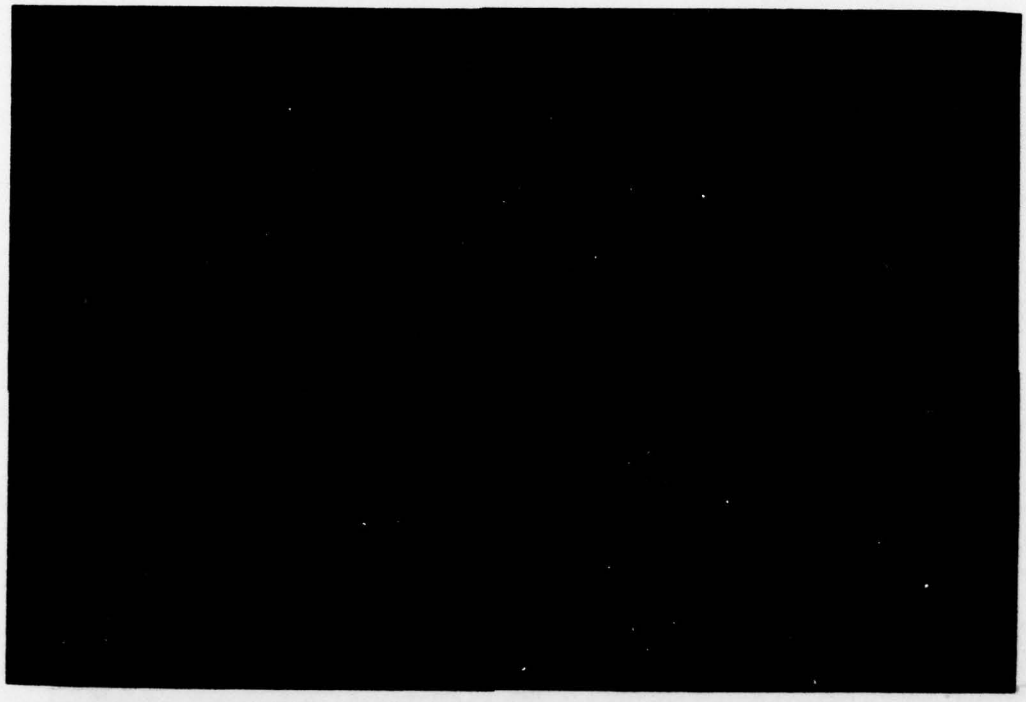

Figure 5-36. Difference Image Generated for the Run Comparing Azimuth - Look 2, Pass 1 to Azimuth - Look 2, Pass 2

Figure 5-37. Difference Image Generated for the Run Comparing the Noncoherent Average of Looks 1 and 2 for Pass 1 to the Noncoherent Average of Looks 1 and 2 from Pass 2.

5.2 FLAMR DATA

5.2.1 Processing Results

Two sets of FLAMR Digital Radar data were received by Digital Image Systems Division. The first set of data was not acceptable. Gaps in the distribution were present indicating that an error occurred when the data was recorded on magnetic tape. A second set of data was requested and received. Stripping details indicated:

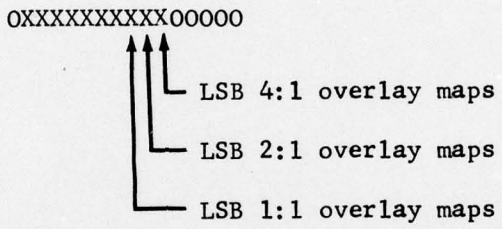

Figure 5-38. Bit Placement

Data was recorded in 16-bit fields with bit placement as indicated by Figure 5-38. The data received was FLAMR strip map SASM data. Upon initial examination, it was discovered that the bottom bit for all overlay maps was always zero. This being the case, stripping was completed using only the upper seven bits of each of the indicated fields. Histograms generated using the data removed in this fashion are as found in Figure 5-39, 4:1 overlay map pass 1; Figure 5-40, 2:1 overlay map pass 1; Figure 5-41, 1:1 overlay map pass 1. These histograms seem to indicate some sort of signal clipping had been applied to the data. This was confirmed on a later visit to the FLAMR facilities. The effects of this signal clipping are also apparent on the images found in Figures 5-42 and 5-43. Areas of strong return seem to be filled with unexplanable discontinuous returns. In addition to this problem, a majority of the pass is returns from the ocean or results of the signal clipping zeroes. Since the matching metric in the strip processor is the correlation coefficient, strips placed over this area become detrimental to the registration process. Registration trials using 6-bit files of the

AD-A056 953 CONTROL DATA CORP MINNEAPOLIS MINN F/G 17/9
DIGITAL MODULAR CHANGE DETECTOR.(U)
MAY 78 R DENNY, M BAYNES, W MCLURE F30602-73-C-0141
UNCLASSIFIED RADC-TR-78-104 NL

3 OF 3
AD
A056953

END
DATE
FILMED
9-78
DDC

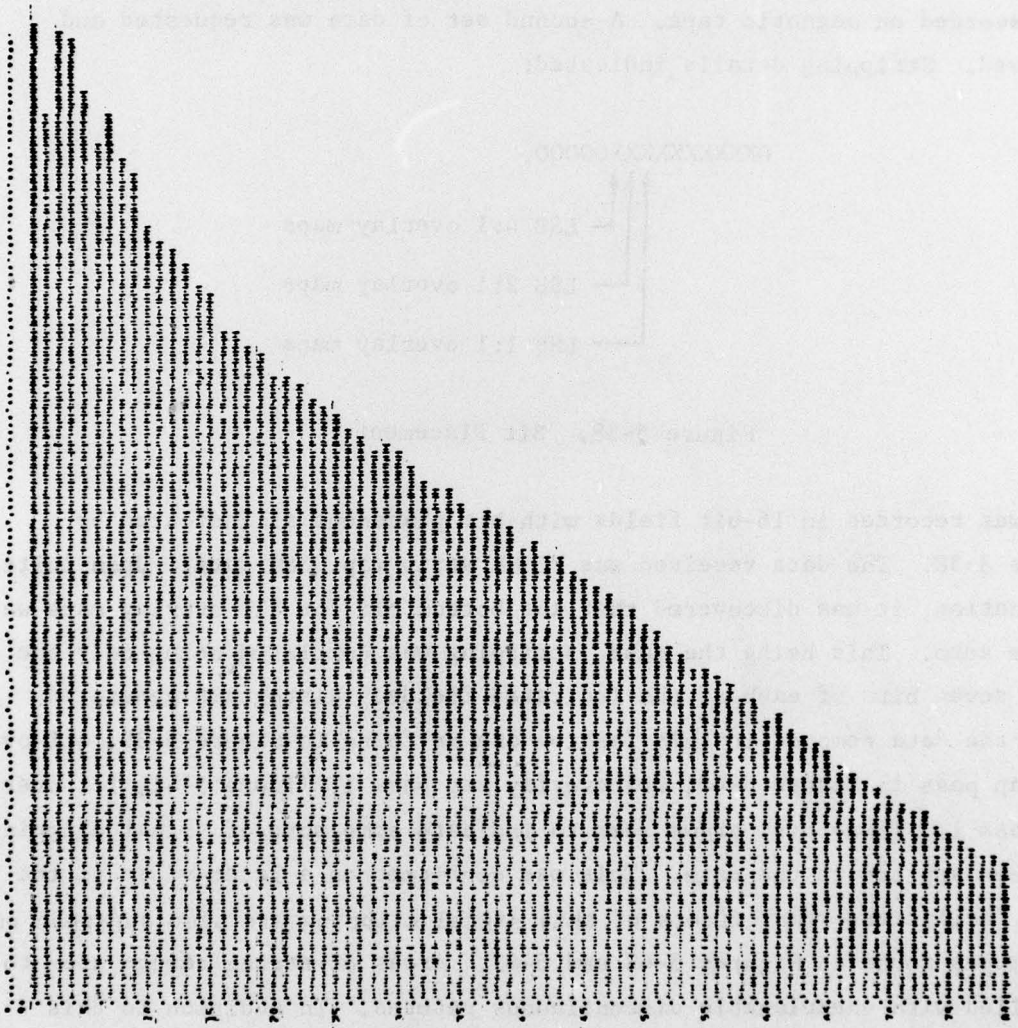

Figure 5-39. FLAMR 4:1 Overlay - Pass 1

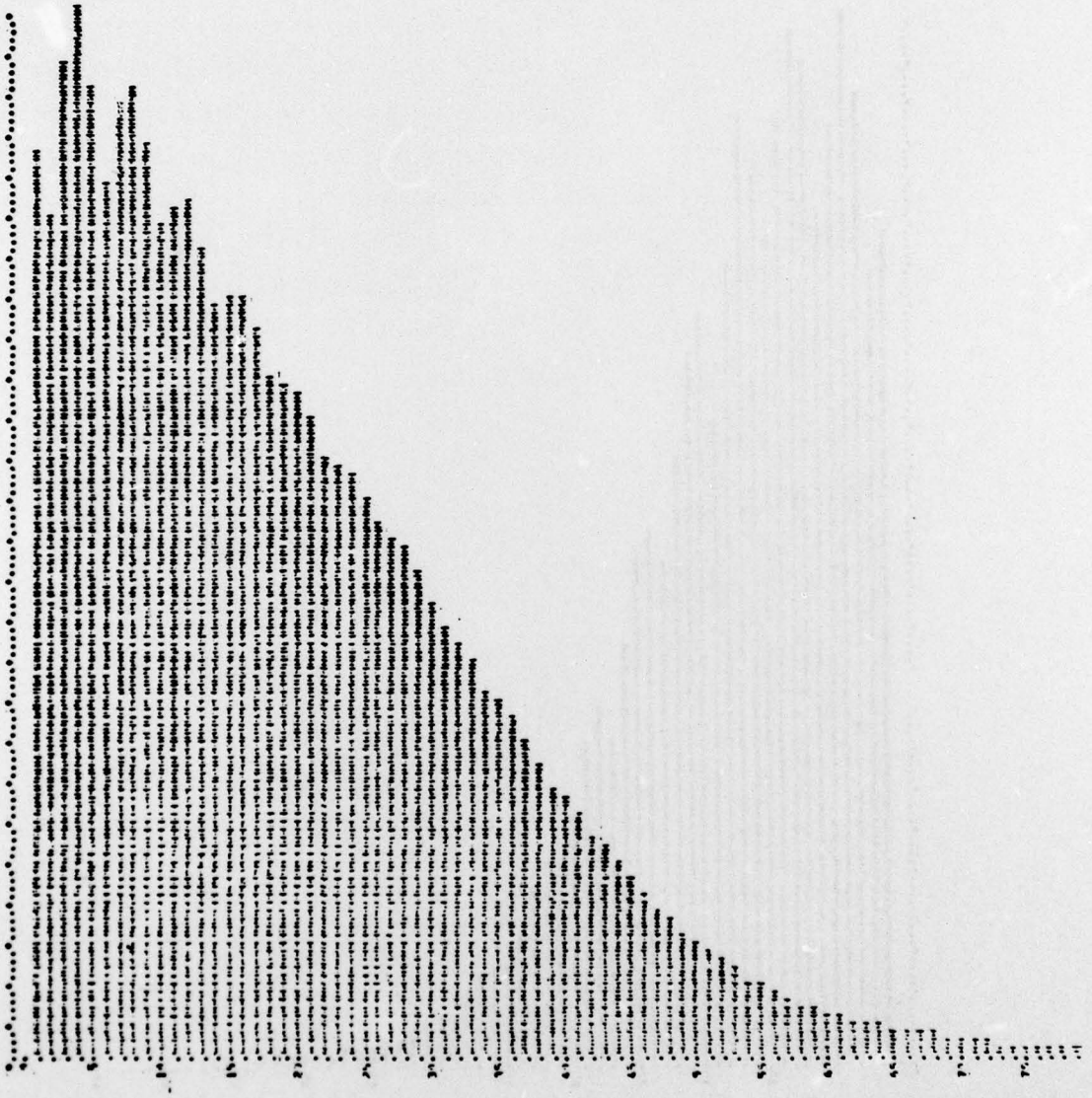

Figure 5-40. FLAMR 2:1 Overlay - Pass 1

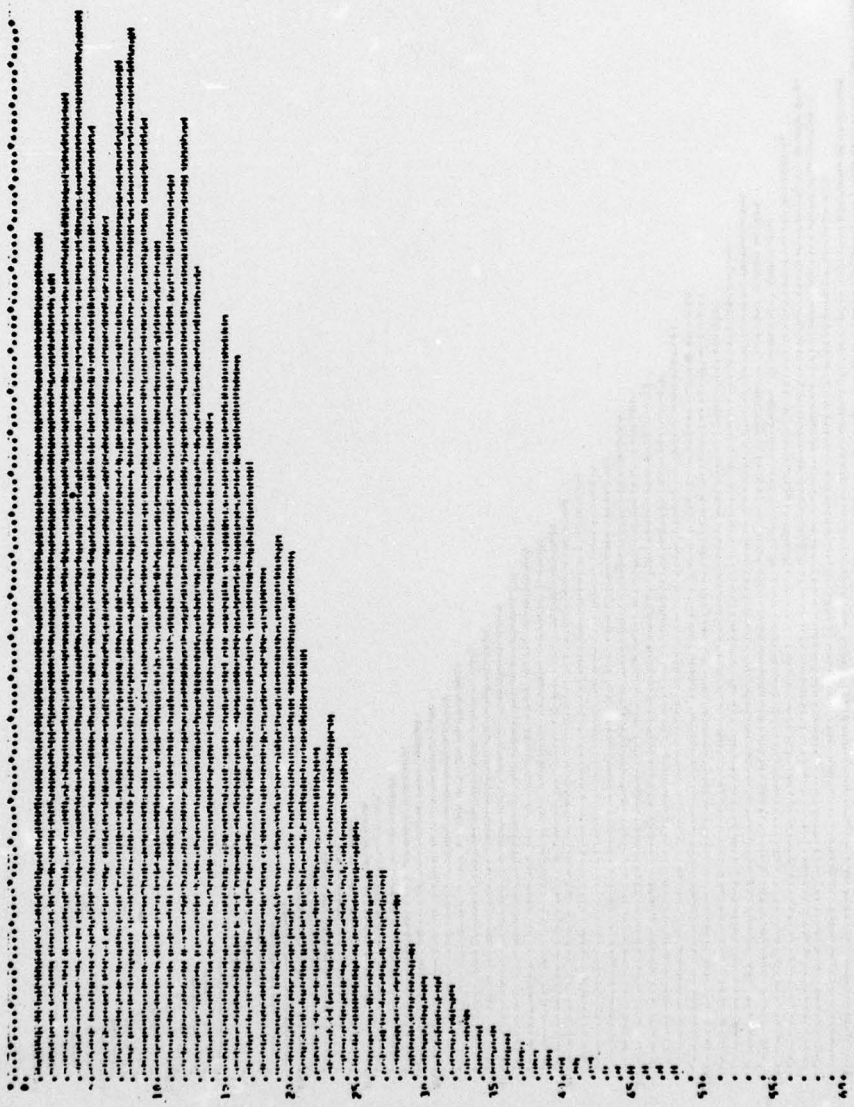

Figure 5-41. FLAMR 1:1 Overlay - Pass 1

FLAMR 7-BIT DATA

1:1 Overlay Pass 1

2:1 Overlay Pass 1

4:1 Overlay Pass 1

Figure 5-42. Effects of Signal Clipping

FLAMR 7-BIT DATA

1:1 Overlay Pass 2

2:1 Overlay Pass 2

4:1 Overlay Pass 2

Figure 5-43. Effects of Signal Clipping

4:1 overlay maps from each pass were made despite these problems, and results are as indicated by the difference image seen in Figure 5-44. Registration appears quite good in all areas where a sufficient amount of data exists for a majority of the strips crossing the images. In areas out in the ocean, registration is obviously inaccurate, for example, the ends of the dock. Considering the data, this is not unexpected. It should be noted that strips in that area are being roughly guided by strips covering ground data. As soon as strips over the water start encountering returns, their registration improves. A statistical analysis of the registration accuracy was done in an area where a majority of the images consisted of ground coverage. This statistical evaluation was done using program WECK. The results indicated an RMS error or .63 pixels. This indicates the automatic strip process is capable of registering this form of digital radar. No additional processing was done for the reasons indicated earlier.

Figure 5-44. Difference Image Obtained Using 4:1 Overlay Maps From Each Pass